

Ecosystem Recovery from Acid Precipitation: Carbon and Nitrogen Cycling in  
the Soil-Stream Continuum

by

Richard Ernest Marinos

Environment  
Duke University

Date: \_\_\_\_\_

Approved:

\_\_\_\_\_  
Emily S. Bernhardt, Supervisor

\_\_\_\_\_  
James B. Heffernan

\_\_\_\_\_  
Daniel D. Richter

\_\_\_\_\_  
Emma J. Rosi

Dissertation submitted in partial fulfillment of  
the requirements for the degree of Doctor  
of Philosophy in Environment  
in the Graduate School of Duke University

2018

ABSTRACT

Ecosystem Recovery from Acid Precipitation: Carbon and Nitrogen Cycling in  
the Soil-Stream Continuum

by

Richard Ernest Marinos

Environment  
Duke University

Date: \_\_\_\_\_

Approved:

\_\_\_\_\_  
Emily S. Bernhardt, Supervisor

\_\_\_\_\_  
James B. Heffernan

\_\_\_\_\_  
Daniel D. Richter

\_\_\_\_\_  
Emma J. Rosi

An abstract of a dissertation submitted in partial  
fulfillment of the requirements for the degree of  
Doctor of Philosophy in Environment  
in the Graduate School of Duke University

2018

Copyright by  
Richard Ernest Marinos  
2018

## Abstract

While the problem of acid precipitation has been greatly reduced across the developed world, acid-impaired ecosystems still bear important legacies of historic acid deposition, and these ecosystems are only slowly beginning to recover. Early evidence suggests that this recovery may have multiple unexpected, substantial impacts on ecosystem carbon (C) and nitrogen (N) cycling, including large reductions in soil organic C and N pools and greatly increased export of dissolved organic C to aquatic ecosystems. These losses of soil C and N, driven by ecosystem recovery from acid precipitation, have the potential to dwarf any gains in biomass pools due to enhanced forest growth. The mechanisms driving these changes remain poorly understood, however. In this work, I ask the following questions: a) How does ecosystem recovery from acid precipitation alter soil C and N cycling, and b) what are the consequences of these changes for ecosystem N retention?

A watershed acid remediation experiment, performed at Hubbard Brook, White Mountains National Forest, New Hampshire, offers an opportunity to study *now* processes of ecosystem recovery from acid precipitation that will take decades to centuries to occur naturally. In this experiment, researchers applied calcium (Ca) silicate to a watershed to restore soil Ca fertility and raise soil pH. This treatment caused a rapid, substantial decrease in soil organic C, and greatly increased streamwater export of

inorganic nitrogen. My dissertation examines my research questions through the lens of this experiment.

In the first part of my dissertation (Chapter 2), I examined how changes to soil pH and Ca fertility, individually and together, drive changes in the solubility and respiration of soil C, and how vegetation mediates these effects. I examined this topic through a soil mesocosm experiment in which I modified soil pH and soil Ca status individually and in combination. I found that there was a strong interactive effect between increases in soil pH and the presence of vegetation. Increasing soil pH increased soil respiration and soil C solubility, but only in the presence of sugar maple (*Acer saccharum*) roots. I also found that Ca fertilization stimulated plant growth but had no effect on soil C dynamics. This suggests that vegetation and soil microbiota may respond to different aspects of ecosystem recovery from acid precipitation, with vegetation sensitive to changes in soil Ca content and microbiota sensitive to changes in soil pH.

In the second part of my dissertation (Chapter 3), I performed a field-based study to examine how the acid remediation treatment altered soil N cycling. I found that the acid remediation treatment increased both gross N mineralization and N uptake in the leaf litter, causing an accelerated N cycle. This accelerated N cycling resulted in larger inorganic N pools throughout the soil profile. These observed changes in N cycling

contrast with earlier studies showing no treatment effect on N cycling rates, and this lag may be coupled to changes in plant community structure.

In the last part of my dissertation (Chapter 4), I examined how these changes in soil N cycling resulted in changes to ecosystem N export, using a combination of re-analysis of long term data sets and intensive stream monitoring. I found that, as a result of the Ca treatment, flushing of inorganic N during storms became a substantially more important mechanism of ecosystem N loss. I found evidence that the flushing of N during stormflow was the result of the mobilization of distal, hydrologically disconnected pools of soil N. This suggests that changes in forest floor N cycling, observed in Chapter 3, were responsible for this response. Finally, I found that in-stream uptake of N was significantly enhanced during baseflow conditions in the Ca-enriched watershed, reducing N export during baseflow.

This dissertation adds new mechanistic insight into the drivers by which ecosystem recovery from acid precipitation will affect C and N cycling. It demonstrates that, while acid precipitation has abated in the developed world, its legacy effects will remain with us for a long while. The changes to ecosystem C and N cycling studied here are concerning from the perspectives of climate change and loading of nutrients to aquatic ecosystems. This suggests the need for further work that couples vegetation dynamics, changes to geochemical properties of soils, and watershed hydrology.

## **Dedication**

To Ernest and Karen, who showed me the wonder of the natural world at a young age,

To Cari, who keeps that childlike wonder alive in me today, and

To Lillian, who I hope will inherit a world as wonderful as the present one.

# Contents

Abstract .....	iv
List of Tables .....	xi
List of Figures .....	xii
Acknowledgements .....	xiv
1. Introduction .....	1
2. Soil carbon losses due to higher pH offset vegetation gains due to calcium enrichment in an acid mitigation experiment .....	8
2.1 Introduction .....	8
2.2 Methods .....	12
2.2.1 Mesocosm construction and incubation .....	13
2.2.2 Soil amendments .....	14
2.2.3 Mesocosm harvest .....	15
2.2.4 Plant measurements .....	16
2.2.5 Soil analyses .....	16
2.2.6 Statistical analysis .....	18
2.3 Results .....	19
2.3.1 Treatment effects on soil acid-base status .....	19
2.3.2 SOC dynamics in unplanted mesocosms .....	22
2.3.3 Plant responses to soil amendments .....	24
2.3.4 SOC dynamics in planted mesocosms .....	25
2.4 Discussion .....	26

3. Ecosystem recovery from acid precipitation drives enhanced soil nitrogen cycling ....	34
3.1 Introduction.....	34
3.2 Methods .....	38
3.2.1 Site description .....	38
3.2.2 Soil collection .....	39
3.2.3 Laboratory analysis.....	41
3.2.4 Statistical analysis.....	44
3.3 Results .....	45
3.4 Discussion.....	57
3.5 Conclusions .....	62
4. A watershed acid rain remediation experiment increases the flashiness of terrestrial nitrogen export but increases in-stream nitrogen retention .....	63
4.1 Introduction.....	63
4.2 Methods .....	67
4.2.1 Study site .....	67
4.2.2 Storm event nitrate dynamics in the long-term record.....	68
4.2.3 High-frequency storm nitrate dynamics .....	69
4.2.4 In-stream nitrate uptake .....	71
4.3 Results .....	73
4.3.1 Storm nitrate c-Q dynamics .....	73
4.3.2 In-stream uptake of nitrate.....	80
4.4 Discussion.....	82
5. Conclusions.....	90

Appendix A: Soil carbon losses due to higher pH offset vegetation gains due to calcium enrichment in an acid mitigation experiment: Supplement .....	97
A.1 Preliminary Experiment: Laboratory Soil Manipulations .....	97
A.1.1 Supplemental methods.....	97
A.1.2 Supplemental results .....	97
A.2 Plant morphological trait analysis .....	100
A.2.1 Supplemental methods.....	100
A.2.2 Supplemental results .....	101
A.3 Soil analyses .....	102
A.3.1 Supplemental methods.....	102
A.3.1.1 Soil physical and chemical analyses.....	102
A.3.1.2 Microbial respiration potential assays .....	102
A.3.2 Supplemental results .....	104
Appendix B: A watershed acid rain remediation experiment increases the flashiness of terrestrial nitrogen export but increases in-stream nitrogen retention: Supplement.....	107
B.1 Supplemental methods.....	107
B.2 Supplemental results and discussion.....	107
Works Cited .....	109
Biography .....	128

## List of Tables

Table 1: Unplanted mesocosms - soil chemical and biological properties by horizon. ....	20
Table 2: Planted mesocosms - soil chemical and biological properties by horizon.....	21
Table 3: Soil properties related to soil C cycling.....	55
Table 4: Plant biomass and morphological traits.....	101
Table 5: Soil exoenzyme potential assays. ....	105

## List of Figures

Figure 1: Water-extractable organic carbon. ....	23
Figure 2: Soil respiration potential. ....	24
Figure 3: Soil amendment effects on sugar maple sapling growth. ....	25
Figure 4: Soil acid-base properties. ....	46
Figure 5: Soil inorganic N concentrations by horizon. ....	48
Figure 6: Whole-profile soil inorganic N pools for the forest floor and 0 - 10 cm mineral soil. ....	49
Figure 7: Net N cycling rates by horizon. ....	51
Figure 8: Gross N cycling rates by horizon for spring 2016 soil samples. ....	52
Figure 9: A N budget “snapshot” for the Oie horizon in spring 2016, reflecting the differences in N pools and gross process rates that were measured. ....	54
Figure 10: Correlations between C mineralization and (a) gross and (b) net N mineralization for forest floor soil samples. ....	56
Figure 11: Gross and net N cycling rates for spring 2016, disaggregated by microtopographic position. ....	57
Figure 12: Instantaneous NO <sub>3</sub> <sup>-</sup> flux in three watersheds at HBEF from 1 January 1991 to 30 June 2016. ....	74
Figure 13: Slopes of the c-Q relationship for high-flow events captured in the weekly HBEF stream chemistry record. ....	75
Figure 14: Summary statistics by period and watershed of event c-Q slope data, disaggregated by season. ....	77
Figure 15: High-frequency NO <sub>3</sub> <sup>-</sup> c-Q relationships for the twelve largest discrete storm events captured using optical NO <sub>3</sub> sensors. ....	79

Figure 16: The mean NO <sub>3</sub> <sup>-</sup> flux by month observed at the weir of the CaSiO <sub>3</sub> -enriched and BGC reference watersheds, relative to the maximum flux observed upstream.....	81
Figure 17: The relationship between the NO <sub>3</sub> <sup>-</sup> flux ratio and discharge. ....	82
Figure 18: A nitrogen budget for the Ca-enriched watershed, highlighting the large discrepancy in ecosystem N balance that continues to be a mystery.....	93
Figure 19: Short term soil microbial respiration potential of soils in laboratory soil manipulations.....	99
Figure 20: Relationships between WEOC and short-term soil microbial respiration across treatment groups.....	106
Figure 21: Potential denitrification rates of four replicate debris dam sediment samples. ....	108

## Acknowledgements

I foremost want to acknowledge the immeasurable contributions of my advisor Emily Bernhardt to my scientific, professional and personal development. I'm deeply grateful for her engagement and support. Second, I thank my partner Cari Ficken, who keeps me focused on the big picture, serves as my sounding-board for half-baked ideas, and patiently helps me improve as a science communicator. She also has helped me understand what it means to do good science as part of a well-centered life, and she sets an example for me in her perseverance through trying circumstances. I thank Emma Rosi, Jim Heffernan and Dan Richter, my committee members, for their advice and encouragement. I also thank Rob Jackson for taking a risk on an unknown quantity when he accepted me as his student at Duke, and also for his support in the early years of my academic program.

This work would not have been possible without the support of the many researchers who have worked at Hubbard Brook, and whose work contextualizes and enriches my own. In particular I would like to thank Gene Likens, Don Buso, Melany Fisk, Chris Johnson, Charley Driscoll, Peter Groffman, Christie Goodale, and Scott Bailey for helping me see the forest from different angles and for encouraging me along the way. I thank Chris Johnson, Charley Driscoll, Amey Bailey, Don Buso, Tammy Wooster, Lindsey Rustad and John Campbell for providing me with the long-term data that were

the foundation of my work. Finally, I thank Ailis Clyne and Geoff Wilson for their friendship and the multiple ways they helped me at Hubbard Brook.

I am also deeply thankful for the intellectual community at Duke that has supported me along the way. Ben Colman, in particular, was a wonderful scientific mentor to me. I thank all the members of the Bernhardt lab for their support and feedback. I would particularly like to recognize Marie Simonin, Matt Ross, Joanna Blaszczak, Jenny Rocca, Jess Brandt and Jackie Gerson, who have all improved greatly the grants and papers I've written and the talks I've prepared. I thank Nia Bartolucci, Steve Anderson, Julian Wilson, Eric Zhang and Tong Fu for their excellent help in the lab. I thank Michael Barnes for spot-on horticultural advice and Brooke Hassett for many patient hours spent in the weeds of science with me. I would like to give a warm hug to Martin Doyle for hosting the annual River Retreat, which renewed my enthusiasm for science every January. I would like to re-thank Emily Bernhardt and Jim Heffernan because they were extremely patient and understanding with me while I was their teaching assistant and I had a newborn at home. Finally, I'd like to thank Meg Avery, who pulled so many strings for me that I'm surprised the Nicholas School didn't unravel.

I thank my parents Bob and Nancy and my mother-in-law Ayla for their unflagging support and love. Other people who have shaped this work in indirect but

important ways include Rosa Newman-Hall, Randy Mecerdy, Siobhan Fennessy, and Roger Kwidja.

This research was funded through many lines of support. I would like to recognize the NSF Graduate Research Fellowship Program, an NSF Doctoral Dissertation Improvement Grant (DEB-1701920), a research travel award provided by Duke's William and Janet Hunt Graduate Fellowship Fund, and Duke's Aleane Webb Dissertation Research Fellowship. Further support was provided through the NSF LTER and LTREB programs, and the Cary Institute for Ecosystem Studies. The Hubbard Brook Research Foundation gave me an important in-kind donation of housing and lab space for two years, and Emily Bernhardt and Justin Wright gave me a well-maintained Toyota Corolla.

This dissertation is a contribution of the Hubbard Brook Ecosystem Study. Hubbard Brook is part of the Long-Term Ecological Research (LTER) network, which is supported by the National Science Foundation. The Hubbard Brook Experimental Forest is operated and maintained by the U.S. Forest Service, Northern Research Station, Newtown Square, Pennsylvania.

# 1. Introduction

The coupling of ecosystem energetics and organismal stoichiometry has been a central organizing principle of ecosystem ecology since Lindeman's (1942) pioneering work that linked nutrient availability, phytoplankton productivity and organic sediment accumulation in shallow lakes. Early hypotheses that examined this coupling proposed that vegetation dynamics during successional development were the primary controls on ecosystem carbon (C) balance and nutrient retention (Odum 1969, Vitousek and Reiners 1975). Much empirical work has borne out the general outlines of these hypotheses in forested ecosystems. Ecosystem C stocks, both in biomass and in soil pools, have been shown to track successional development (Covington 1981, Chapin et al. 1994, Richter et al. 1999, Post and Kwon 2000) and ecosystem nutrient retention is also strongly controlled by disturbance and subsequent recovery (Bormann and Likens 1979, Grogan et al. 2000, Kreuzweiser et al. 2008). Nonetheless, other studies have shown patterns of patterns of soil C aggradation (e.g. Zhou et al. 2006) and ecosystem nutrient retention (e.g. Aber et al. 1998, Yanai et al 2013) that do not conform to predictions based on successional dynamics, making clear the limits of considering vegetation as the primary control on these processes. Explanations for these discrepancies have been found with new insights into the mechanisms soil organic matter (SOM) stabilization (Sutton and Sposito 2006, Schmidt et al. 2011) and soil retention of legacy nutrient inputs (Van Meter et al. 2016). This has brought renewed attention to the central role that the

physical, chemical and biological properties of soils (and human alteration to these properties) play in controlling ecosystem C balance and nutrient retention.

A key pathway by which humans alter soil properties controlling ecosystem C balance and nutrient retention is through acid precipitation (Likens et al. 1996). Acid precipitation across the developed world peaked in the 1970s, but clean air legislation has resulted in dramatic reductions of acid deposition over the past thirty years (Driscoll et al. 2016). Nonetheless, forests across North America and Europe remain severely impacted by the legacies of over a hundred years of acid deposition. These legacies include soil acidification, low soil fertility of cation nutrients, elevated levels of toxic inorganic aluminum (Al), and increased morbidity of vegetation (Likens et al. 1996, Driscoll et al. 2001, Joslin et al. 1992, Sullivan et al. 2013). Terrestrial ecosystem recovery from acid precipitation is likely to occur very gradually, and the trajectories of this recovery are likely to bring forested ecosystems to different biogeochemical and ecological states than in pre-acid precipitation conditions (Likens and Buso 2012). Some recovery metrics, such as increases in soil pH in organic soil horizons, have gradually started to recover (Kirk et al. 2010, Lawrence et al. 2015). Others, such as increases in mineral soil pH and the restoration of soil Ca fertility through weathering inputs, are likely to occur over decades to centuries and will likely not result in full recovery to pre-acid deposition conditions (Likens et al. 1996).

Despite the fact that forested ecosystems have only begun to recover from acid precipitation, there is mounting evidence that this incipient recovery is altering ecosystem C balance and nutrient retention. Substantial declines in soil organic matter pools across North America and Europe have been linked to ecosystem recovery from acid precipitation (Oulelhe et al. 2011, Lawrence et al. 2012). Recovery has also been shown to drive elevated export of dissolved organic matter to headwater streams and lakes (Monteith et al. 2007, Evans et al. 2012). These changes in soil C dynamics suggest that acid precipitation was a key driver in the stabilization of soil organic matter, and that, with reductions in acid precipitation, this organic matter is rapidly being liberated. These large decreases in soil organic matter have the potential to dwarf any increases in biomass C due to vegetation recovery and may substantially diminish or eliminate the C sink in these forests. Although a variety of geochemical mechanisms have been proposed that could drive these changes (Clarholm and Skjellberg 2013), there is currently no consensus on the why these ecosystem losses of carbon are occurring and how much they will continue to change ecosystem C balance.

A watershed-scale acid rain remediation experiment, performed at Hubbard Brook Experimental Forest (White Mountains National Forest, NH) in 1999, offers an opportunity to examine potential mechanisms by which ecosystem recovery from acid precipitation may drive altered soil carbon and nutrient dynamics. The experiment also offers a window into how ecosystems may function as they recover from acid

precipitation more fully over the coming decades to centuries. In the experiment, researchers applied powdered calcium silicate ( $\text{CaSiO}_3$ ) to an 11 ha watershed in order to restore soil Ca fertility and slightly elevate soil pH. Many of the predicted effects of this experiment, such as increased aboveground biomass (Battles et al. 2014), sugar maple (*Acer saccharum*) recruitment (Juice et al. 2006), and stream acid-neutralizing capacity (Cho et al. 2012) came to pass. However, two of the most dramatic effects of the treatment were wholly unpredicted: First, the treatment caused a massive loss of soil organic matter. In the fourteen years following the  $\text{CaSiO}_3$  addition, the forest floor and top 10 cm of mineral soil lost  $31.9 \text{ Mg C ha}^{-1}$ , a 35% loss of SOC equivalent to  $\sim 1/3$  of the aboveground biomass C (Johnson et al. 2014). Second, the treatment caused greatly enhanced nitrogen (N) export in streamflow, with steadily increasing nitrate ( $\text{NO}_3^-$ ) flux that in 2013 reached 30 times that of the reference watershed at Hubbard Brook (Rosi-Marshall et al. 2016). These results show that the impacts on C and N dynamics of continued ecosystem recovery from acid precipitation are likely to be profound.

For my dissertation, I worked within the context of the acid remediation experiment at HBEF to examine how ecosystem recovery from acid precipitation alters coupled ecosystem C and N processes. I examined how recovery controls soil C and N cycling, how these changes control export of N to receiving headwaters, and how in-stream N processing responds to increased N loading. I address these questions in three research chapters:

In Chapter 2, entitled “Soil carbon losses due to higher pH offset vegetation gains due to calcium enrichment in an acid mitigation experiment”, I examine geochemical and vegetation controls on the solubility and respiration of soil organic matter, using a controlled mesocosm approach to tease apart the drivers behind enhanced C loss. In this experiment, I modified soil pH and soil Ca status individually and in combination. I found that there was a strong interactive effect between increases in soil pH and the presence of vegetation. Increasing soil pH increased soil respiration and soil C solubility, but only in the presence of sugar maple (*Acer saccharum*) roots. I also found that Ca fertilization stimulated plant growth but had no effect on soil C dynamics. This suggests that vegetation and soil microbiota may respond to different aspects of ecosystem recovery from acid precipitation, with vegetation sensitive to changes in soil Ca content and microbiota sensitive to changes in soil pH.

In Chapter 3, entitled “Ecosystem recovery from acid precipitation drives enhanced soil nitrogen cycling,” I examined gross and net N cycling rates in a plot-based study to determine how ecosystem recovery from acid precipitation drives enhanced N export from soils. I found that the acid remediation treatment increased both gross N mineralization and N uptake in the leaf litter, causing an accelerated N cycle. This accelerated N cycling resulted in larger inorganic N pools throughout the soil profile. These observed changes in N cycling contrast with earlier studies showing no treatment effect on N cycling rates, and this lag may be coupled to changes in plant community

structure. There was no direct relationship between soil geochemical properties and N cycling, further supporting the idea that changes to N cycling were due to changes in the plant community.

In Chapter 4, “A watershed acid rain remediation experiment increases the flashiness of terrestrial nitrogen export but increases in-stream nitrogen retention”, I examine how enhanced terrestrial cycling of N manifests in patterns of stream N export and retention, using watershed outlet chemistry data and synoptic stream surveys. I found that, as a result of the Ca treatment, flushing of inorganic N during storms became a substantially more important mechanism of ecosystem N loss. I found evidence that the flushing of N during stormflow was the result of the mobilization of distal, hydrologically disconnected pools of soil N. This suggests that changes in forest floor N cycling, observed in Chapter 3, were responsible for this response. Finally, I found that in-stream uptake of N was significantly enhanced during baseflow conditions in the Ca-enriched watershed, reducing N export during baseflow.

This dissertation adds new mechanistic insight into the drivers by which ecosystem recovery from acid precipitation will affect C and N cycling. It demonstrates that, while acid precipitation has abated in the developed world, its legacy effects will remain with us for a long while. The changes to ecosystem C and N cycling studied here are concerning from the perspectives of climate change and loading of nutrients to

aquatic ecosystems. This suggests the need for further work that couples vegetation dynamics, changes to geochemical properties of soils, and watershed hydrology.

## **2. Soil carbon losses due to higher pH offset vegetation gains due to calcium enrichment in an acid mitigation experiment**

### ***2.1 Introduction***

Many temperate forest ecosystems across North America and Europe show incipient signs of recovery from acid precipitation, and recent research suggests that this recovery profoundly alters soil organic carbon (SOC) dynamics. Substantial declines in SOC stocks have been linked to reduced acid deposition in conifer forests across both continents (Lawrence et al. 2012; Oulehle et al. 2011). Decreases in acid deposition have also been shown to drive enhanced fluxes of SOC into lakes and headwater streams (Monteith et al. 2007; Evans et al. 2008). These losses are important to overall ecosystem carbon (C) balance, as SOC comprises more than 80% of total C stocks in these ecosystems (Scharlemann et al. 2014). Although temperate forests are currently considered net sinks of C (Pan et al. 2011) and recovery from acid precipitation may increase net primary productivity (Battles et al. 2014), these forests may become net sources of C if recovery also drives substantial losses of SOC.

The legacies of anthropogenic acid precipitation include decreased soil pH, increased concentrations of toxic monomeric aluminum (Al) in soil solution, and a profound loss of soil cationic nutrients, in particular calcium (Ca) (Ulrich et al. 1980; Likens et al. 1996). In many forests, these soil properties have begun to recover slowly (Hruska et al. 2002; Lawrence et al. 2015), but maximum recovery will likely take

decades to centuries (Driscoll et al. 2001). These soil acid-base properties often do not recover in tandem, driven by differences in geology, the severity of historic acid deposition, and vegetation dynamics (Lawrence et al. 2015; Clarholm and Skjellberg 2013; Nezat et al. 2004). It is thus important to understand how each of these soil chemical properties affects SOC dynamics separately and together to predict the overall SOC impacts of recovery from acid precipitation in different forest ecosystems.

Manipulative acid remediation experiments offer predictions of how SOC dynamics may change as forests recover more fully over the coming decades. Lime ( $\text{CaCO}_3$ ) treatments have been shown to increase concentrations of dissolved organic carbon (DOC) in soil solution, whereas experimental acidification treatments have been shown to decrease DOC concentrations (Driscoll et al. 1996; Ekstrom et al. 2011). Two whole watershed acid remediation experiments have resulted in opposite conclusions about the impact of rising soil Ca and pH on SOC stocks. At the Hubbard Brook Experimental Forest (HBEF) (New Hampshire, U.S.A.), a watershed-scale wollastonite ( $\text{CaSiO}_3$ ) enrichment led to an increased extent of leaf litter decomposition (Lovett et al. 2016) and a 35% decline in SOC stocks in the decade following enrichment (Johnson et al. 2014). In contrast, at Woods Lake (New York, U.S.A.), two decades after a watershed lime treatment, SOC stocks in the treated watersheds were more than double those in adjacent reference watersheds (Melvin et al. 2013). Differences between these two large-scale experiments could be due to differences in the relative changes in soil Ca versus

soil pH. At Woods Lake, approximately four times more Ca was applied in the liming treatment than at Hubbard Brook, but increases in soil pH were roughly comparable. Also, in plot-scale  $\text{CaSiO}_3$  enrichment studies at HBEF, where the levels of enrichment were five times higher than in the watershed experiment, researchers found decreased SOC solubility (Balara et al. 2015) and decreased decomposition of older SOC, despite higher leaf litter turnover (Minick et al. 2017).

In each of these field experiments, researchers altered many soil chemical properties simultaneously, making it difficult to resolve the specific impacts on SOC dynamics of increased Ca fertility, soil pH, and ionic strength of soil solution. Increases in soil pH and Ca fertility are likely to have opposite effects on SOC solubility, and divergent impacts on microbial activity and plant productivity. In acid soils, the solubility of SOC increases with soil pH as a result of the destabilization of micelle-like associations of SOC molecules that are stable at low pH (Sutton and Sposito 2005). Elevated soil pH can also reduce SOC sorption onto soil minerals and complexation with iron and Al, increasing C bioavailability (Clarholm and Skjellberg 2014; Newcomb et al. 2017). By contrast, increased soil Ca concentrations may stabilize SOC and decrease its bioavailability by forming “cation bridges” between SOC molecules (Mouvenchery et al. 2011; Balara et al. 2015). There are many reasons to expect enhanced microbial activity as soil pH increases. The pH optima of many catalytic exoenzymes are substantially higher than soil pH in many acid-impacted forests (Niemi and Vepsäläinen 2005),

mycorrhizal colonization is substantially suppressed in very acidic soils (Coughlan et al. 2000), and Al toxicity at low soil pH can substantially depress microbial biomass and activity (Illmer et al. 2003). Low soil pH can also suppress soil faunal activity and associated decomposition (Geissen and Brümmer 1999). Ca fertilization has also been hypothesized to stimulate microbial activity by alleviation of Ca limitation in fungi (Lovett et al. 2016). Finally, both Ca fertility and soil pH can strongly impact vegetation dynamics. Reduced Al stress at higher soil pH can promote tree growth (Halman et al. 2013). Increased Ca fertility may result in increased aboveground plant growth, especially for Ca-sensitive species such as sugar maple (*Acer saccharum*) and red spruce (*Picea rubra*) (Baribault et al. 2010; Halman et al. 2014). But increased Ca fertility may also decrease fine root growth (Fahey et al 2016), reducing inputs of root litter which are known to be relatively stable in soils (Schmidt et al. 2011). This large suite of mechanisms suggests that SOC responses to ecosystem recovery from acid precipitation are likely to be complex and possibly synergistic, with soil pH and Ca status mediating interactions among plants, microbes, and extant SOC pools.

Here, we experimentally tested the impact of increasing soil pH (alkalinity treatment) and soil exchangeable calcium (Ca treatment), separately and in combination, on SOC solubility, microbial activity and plant growth. The choice of our soil amendments allowed us to independently alter soil pH and Ca concentrations, permitting us mechanistic understanding into the geochemical factors controlling plant

and SOC dynamics, in contrast to most studies which alter these properties in tandem. Using acid-impacted soils from HBEF, we performed a year-long mesocosm experiment to examine the long-term effects of these soil amendments on SOC dynamics, in mesocosms both with and without sugar maple saplings. We expected that the alkalinity treatment would increase SOC solubility and the Ca treatment would decrease SOC solubility in both planted and unplanted mesocosms. Further, we expected that, in the alkalinity treatment, increases in SOC solubility would be correlated with enhanced microbial respiration and other metrics of soil microbial activity, with the opposite effect observed in the Ca treatment. Finally, in the planted mesocosms, we expected that both treatments would enhance plant growth and fresh C inputs into the soil, and that this would amplify the predicted increase of microbial activity in the alkalinity treatments and mitigate the predicted decrease in the Ca treatments.

## **2.2 Methods**

This experiment was designed to strike a balance between the limited realism of laboratory manipulations of soil chemistry and the high variability of field-based measurements. Laboratory manipulations of pH and Ca fertility often introduce ionic strength artifacts that severely limit potential inferences (Appendix A), or else require invasive soil manipulations (as in Wittinghill and Hobbie (2011)). As is common in complex, formerly-glaciated terrain such as this study site, high within-plot variability of soil microbial activity (CV of heterotrophic respiration = 52%) (Groffman 2015) makes

detecting all but the largest changes in SOC dynamics challenging. By performing a long-term, freely draining mesocosm experiment, we allowed time for the soil microbial community to adapt to novel chemical conditions, ionic strength issues were minimized by leaching of the soil profile, and soil structure was able to re-establish. By using a homogenized soil taken from an acid impacted forest, we were able to control for issues of fine-scale spatial heterogeneity in soils.

### **2.2.1 Mesocosm construction and incubation**

In June 2016, we collected soil from a 4 m<sup>2</sup> area within an acid-impacted hardwood stand in HBEF. The soil was a typical Spodosol in a stand dominated by sugar maple (*Acer saccharum*) and American beech (*Fagus grandifolia*). We bulked soil by horizons: the Oi/Oe horizon (referred to here as leaf litter); Oa/A horizon (organic horizon); and mineral soil from 0 to 10 cm depth, comprising E, Bh and Bs horizon soils (mineral horizon). We sieved the soils (to pass a 6.4 mm screen for leaf litter and a 3.2 mm screen for organic and mineral horizons) and homogenized them by shovel. To build each mesocosm, we reconstructed the soil profile by layering, loosely-packed, 293g (dry mass) mineral soil, 227g humic soil, and 25g leaf litter into 100 2.5 L plastic pots. In half of the mesocosms, we planted 3-year-old, bare root sugar maple saplings from the New Hampshire State Forest Nursery (Boscawen, NH), and we left the remaining 50 unplanted. To allow mesocosms to recover from disturbance effects due to transplanting and construction, we pre-incubated them outdoors at HBEF from June to August 2016.

We then transported them to the greenhouse facility at Duke University (Durham, NC) in September, briefly maintaining them indoors and then moving them to an enclosed area outside. In early November 2016, shortly before the maples senesced, we applied the chemical amendments described in the following section. To prevent soil freezing and sapling mortality during the winter, if temperatures were forecast to be below 0°C for more than one day, the mesocosms were covered with a tarp shelter and the air in the shelter was heated to 2 °C. In late January, we calculated that, due to an atypically warm winter, the maples would not receive sufficient chilling degree-days to ensure the breaking of dormancy in the spring (Donnelly 1973). We therefore moved the mesocosms into cold storage at 4°C for six weeks starting in early February 2017. In mid-March 2017, we returned the seedlings to the exterior greenhouse space until harvest in mid-July 2017. Throughout the experiment, the mesocosms were monitored at least weekly and watered and weeded as necessary.

### **2.2.2 Soil amendments**

In early November 2016, we treated each soil horizon in the mesocosms with one of the following amendments: calcium chloride to increase soil exchangeable Ca twofold (Ca treatment); potassium hydroxide to increase soil pH by one unit (alkalinity treatment); a combination Ca x alkalinity treatment; a deionized water control (Control); or a potassium chloride control (K Control). The K Control matched the ionic strength of the Ca x alkalinity treatment and was included to account for effects of osmotic stress

and potassium fertilization that resulted from the Ca and alkalinity treatments. We destructively sampled five spare mesocosms to determine the appropriate concentrations of each soil amendment. The appropriate amounts of potassium hydroxide to achieve the desired alkalinity treatment effect in each horizon were determined by titration of soil slurries using a DL-18 autotitrator (Mettler-Toledo, Columbus, OH). Appropriate amounts of Ca addition were determined by measuring exchangeable Ca in each horizon using the methods described in Appendix A. We amended each soil horizon separately by injecting treatment solution throughout each horizon with a spinal tap needle. In total, we had 10 planted and 10 unplanted replicates per treatment.

### **2.2.3 Mesocosm harvest**

In mid-July 2017, we destructively harvested all mesocosms, separating and bulking soils by horizon. For planted mesocosms, we carefully separated plant roots from the soil, washed the remaining soil from the roots, and kept the roots moist for same-day morphological analysis. We stored soils at 4°C until analysis. All soil analyses were performed within ten days of harvest, and 17% of the total sample load consisted of analytical replicates and blanks. An insufficient mass of leaf litter soil was recovered to perform the analyses, so these samples were discarded.

## **2.2.4 Plant measurements**

At the time of planting, we estimated the initial dry biomass of each bare root sapling by adjusting the fresh mass by the mean moisture content measured on 12 spare saplings. At harvest, we measured the final biomass of each plant as well as a suite of root and leaf morphological traits. We divided plants into leaf, stem, coarse root (> 2 mm) and fine root (< 2 mm) components. The methods of the morphological analyses are presented in Appendix A. Following morphological analysis, we dried plant samples at 60 °C for 7 d and weighed each biomass component. We summed these components to calculate total plant biomass and calculated the relative growth rate (RGR) of each plant using the equation in Hunt (1982).

## **2.2.5 Soil analyses**

We measured soil water content, percent organic matter, pH, total dissolved solids, exchangeable Ca and exchangeable Al using standard methods described in Appendix A. We measured organic-bound Al via a batch extraction process that modified the protocol in Gu et al. (2017). We extracted organic-bound Al using a 0.5 M cupric chloride solution in a 5:1 extractant: soil suspension, agitating these samples on an end-over shaker for 24 h. We filtered these extracts through Acrodisc 0.2 µm polysulfone membrane filters (Pall Corporation, Port Washington, NY) and analyzed them by flame AA spectrometry on a PE 3100 spectrometer (Perkin-Elmer, Waltham, MA).

We used substrate-induced respiration (SIR) as an index of microbial biomass, following the protocol in Fierer et al. (2003). We performed long term C mineralization assays on all soils, beginning these assays within three hours of the harvest of each mesocosm in an effort to capture the transient effects of root-mediated processes. In these assays, we measured cumulative respiration over 24 h on days 1, 2, 4, 8, 16, 35, and 75 post-harvest. Our protocol slightly modified standard methods and is further described in Appendix A. We did not conduct separate short-term C mineralization assays, but instead calculated total soil respiration over the first week of the long-term incubations, estimating respiration on days that it was not measured by linear interpolation of the measured respiration rates. To assess potential soil enzyme activity, we measured a suite of C-degrading enzyme activities ( $\alpha$ -glucosidase, AG;  $\beta$ -glucosidase, BG; cellobiohydrolase, CB; xylosidase, XYL, and N-acetyl glucosaminidase, NAG) as well as phosphatases (PHOS) following the microplate enzyme assay protocol of Bell et al. (2013).

We used water-extractable organic carbon (WEOC) as a measure of SOC solubility. Within 4 hours of harvest, we extracted 8 g of field-moist soil in 40 mL of low-OC deionized water. Slurries were shaken at 60 rpm on an end-over shaker for 16h, centrifuged at 3500 rpm for 15 minutes, and filtered through an Acrodisc 0.2  $\mu$ m polysulfone membrane filter. The filters were rinsed with 10 ml of sample prior to sample collection. Total organic carbon content was measured on a TOC-V combustion

analyzer (Shimadzu Corporation, Koyoto, Japan). We quantified WEOC molecular characteristics by spectrophotometric methods. Absorbance spectra of samples were measured from 220 to 500nm using a Genesys 10S spectrometer (Thermo-Fisher, Waltham, MA). Specific UV absorbance at 280nm ( $SUVA_{280}$ ), a measurement positively correlated with the proportion of aromatic moieties in a sample, was calculated as the sample's absorbance at 280 nm divided by concentration of dissolved organic carbon in units of  $mg\ L^{-1}$  (Chin et al. 1994). The  $E2:E3$  ratio, which is inversely correlated with the mean molecular weight of dissolved organic carbon, was calculated as the ratio of absorbance at 255 and 365 nm (Avagyan et al. 2014).

### **2.2.6 Statistical analysis**

All statistical analyses were performed in R (R Core Development Team 2017). No microbial or plant measurements showed any significant difference between the Control treatment and the K Control treatment (student's t test,  $\alpha=0.05$ ), suggesting that our concern over artifacts from potassium fertilization and osmotic stress was unwarranted. We therefore dropped this treatment from further analysis in order to allow analysis of the experiment as a balanced  $2 \times 2$  factorial design. We analyzed the effects of chemical amendments with 2-way (Ca x alkalinity) ANOVA models. Each soil horizon was analyzed in a separate model, and the unplanted mesocosms were analyzed separately from the planted mesocosms. All ANOVAs for each response variable were thus performed four times, so the significance of model terms was evaluated at  $\alpha = 0.05 /$

4 = 0.0125 to account for multiple comparisons. In models where the interaction term was not significant but main effects were, we report results from a reduced model with main effects only.

## **2.3 Results**

### **2.3.1 Treatment effects on soil acid-base status**

The soil amendments significantly increased soil pH and Ca fertility, but to a lesser extent than intended. Across planted and unplanted mesocosms, the alkalinity treatment increased soil pH, relative to controls, by a mean of 0.82 units in the organic horizon ( $p < 0.001$ ) and by 0.75 units in the mineral horizon. There was no effect of the Ca treatment on soil pH. The Ca treatment increased exchangeable Ca, relative to the controls, from 12.3 to 18.0  $\mu\text{mol gds}^{-1}$  in the organic horizon ( $p < 0.001$ ) and from 0.52 to 1.08  $\mu\text{mol gds}^{-1}$  in the mineral soil ( $p < 0.001$ ) (Tables 1 and 2). Despite no addition of Ca in the alkalinity treatment, the alkalinity treatment increased exchangeable Ca from 12.3 to 14.5  $\mu\text{mol gds}^{-1}$  in the organic horizon and 0.52 to 1.00  $\mu\text{mol gds}^{-1}$  in the mineral soil ( $p < 0.001$ ), possibly due to displacement of Ca by K on the exchange complex and subsequent leaching in the leaf litter and organic horizons. These data, disaggregated by planting status, are presented in Tables 1 and 2.

**Table 1: Unplanted mesocosms - soil chemical and biological properties by horizon. Means and standard errors (in parentheses) of 10 replicates. Bold indicates significant difference from control (Tukey's test,  $\alpha=0.0125$ ).**

	Unplanted Mesocosms			
	Control	Ca	Alk.	Ca x Alk.
<b><u>Organic Horizon</u></b>				
<i>Chemical Properties</i>				
Soil Moisture (% GWC)	49.9 (0.6)	49.4 (0.8)	<b>54.5 (0.9)</b>	52.1 (0.7)
Organic Matter (% LOI)	35.0 (1.2)	35.5 (0.6)	36.3 (0.8)	36.0 (0.9)
pH <sub>H2O</sub>	3.95 (0.27)	4.10 (0.18)	<b>4.77 (0.14)</b>	<b>4.80 (0.09)</b>
Exchangeable Ca ( $\mu\text{mol gds}^{-1}$ )	11.7 (1.06)	<b>18.1 (1.17)</b>	15.4 (1.10)	<b>21.2 (1.30)</b>
Exchangeable Al ( $\mu\text{mol gds}^{-1}$ )	8.71 (0.43)	9.14 (0.63)	<b>4.09 (0.64)</b>	<b>4.69 (0.76)</b>
Organic-bound Al ( $\mu\text{mol gds}^{-1}$ )	27.1 (2.32)	26.2 (2.55)	28.7 (2.36)	27.0 (2.64)
Total Dissolved Solids ( $\mu\text{g gds}^{-1}$ )	469 (24)	439 (30)	<b>739 (24)</b>	<b>618 (26)</b>
<i>Microbial Activity</i>				
Mic. Biomass (SIR) ( $\mu\text{g gds}^{-1} \text{d}^{-1}$ )	104.2 (6.7)	121.2 (11)	<b>139.2 (7.4)</b>	132.1 (7.1)
Enz. Activity Sum ( $\text{nmol gds}^{-1} \text{h}^{-1}$ )	266.6 (27)	297.8 (21)	318.1 (21)	329.3 (38)
<i>Soluble Carbon Quality</i>				
SUVA <sub>280</sub> ( $\text{m}^{-1}$ )	4.330 (0.041)	4.170 (0.048)	4.164 (0.028)	4.438 (0.200)
E2:E3	4.023 (0.019)	4.064 (0.022)	3.923 (0.025)	3.951 (0.038)
<b><u>Mineral Horizon</u></b>				
<i>Chemical Properties</i>				
Soil Moisture (% GWC)	39.2 (0.3)	38.5 (0.7)	40.9 (1.4)	38.2 (0.4)
Organic Matter (% LOI)	9.6 (0.61)	8.8 (0.23)	9.2 (0.01)	9.1 (0.08)
pH <sub>H2O</sub>	4.10 (0.20)	4.05 (0.06)	<b>4.55 (0.12)</b>	<b>4.61 (0.09)</b>
Exchangeable Ca ( $\mu\text{mol gds}^{-1}$ )	0.48 (0.02)	<b>0.98 (0.07)</b>	<b>0.79 (0.05)</b>	<b>64.0 (4.6)</b>
Exchangeable Al ( $\mu\text{mol gds}^{-1}$ )	16.1 (0.55)	17.7 (0.85)	16.0 (1.03)	15.5 (0.76)
Organic-bound Al ( $\mu\text{mol gds}^{-1}$ )	67.0 (4.86)	66.6 (5.20)	66.0 (4.96)	62.4 (6.81)
Total Dissolved Solids ( $\mu\text{g gds}^{-1}$ )	346 (23)	318 (23)	410 (27)	386 (23)
<i>Microbial Activity</i>				
Mic. Biomass (SIR) ( $\mu\text{g gds}^{-1} \text{d}^{-1}$ )	48.8 (1.8)	51.6 (1.2)	52.3 (2.2)	53.5 (1.2)
Enz. Activity Sum ( $\text{nmol gds}^{-1} \text{h}^{-1}$ )	161.5 (19)	144.9 (9.4)	161.9 (16)	165 (15)
<i>Soluble Carbon Quality</i>				
SUVA <sub>280</sub> ( $\text{m}^{-1}$ )	3.390 (0.083)	<b>3.085 (0.065)</b>	3.540 (0.085)	3.625 (0.063)
E2:E3	5.054 (0.081)	5.313 (0.08)	4.903 (0.076)	4.82 (0.056)

**Table 2: Planted mesocosms - soil chemical and biological properties by horizon. Means and standard errors (in parentheses) of 10 replicates. Bold indicates significant difference from control (Tukey's test,  $\alpha=0.0125$ ).**

	Planted Mesocosms			
	Control	Ca	Alk.	Ca x Alk.
<b><u>Organic Horizon</u></b>				
<i>Chemical Properties</i>				
Soil Moisture (% GWC)	55.1 (1.1)	54.7 (1.2)	56.1 (1.1)	<b>48.7 (2.4)</b>
Organic Matter (% LOI)	34.8 (1.5)	35.4 (0.6)	34.5 (0.4)	34.4 (1.1)
pH <sub>H2O</sub>	3.70 (0.20)	3.91 (0.10)	<b>4.51 (0.08)</b>	<b>4.36 (0.15)</b>
Exchangeable Ca ( $\mu\text{mol gds}^{-1}$ )	12.8 (0.91)	<b>18.0 (0.74)</b>	13.7 (0.79)	<b>19.4 (1.54)</b>
Exchangeable Al ( $\mu\text{mol gds}^{-1}$ )	15.1 (0.82)	11.8 (0.89)	<b>11.0 (0.98)</b>	<b>7.24 (0.80)</b>
Organic-bound Al ( $\mu\text{mol gds}^{-1}$ )	26.0 (2.60)	25.9 (2.33)	31.6 (3.71)	28.2 (2.58)
Total Dissolved Solids ( $\mu\text{g gds}^{-1}$ )	525 (36)	498 (24)	632 (42)	<b>661 (28)</b>
<i>Microbial Activity</i>				
Mic. Biomass (SIR) ( $\mu\text{g gds}^{-1} \text{d}^{-1}$ )	128.5 (9.7)	140.2 (6.9)	154 (13)	154.3 (8.3)
Enz. Activity Sum ( $\text{nmol gds}^{-1} \text{h}^{-1}$ )	376.8 (44)	368.4 (24)	365 (36)	330.7 (38)
<i>Soluble Carbon Quality</i>				
SUVA <sub>280</sub> ( $\text{m}^{-1}$ )	4.046 (0.056)	4.062 (0.062)	4.232 (0.084)	4.035 (0.110)
E2:E3	4.214 (0.031)	4.172 (0.030)	4.088 (0.040)	4.152 (0.033)
<b><u>Mineral Horizon</u></b>				
<i>Chemical Properties</i>				
Soil Moisture (% GWC)	38.3 (0.9)	37.2 (0.8)	37.7 (0.7)	36 (1.8)
Organic Matter (% LOI)	9.3 (0.21)	9.1 (0.06)	9.1 (0.13)	9.5 (0.44)
pH <sub>H2O</sub>	3.97 (0.19)	4.17 (0.07)	<b>5.01 (0.08)</b>	<b>4.92 (0.06)</b>
Exchangeable Ca ( $\mu\text{mol gds}^{-1}$ )	0.68 (0.05)	<b>1.03 (0.05)</b>	<b>1.07 (0.07)</b>	<b>1.63 (0.16)</b>
Exchangeable Al ( $\mu\text{mol gds}^{-1}$ )	18.3 (0.76)	16.2 (0.58)	<b>13.9 (0.63)</b>	<b>14.6 (0.69)</b>
Organic-bound Al ( $\mu\text{mol gds}^{-1}$ )	63.1 (4.36)	67.4 (5.00)	69.1 (5.35)	66.8 (5.04)
Total Dissolved Solids ( $\mu\text{g gds}^{-1}$ )	301 (27)	282 (21)	326 (23)	325 (22)
<i>Microbial Activity</i>				
Mic. Biomass (SIR) ( $\mu\text{g gds}^{-1} \text{d}^{-1}$ )	56.9 (2.9)	57 (1.3)	58.6 (3.1)	57.5 (1.7)
Enz. Activity Sum ( $\text{nmol gds}^{-1} \text{h}^{-1}$ )	155 (21)	139.9 (11)	144.4 (12)	163.3 (17)
<i>Soluble Carbon Quality</i>				
SUVA <sub>280</sub> ( $\text{m}^{-1}$ )	2.977 (0.049)	2.972 (0.047)	<b>3.587 (0.066)</b>	<b>3.439 (0.061)</b>
E2:E3	5.561 (0.053)	5.541 (0.055)	<b>4.943 (0.05)</b>	<b>5.026 (0.046)</b>

The alkalinity treatment decreased exchangeable Al in the organic horizon soils of the planted mesocosms from a mean of 15.2 to 10.9  $\mu\text{mol gds}^{-1}$  ( $p = 0.003$ ) and from 8.67 to 4.13  $\mu\text{mol gds}^{-1}$  in the unplanted mesocosms ( $p < 0.001$ ). In the organic horizon of the planted mesocosms, the Ca treatment also decreased exchangeable Al from 15.2 to 11.5  $\mu\text{mol gds}^{-1}$  ( $p < 0.001$ ) but no effect of the Ca treatment was observed in the planted mesocosms. In the planted mesocosms, the alkalinity treatment decreased mineral horizon exchangeable Al from a mean of 17.6 to 14.6  $\mu\text{mol gds}^{-1}$  ( $p < 0.001$ ), but there was no effect of the alkalinity treatment on exchangeable Al in the unplanted mineral horizon soils. There was no effect of the Ca treatment on mineral horizon exchangeable Al in either planted or unplanted mesocosms. Organic-bound Al was not significantly affected by any treatment in either horizon (Table 1, Table 2). Soil solution ionic strength was modestly elevated by the alkalinity treatment in organic horizon soils, but otherwise there was no effect of the treatments on ionic strength (Table 1, Table 2).

### **2.3.2 SOC dynamics in unplanted mesocosms**

In the unplanted mesocosms, both soil amendments altered SOC solubility but neither altered microbial activity. The Ca treatment reduced WEOC concentrations by 19% ( $p = 0.003$ ) and 43% ( $p < 0.001$ ) in the organic and mineral horizons, respectively. The alkalinity treatment decreased WEOC in organic horizon soils by 17% ( $p=0.011$ ) but had no effect on WEOC in mineral soils (Figure 1). Neither treatment significantly impacted the metrics of WEOC quality that we examined (Table 1). There was no

significant effect of either soil amendment on short-term or long-term soil respiration potential (Figure 2 a,b, left panes) or exoenzyme activity potential (Table 1 and Appendix A: Table 4). The alkalinity treatment increased microbial biomass by 20% in organic horizon soils ( $p = 0.008$ ), but no other treatment effects on microbial biomass were observed.

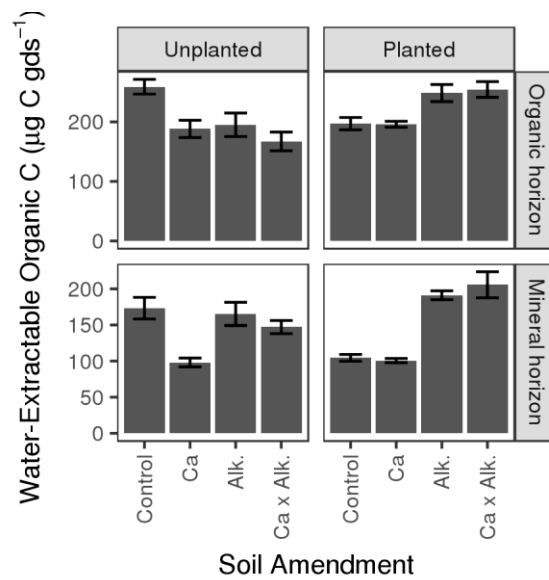


**Figure 1: Water-extractable organic carbon. The left column shows data for unplanted mesocosms, and the right column planted. Error bars are +/- 1 standard error.**

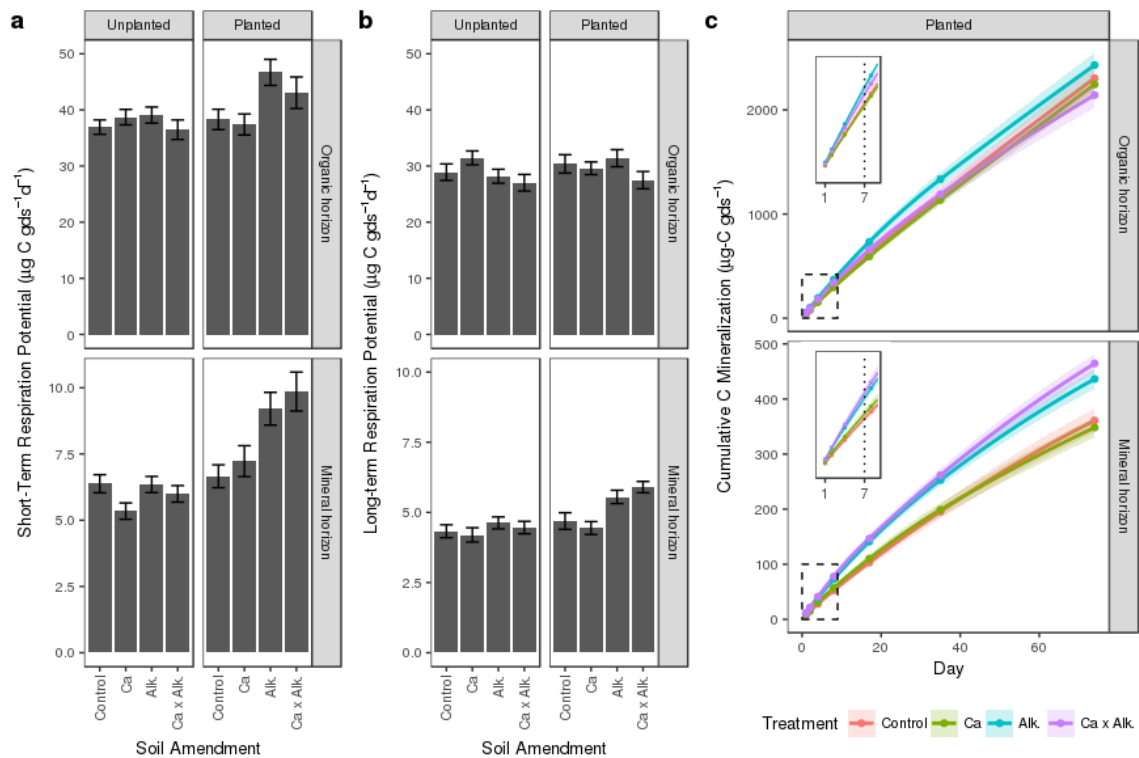


**Figure 2: Soil respiration potential. (a) Mean short-term (days 1-7) respiration potential. Error bars are  $\pm 1$  SE. (b) Mean long-term respiration potential (days 8-74). Error bars are  $\pm 1$  SE. (c) Cumulative 74-day soil respiration. Days that measurements were performed are indicated with points. Envelopes are  $\pm 1$  SE. (inset) Detail view of cumulative respiration on days 1-8. The dotted line indicates the end of the short-term respiration measurement period on day 7.**

### 2.3.3 Plant responses to soil amendments

The Ca treatment increased the relative growth rate of saplings by 22% ( $p=0.022$ , Figure 3 a), but the alkalinity treatment had no significant effect on sapling growth. Despite this Ca treatment effect on plant growth, we measured no significant differences in fine root biomass across the treatments (Figure 3 b). Mean fine root density among all mesocosms was  $324 \text{ g m}^{-3}$ , considerably lower than the mean root density ( $1519 \text{ g m}^{-3}$ )

reported for the forests from which these soils were collected (Fahey and Hughes 1994). There were no effects of any treatment the plant morphological traits that we examined (Appendix A: Table 3).

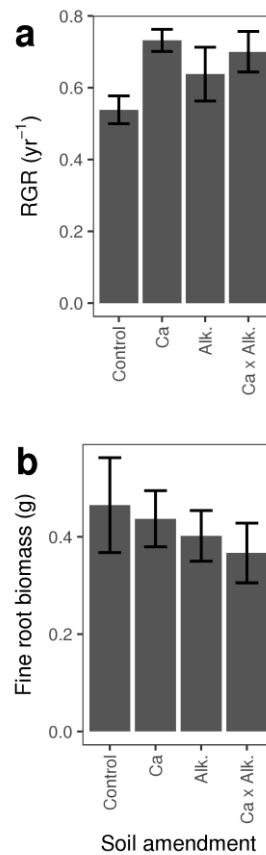


**Figure 3: Soil amendment effects on sugar maple sapling growth. Error bars are  $\pm 1$  SE. (a) Annual relative growth rate. (b) Total fine root (< 2mm diameter) biomass.**

### 2.3.4 SOC dynamics in planted mesocosms

In the planted mesocosms, the alkalinity treatment significantly increased SOC solubility and microbial respiration, but there was no effect of the Ca treatment. The alkalinity treatment increased WEOC concentrations by 28% in the organic horizon ( $p = 0.002$ ) and 93% in the mineral horizon ( $p < 0.001$ ) (Figure 1). In the mineral horizon, the

increased concentration of WEOC was accompanied by increased molecular weight (alkalinity effect on E2:E3 ratio = -0.566,  $p < 0.001$ ) and increased aromaticity (alkalinity effect on  $SUVA_{280} = 0.538$ ,  $p < 0.001$ ) of the WEOC (Table 2). The alkalinity treatment increased short term (day 1 to 7) respiration relative to the control by 18.5% ( $p = 0.003$ ) in the organic horizon and 37.2% ( $p < 0.001$ ) in the mineral horizon (Figure 2 a,c, right panes). These increases in respiration were not accompanied by increases in microbial biomass or exoenzyme activity potential (Table 2). The alkalinity effect on microbial respiration did not continue throughout the course of the long-term soil incubations (Figure 3 b,c). In the organic horizon, alkalinity had a significant positive effect on respiration potential through the day 8 measurement ( $p = 0.013$ ), but not on any subsequent measurement date. We observed a similar trend in the mineral soil horizon, where we observed a significant increase in respiration in the alkalinity treatments through day 16 ( $p = 0.001$ ), after which these treatments were indistinguishable from the control.

## **2.4 Discussion**

This experiment provides evidence that acid rain recovery may lead to shifts in both the amount and the distribution of ecosystem carbon stocks. The magnitude and direction of this change is uncertain, as it may depend on the balance between enhanced forest growth in response to rising soil Ca and enhanced soil organic matter turnover in response to rising soil pH. In our experiment, plant growth was only stimulated by Ca

amendment, while microbial respiration was only stimulated by increases in soil alkalinity. The effects of both soil amendments were entirely dependent on the presence of plants, as effects of the alkalinity treatment on microbial respiration only observed in the planted mesocosms.

We found that Ca fertilization increased growth of sugar maple saplings. This suggests that alleviation of Ca limitation can account for the enhanced aboveground productivity of sugar maple and increased sugar maple sapling recruitment previously observed in field acid remediation experiments (Battles et al. 2014; Juice et al. 2006). Since our pH treatment did not affect plant growth, our results do not support the alternative hypothesis, posed by Juice et al. (2006), that elevated soil pH, resulting in lower Al stress, may drive enhanced productivity in sugar maples in these soils. We also found that fine root biomass and morphological root traits were not significantly affected by any of the soil amendments. This is in contrast to Fahey et al. (2016), who showed that the watershed acid remediation experiment at HBEF significantly reduced fine root biomass in the treatment watershed, suggesting a reallocation of C from belowground to aboveground production. In our experiment, Ca amendment therefore increased maple sapling growth, but did not alter patterns of C allocation or root structure.

Our data show that plants play a key role in mediating the response of soil microbial activity. We predicted that the alkalinity treatment would increase microbial

respiration in both the planted and unplanted mesocosms, but we only observed this effect in the planted mesocosms. Moreover, the increase in respiration was transient following the removal of roots from the soil, suggesting that plants are substantially mediating the effect of increased soil pH on microbial activity. The rhizosphere is widely recognized as an important hotspot of SOC cycling (Finzi et al. 2015), but the alkalinity mesocosms did not have higher (total or fine) root mass. The observed increase in short-term respiration potential therefore was not simply due to a greater proliferation of roots, and thus a greater proportion of rhizosphere soil in our samples. Enhanced exoenzyme production by mycorrhizae and free-living microbes cannot account for the increased respiration either; our analysis of exoenzyme activity showed no differences between treatments, and furthermore arbuscular mycorrhizal trees such as sugar maples are not thought to invest heavily in exoenzyme production (Phillips et al. 2013). The exact mechanism by which plants mediated the response of microbial activity to the alkalinity treatment thus remains unresolved.

It is possible that the respiration response to the alkalinity treatment in planted mesocosms could be due to an increase in inputs of recent photosynthate to the soil as rhizosphere carbon flux (RCF, i.e. root exudation, mycorrhizal allocation, and rhizodeposition), with these increased inputs stimulating decomposition of extant pools of SOC. It is implausible though that the microbial respiration of RCF alone could account for the observed increases in microbial respiration. The cumulative increase in

respiration observed over seven days in the planted alkalinity treatments over is greater than a quarter of the total annual RCF for maple saplings estimated by Phillips and Fahey (2005), when scaled to the mean biomass of our saplings. Further, a large amount of RCF is used in the production of mycorrhizal biomass that is resistant to decomposition (Olsson and Johnson 2005), and so would not be immediately respired following the removal of plant roots. Therefore, we conclude that respiration of increased RCF likely could only account for a portion of the increased respiration in alkalinity-treated planted soils, and that the majority of the increase was due to respiration of extant SOC pools.

Our data are consistent with the hypothesis that the alkalinity treatment makes extant SOC stocks more susceptible to decomposition, but that the respiration of this SOC is only possible with the addition of labile RCF inputs from plant roots causing a priming effect (Fontaine et al. 2007). This would explain why the respiration response in the planted mesocosms was transient, as well as why the unplanted mesocosms showed no respiration response to the alkalinity treatment. This is also consistent with data from our preliminary experiment (Appendix A) that showed higher rates of microbial respiration in soils that had been recently excavated from pedons containing substantially higher root densities than in the mesocosms. Further work examining the role of RCF in controlling soil responses to recovery from acid precipitation is

warranted. Overall, our data suggest that plant-mediated microbial decomposition may drive losses of SOC as forest ecosystems recover from acid deposition.

We did not find any evidence that microbial activity in the control soils was directly constrained by low pH or Ca fertility. We had hypothesized that alleviation of Al stress caused by increasing soil pH could increase microbial activity. Although the alkalinity treatment did decrease levels of exchangeable Al, this was not accompanied by a consistent response in soil microbial respiration. Overall, the changes in exchangeable Al pools were relatively minor. We found no evidence of Ca limitation of microbial activity, as the Ca treatment had no impact on microbial respiration or biomass.

Consistent with theory and laboratory experiments, we hypothesized that the alkalinity treatment would increase C solubility and the Ca treatment would decrease solubility, potentially driving SOC bioavailability and respiration. We observed the predicted effect of the alkalinity treatment in the planted mesocosms but not the unplanted mesocosms, and we observed the predicted effect of the Ca treatment in the unplanted mesocosms but not the planted mesocosms. These contrasting results show that the controls on SOC solubility that pertain here are more complicated than straightforward geochemical controls. WEOC is often considered to represent a microbially-available fraction of SOC (Boyer and Groffman 1996), but experiment-wide there was only very weak correlation between respiration and WEOC (Appendix A:

Figure S3), showing that in this experiment WEOC and respired carbon likely represent distinct pools of SOC. In the case of the planted mesocosms, the increase in mineral horizon WEOC corresponded with a significant increase in the molecular weight and aromaticity of the WEOC, making the mineral horizon WEOC more closely resemble the quality of organic horizon WEOC. We speculate that leaching of SOC from the organic horizon in planted pots accounts for the large increase in WEOC in the mineral horizon, accounting for the change in molecular characteristics, but why this effect was only observed in the planted mesocosms is unclear. Any changes in SOC solubility were not due to changes in the complexation of SOC with Al, as there was no-effect of any treatment on organic-bound Al. The divergent responses of SOC solubility between the planted and unplanted mesocosms remain difficult to interpret and suggest that controls on SOC solubility are more complicated than we initially hypothesized.

One of the motivations of this study was to understand the mechanisms by which the watershed acid remediation treatment at HBEF, which both increased soil pH and Ca fertility, impacted SOC dynamics, leading to a 35% decline in SOC stocks. Using the ecosystem C budget prepared by Fahey et al. (1995) for the reference watershed at HBEF, we calculated whether the increases in respiration observed in the alkalinity treatment, when scaled to the respiratory terms of the C budget, could account for the decline in SOC stocks, assuming all other budget compartments were at steady state. We found that the increases in respiration rates would only account an 11% decline in SOM

stocks, not the observed 35% decline, although this itself would represent a loss of over 1 Mg C ha<sup>-1</sup>.

The soil amendments performed in these experiments were intended to simulate a realistic level of ecosystem recovery from acid precipitation (albeit over a much shorter time period.) In the organic horizon soils, the changes in soil pH and Ca fertility caused by the soil amendments are at the high end of the range of shifts observed to have occurred naturally over the last 24 years at other sites across the northeastern U.S. (Lawrence et al. 2015). As natural recovery of soil pH and cationic fertility in mineral soils has not yet been observed in the field, it remains an open question whether the mineral horizon amendments represent a realistic possible future ecosystem state. We do acknowledge that these soil amendments change soil pH and Ca status in an artificial way, but care was taken to account for potential experimental artifacts. The potassium chloride control treatment allowed us to disentangle the effect of potassium fertilization from the pH effect of the potassium hydroxide addition, and the freely-draining mesocosms allowed added chloride in the Ca treatment to leach, resulting in only minimal differences in soil solution ionic strength by the time the experiment concluded.

We found that, in simulated forest soil recovery from acid precipitation, increases in soil pH caused a marked increase soil respiration and SOC solubility, and enhanced Ca fertility drove increases in primary productivity. These changes to soil C stocks are concerning, as they may represent a substantial net source of C to the

atmosphere. Plants were shown to play a central role in promoting respiration and SOC solubility, as the treatment effect of increased soil pH was only observed in the planted mesocosms. The mechanisms underpinning plant mediation of these SOC dynamics remain obscure, but this work suggests the need for continued work on microbial priming and rhizosphere C fluxes in the context of acid precipitation research.

## **3. Ecosystem recovery from acid precipitation drives enhanced soil nitrogen cycling**

### ***3.1 Introduction***

Soil acidity modifies the bioavailability of organic matter and determines both the structure and activity of soil microbial communities, thus playing a central role in mediating coupled soil carbon (C) and nitrogen (N) dynamics (Schmidt et al. 2011, Coughlan et al. 2000, Rousk et al. 2009, Illmer et al. 2003). Despite the importance of acidity as a master driver of soil biogeochemical cycling, the impacts of rapid changes (i.e. over decades to centuries) in soil acidity are seldom considered in long-term projections of ecosystem dynamics. This is a critical knowledge gap, because while soil acidity is generally stable over intermediate timescales (Slessarev et al. 2016), anthropogenic acid deposition (hereafter referred to as 'acid rain') has caused severe soil acidification over the past century (Likens et al. 1996). Following this acidification, clean air regulations have resulted in substantial reductions in soil acidity in the developed world over the course of a few decades (Kirk et al. 2010, Lawrence et al. 2012, Lawrence et al. 2015). These rapid decreases in soil acidity have been linked to declines in soil organic matter (Oulehle et al. 2011, Lawrence et al. 2012) and increased hydrologic export of DOC (Monteith et al. 2007, Erlandsson et al. 2011) across eastern North America and western Europe. Although there are many mechanisms by which soil acidity may alter soil C and N cycling, process-based biogeochemical models (e.g. DayCent, CLM-CN, Biome-BGC) generally do not explicitly include any links between

soil acidity and C and N process rates (Thornton 2005, Parton et al. 1998, Oleson et al. 2013). Understanding long-term trajectories of ecosystem recovery from acid rain, and their implications for global C and N stocks, will require a more thorough understanding of how rapid anthropogenic changes in soil acidity affect ecosystem C and N storage, cycling, and loss.

There are a variety of mechanisms through which soil deacidification is likely to impact ecosystem structure and function. Several dominant tree species have proven very sensitive to soil acidification, and their declines with acidification may be reversed as ecosystems recover. In eastern North America, the depletion of soil calcium throughout acid rain impacted regions has been linked to declines in sugar maples (*Acer saccharum*) and red spruce (*Picea rubra*) (Joslin et al. 1992, Sullivan et al. 2013). It has been proposed that the decline in sugar maples may lead to substantial changes in soil biogeochemical processes, since sugar maple litter is far more labile than the majority of other tree species throughout their range (Lovett et al. 2002, Hobbie et al. 2007).

These changes in aboveground litter quality due to vegetation shifts have been accompanied by direct effects of soil acidification on belowground biogeochemical cycling. Acidification may result in greater stabilization of soil organic matter (SOM) through changes in SOM structure, association with mineral surfaces, and complexation with aluminum (Al) (Clarholm and Skjellberg 2013), which may reduce carbon and nitrogen mineralization. High soil acidity has been shown to inhibit soil microbial

activity (Illmer et al. 2003, Wolters and Schaffer 1994, Niemi and Vepsäläinen 2005) and to alter the abundance and composition of microbial guilds responsible for key pathways in soil N cycling (Simek and Cooper 2002, Liu et al. 2010, Stempfhuber et al. 2015). Nitrification in particular is known to be sensitive to high soil acidity (Mueller et al. 2012, Li et al. 2018, but see Venterera et al. 2004), and nitrification is a key pathway by which N is mobilized in water and lost from ecosystems (Likens et al. 1969). Finally, soil acidification can decrease soil faunal activity and associated decomposition of SOM (Reich et al. 2005, Geissen and Brummer 1999). Though the effects of soil acidity on above- and belowground C and N cycling are myriad and complex, nearly all pathways suggest the potential for reduced C and N turnover in acidified soils, but these changes may be highly non-linear and subject to threshold effects (Rousk et al. 2009). Thus, as ecosystems recover from acid rain, it remains an open question the extent to which C and N cycling and loss will accelerate as soils become less acidic.

A watershed acid mitigation experiment, performed at Hubbard Brook Experimental Forest (HBEF), induced profound changes in watershed C and N cycling that may foreshadow changes that will occur as forest ecosystems gradually recover from acid rain over the coming decades (Johnson et al. 2014, Rosi-Marshall et al. 2016). In this experiment, a watershed was treated with calcium silicate to elevate soil Ca and pH. In the decade following the treatment, sugar maple biomass and litterfall increased (Battles et al. 2014) but this increase in aboveground biomass C and N was dwarfed by

contemporaneous declines in surficial soil C and N stocks (Johnson et al. 2014). Both foliar and leaf litter N concentrations increased substantially (Lovett et al. 2016, Juice et al. 2006). While these shifts in aboveground and belowground C and N pools occurred within the first several years of treatment, soil solution N fluxes and whole watershed N exports did not increase substantially until 2008, nine years after treatment (Driscoll 2016, Rosi-Marshall et al. 2016). By 2013, watershed N export was thirty times higher than the reference watershed (Rosi-Marshall et al. 2016). Such a dramatic increase in watershed N exports must be the result of altered soil N cycling rates, yet early in the experiment (2000-2002), Groffman et al. (2006) measured no significant treatment effects on gross or net N cycling in the Ca-enriched watershed. Routine summer measurements of net N mineralization and nitrification, which continued into the period of high watershed N export, have similarly showed no response to the watershed treatment (Groffman 2013). Thus, the source of this increased N export and the drivers responsible for its liberation remain unresolved.

Here, we addressed two (non-exclusive) hypotheses that may reconcile the observations that watershed N loss has increased substantially while net N cycling rates remain unchanged. First, we hypothesized that although the treatment enhanced rates of microbial N mineralization, this effect was counterbalanced by enhanced biotic demand for N. If both enhanced mineralization and immobilization result from this acid mitigation experiment, this would result in an accelerated N cycle without any change in

net process rates. A faster N cycle could lead to higher watershed N exports, though, if hydrologic flushing regularly exports N from this high-turnover pool of inorganic N. Second, we hypothesized that Ca enrichment disproportionately affected N cycling in the early spring, when microbial processes dominate the N cycle and plant demand for N is negligible. The majority of annual watershed N export at Hubbard Brook occurs during the spring months (Bernhardt et al. 2005), and previous work has shown that N mineralization and nitrification during the non-growing season accounts for this high export (Pardo et al. 2004, Judd et al. 2005). We examined these hypotheses by measuring both gross and net nitrogen mineralization and nitrification rates during both spring and summer sampling campaigns.

## **3.2 Methods**

### **3.2.1 Site description**

Hubbard Brook Experimental Forest (*White Mountains NF, New Hampshire, USA*) is primarily a mixed hardwood forest composed of American beech (*Fagus grandiflora*), sugar maple (*Acer saccharum*), and yellow birch (*Betula allegheniensis*), with some conifers at higher elevations. Soils are well-drained podzols formed on unsorted glacial till parent material, with a mean depth to bedrock of ~2 m (Johnson et al. 2014). The topography is steep, with the study area having a mean slope of 17° and an elevation between 400 and 800 m (Groffman et al. 2006). The landscape at HBEF is defined by pit-and-mound microtopography caused by tree wind throws. These

depressional pits have been shown elsewhere to play an important role in seedling recruitment, greenhouse gas fluxes, pedogenesis, and hydrologic routing (Schaetzl et al. 1988, Veneman et al. 1984, Phillips et al. 2017, Kooch et al. 2015, Valtera and Schaetzl 2017).

The study was conducted in two small watersheds within HBEF in a paired watershed experimental design. In October 1999, one watershed (Ca-enriched watershed) was treated with powdered, pelletized wollastonite ( $\text{CaSiO}_3$ ) with the goal of replacing soil Ca lost due to anthropogenic acid deposition. The other watershed, located immediately to the west of the long-term biogeochemical reference watershed at HBEF, was maintained as a control (reference watershed). In the Ca-enriched watershed, base saturation of the soil increased from 10% pre-treatment to 19% post-treatment in mineral soil horizons, and the treatment had a complex but overall positive effect on soil pH, which is explored more fully by Johnson et al. (2014).

### **3.2.2 Soil collection**

Soil collection sites were established at six sites within the hardwood vegetation zones of each watershed. In the Ca-enriched watershed, sites were selected immediately downslope of lysimeters which were installed in random locations throughout the watershed as part of a long-term monitoring program (Cho et al. 2010). In the reference watershed, sites were selected randomly using ArcGIS. Because of the potential importance of pit and mound microtopography in driving biogeochemical processes, we

explicitly sampled across this gradient, establishing at each site two plots that spanned the range of pit-and-mound microtopography. One plot was established in a depressional area believed to be a relict pit from an old tree throw, and the other was established on an adjacent convex area thought to be a relict mound. Fresh pits and mounds (those with still-visible root masses) were not sampled. Thus, each watershed contained a total of twelve sampling plots, six in depressional landforms and six in convex landforms.

Soils were sampled on two occasions within each plot, during the peak growing season in early August 2015 (summer) and after snowmelt but before leaf-out in late March 2016 (spring). The former sampling time corresponds to the time period of lowest N flux from watersheds at HBEF, and the latter corresponds to the period of high N flux, a seasonal pattern that has been attributed to the relative demand of vegetation for N (Likens 2013). On both occasions, sampling occurred 2 - 3 days after a rain storm, and soils were at or near field capacity. Soils were collected, bulked by horizon (Oie, Oa, and 0-10 cm mineral soil), and homogenized using the methods that Groffman (2013) employed for long-term soil monitoring at HBEF. Soils used for microbial process rate measurements were stored at 4°C until analysis, which occurred within ten days of sample collection. A subsample of each soil was air-dried and stored for later analysis of soil pH and exchangeable cations.

### 3.2.3 Laboratory analysis

The water content of both field-moist and air-dry soils was determined by gravimetric moisture loss after drying at 60 °C for 48 h in a drying oven. Soil organic matter (SOM) content was determined by mass lost on ignition at 550 °C for 4h in a muffle furnace. Soil pH was measured potentiometrically in a 2:1 water : soil slurry using a Mettler-Toledo DL-18 probe. Exchangeable base cations were extracted from 5g of air-dry soil using 50 ml of 1M ammonium acetate buffered to pH 7. These slurries were rotated at 60 rpm on an end-over shaker for 24h, then vacuum filtered through a Gelman A/E glass fiber filter (1.0 µm nominal pore size). All samples were analyzed for exchangeable Ca on a Perkin Elmer 3100 Flame AA spectrometer, and the spring 2016 samples were further analyzed for K, Mg, and Na. For spring 2016 samples, exchangeable acidity and aluminum (Al) was extracted from 10g of field moist soil (5g for Oie horizon soil) using 50 ml of 2 M potassium chloride, shaken at 120 rpm for 1 h on a shaker table, and gravity filtered through a pre-rinsed Whatman 42 filter (2.5 µm nominal pore size). Exchangeable acidity and exchangeable Al were determined titrimetrically following the method in Abreu et al. (2003), using a Mettler-Toledo DL-18 autotitrator. Cation exchange capacity and base saturation were calculated by summation (Robertson et al. 1999).

Soil ammonium (NH<sub>4</sub><sup>+</sup>) and nitrate (NO<sub>3</sub><sup>-</sup>) pool sizes were determined by extraction of 10g of field moist soil (5g for Oie horizon soil) using 50 ml of 2 M

potassium chloride, shaken at 120 rpm for 1 h on a shaker table and gravity filtered through a pre-rinsed Whatman 42 filter. These extracts were analyzed colorometrically on a Lachat QuikChem flow injection analyzer. To measure potential C mineralization, net N mineralization, and net nitrification, we performed short-term laboratory soil incubations. Field moist soil (10 g for Oa and mineral horizon soils, 5 g for Oie horizon soil) was incubated in the dark for 10 d at 20 °C in a 976 ml glass jar fitted with a butyl rubber septum. After the incubation, headspace gas was sampled with a 1 ml gas syringe. This gas sample was immediately analyzed for CO<sub>2</sub> concentration using a Li-Cor LI-6200 IRGA in a flow injection configuration. C mineralization potential on a basis of per gram of dry soil per day was calculated from accumulation of headspace CO<sub>2</sub> over the course of the incubation. After headspace gas analysis, the samples were analyzed for NH<sub>4</sub><sup>+</sup> and NO<sub>3</sub><sup>-</sup> following the same procedure outlined above. Net N mineralization was calculated as the net increase of NH<sub>4</sub><sup>+</sup>-N and NO<sub>3</sub><sup>-</sup>-N over the course of the incubation, and net nitrification as the net increase of NO<sub>3</sub><sup>-</sup>-N only, each expressed on a per gram of dry soil per day basis. Microbial biomass was measured by the chloroform fumigation-incubation method (Jenkinson and Powlson 1976), with CO<sub>2</sub> production measured in the same manner as in the C mineralization assays.

For the spring 2016 sampling date, we used a laboratory isotopic pool dilution approach to measure potential gross N mineralization, nitrification, and N immobilization, slightly modifying the protocol used by Groffman et al. (2006). Four

replicate 10 g subsamples of each soil (5 g for Oie horizon soil) were weighed into specimen cups and pre-incubated for 12h. Two of these subsamples were then amended with 45  $\mu\text{g}$  of 99 atom %  $^{15}\text{N}$  as  $^{15}\text{NH}_4\text{Cl}$  for measurement of gross N mineralization, and two subsamples were amended with 45  $\mu\text{g}$   $^{15}\text{N}$  as  $\text{K}^{15}\text{NO}_3$  for measurement of gross nitrification. The amendments were dissolved in 1 ml of water that was sprayed slowly onto the soil through a 28 ga. needle, while constantly tumbling the sample to homogenize the application. In order to determine initial pool sizes and isotopic compositions of the soil inorganic N pools, we extracted inorganic N from one of the  $^{15}\text{NH}_4^+$ -amended samples and one of the  $^{15}\text{NO}_3^-$ -amended samples within fifteen to thirty minutes after the labeled N amendment, using the KCl extraction procedure described above. The remaining samples were incubated for 3 d at 20  $^\circ\text{C}$  in the dark and then extracted following the same protocol.  $\text{NH}_4^+$  and  $\text{NO}_3^-$  concentrations were determined by colorometric analysis on a Lachat QuikChem flow injection analyzer. Samples were prepared for isotopic analysis using a diffusion/acid trap method similar to Sorensen and Jensen (1991). The isotopic composition of the samples was measured by EA-IRMS at the Stable Isotope Facility at UC-Davis. Gross process rates were calculated from initial and final pool sizes and isotopic compositions using the equations in Hart et al. (1994).

### 3.2.4 Statistical analysis

All statistical analyses were performed in R v. 3.2.3 (R Core Team, 2017). To test for differences between watersheds for parameters of interest, we performed blocked one-way ANOVA analyses, with topographic position included as a blocking factor. The blocking factor was significant for only 3 out of 69 statistical comparisons performed, below the expected 5% false discovery rate under the null hypothesis of no difference between blocking factor levels, but the blocking factor was nonetheless retained in all models. We analyzed each season and each soil horizon separately. We also fit linear models to test for correlations between soil geochemical properties (pH, base saturation, exchangeable Ca, exchangeable Al) and soil microbial processes. To examine whole-profile soil inorganic N pools, we scaled soil concentration measurements by the mean soil horizon masses reported for each watershed (Johnson and Hamburg 2015, Johnson et al. 2014). We report statistically significant results at  $\alpha = 0.10$ .

To contextualize our findings regarding soil N process rates, we prepared a N budget “snapshot” for the leaf litter horizon (Oie) during the spring sampling campaign. To estimate field N process rates at springtime soil temperatures, we scaled our potential rate measurements obtained at 20 °C to expected rates at 5 °C, based on a  $Q_{10}$  of 2.5, a value reported for organic horizon podzols in Katterer et al. (1999). The organic N pool size in the Oie horizon for the Ca-enriched watershed was taken from Johnson et al. (2014), and the pool size in the reference watershed was computed from soil horizon

mass and % C data from Johnson and Hamburg (2015), assuming the same C:N ratio as in the Ca-enriched watershed. Leaf litter inputs were calculated using leaf litter mass data from Fahey (2016) and litter chemistry data from Lovett et al. (2016). Root litter inputs were estimated from fine root mass data from Fahey et al. (2016), root turnover rates estimated from Tierney and Fahey (2002) and root N concentration data from Fahey et al. (1994). Microbial biomass N was computed with data from Groffman (2013) and Johnson et al. (2014). N deposition estimates were taken from Rosi-Marshall et al. (2016).

### **3.3 Results**

Seventeen years after the initial treatment, soil acid-base status was strongly impacted by  $\text{CaSiO}_3$  treatment in the organic soil horizons, with a more muted response in the mineral soil (Figure 4). Topographic position and season had no significant effect on these soil properties. In the Ca-enriched watershed, soil pH was 0.26 units higher in the Oie horizon ( $p < 0.001$ ) and 0.15 units higher in the Oa horizon ( $p = 0.006$ ), compared to the reference watershed. In the mineral soil, we did not detect a significant difference in soil pH. Exchangeable Al was 86% lower in the Oie horizon ( $p = 0.033$ ) and 38% lower in the Oa horizon ( $p = 0.030$ ) but was not significantly different in the mineral soil. Exchangeable Ca was 2.2-fold higher in the Oie Horizon ( $p < 0.001$ ), 5.6-fold higher in the Oa horizon ( $p < 0.001$ ), and 5.7-fold higher in the mineral horizon ( $p < 0.001$ ). Base saturation was significantly higher in the Ca-enriched watershed in all horizons; in the

Oie horizon, mean base saturation was 89.8% in the Ca-enriched watershed versus 77.8% in the reference watershed ( $p = 0.013$ ), 56.3% versus 20.7% in the Oa horizon ( $p < 0.001$ ) and 18.4% versus 9.0% in the mineral soil ( $p < 0.001$ ).

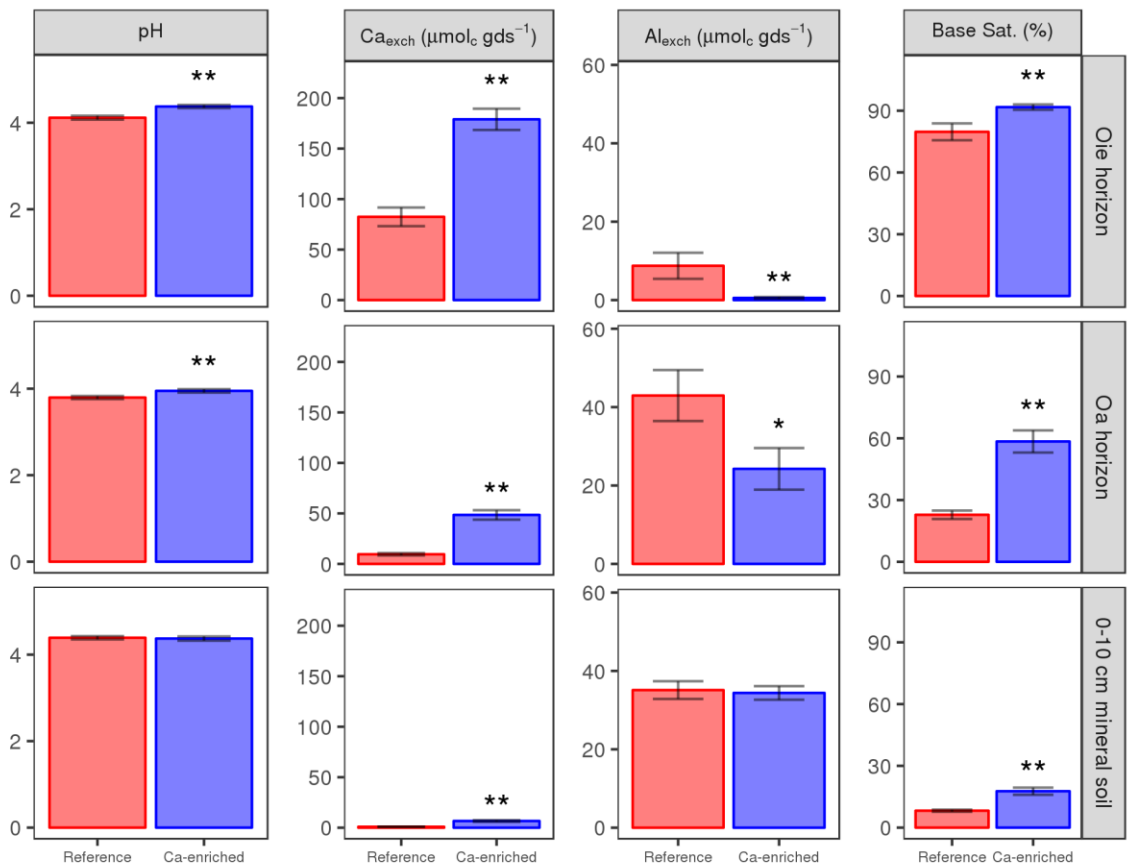


**Figure 4: Soil acid-base properties. Means and standard errors are displayed. Asterisks indicate a significant difference between the Ca-enriched watershed and the reference watershed (\*  $p < 0.10$ , \*\*  $p < 0.05$ ). Soil pH and exchangeable Ca data are aggregated from spring and summer sampling dates. Exchangeable Al and base saturation are data from the spring sampling date only.**

For both sampling dates, soil inorganic N concentrations were generally higher in the Ca-enriched watershed than in the reference watershed during both sampling periods (Figure 5). In absolute terms, the greatest differences in inorganic N

concentrations between watersheds were observed in the Oie horizon, as this horizon contained, on average, 3.5 times the total inorganic N (TIN) of the Oa horizon and 12.0 times the TIN of the mineral horizon. When N concentrations in each horizon (Figure 5) were scaled to the mass of each horizon to estimate whole-profile inorganic N pools on an areal basis,  $\text{NH}_4^+$ ,  $\text{NO}_3^-$ , and TIN pools were all significantly higher in the Ca-enriched watershed for both sampling dates (Figure 6). In the Ca-enriched watershed, whole-profile  $\text{NH}_4^+$  pools were 2.5 times larger than the reference watershed during the summer ( $p < 0.001$ ), and 2.4 times larger in the spring ( $p < 0.001$ );  $\text{NO}_3^-$  pools were 1.4 times larger during the summer ( $p = 0.041$ ) and 4.1 times larger in the spring ( $p < 0.001$ ). Summing these two pools, the TIN pool was 1.8 times larger in the Ca-enriched watershed in the summer ( $p < 0.001$ ) and 2.6 times larger in the spring ( $p < 0.001$ ).

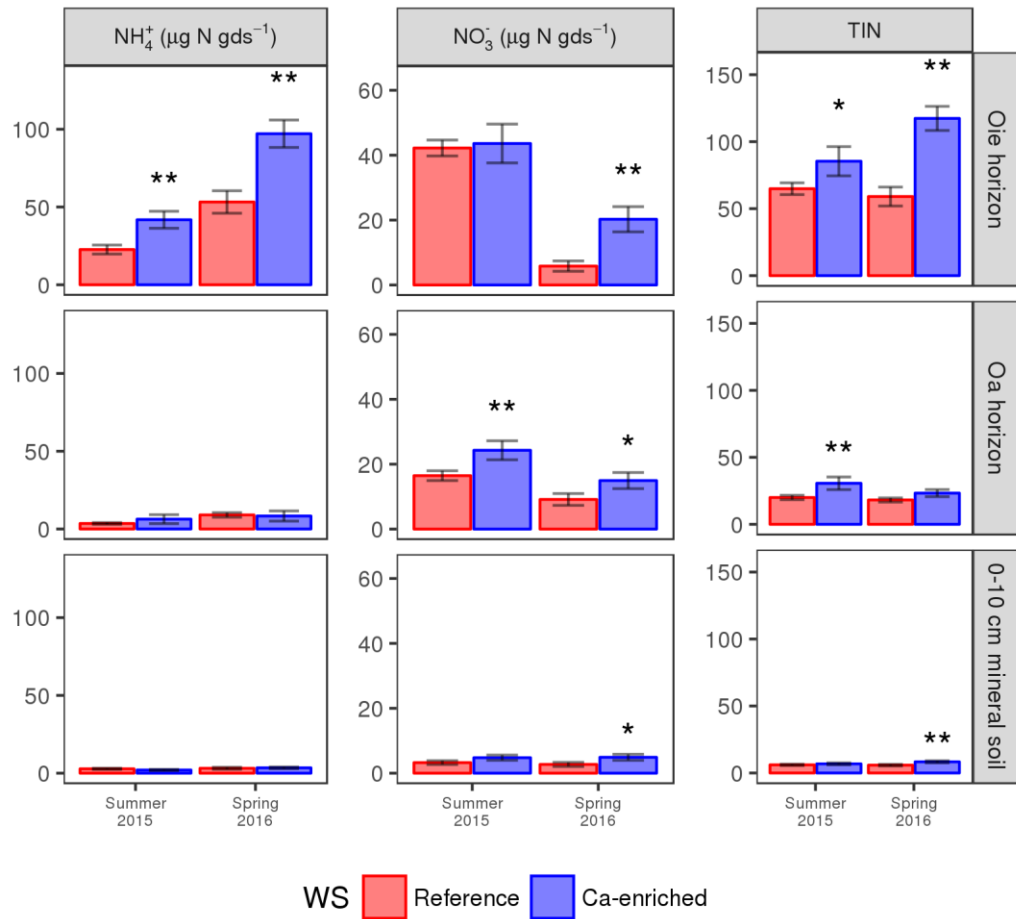
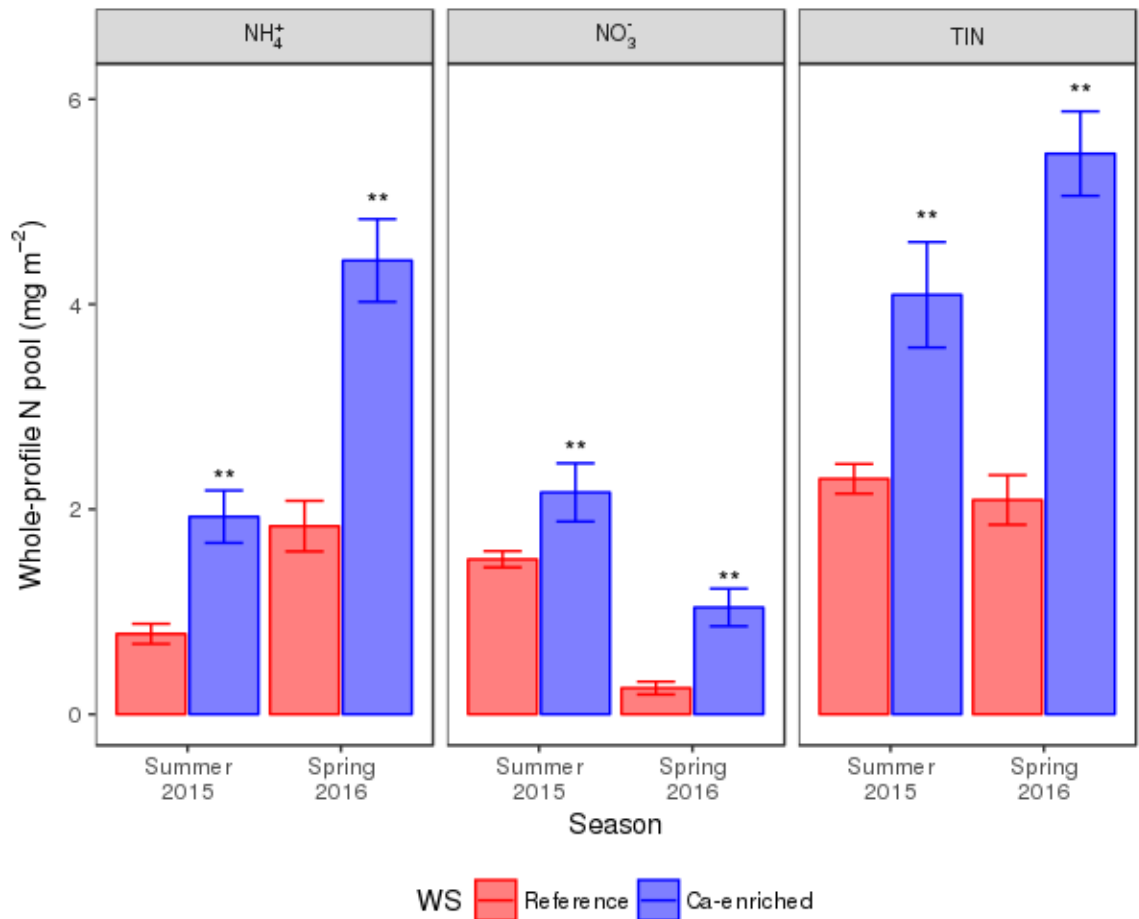


Figure 5: Soil inorganic N concentrations by horizon. Means and standard errors are displayed. Asterisks indicate a significant difference between the Ca enriched watershed and the reference watershed (\*  $p < 0.10$ , \*\*  $p < 0.05$ ).



**Figure 6: Whole-profile soil inorganic N pools for the forest floor and 0 - 10 cm mineral soil. Means and standard errors are displayed. Asterisks indicate a significant difference between the Ca enriched watershed and the reference watershed ( $p < 0.05$ ).**

Gross N cycling rates were elevated in the Ca-enriched watershed relative to the reference watershed, but there were no differences between watersheds in net N cycling rates. Net N mineralization and nitrification were not significantly different in any soil horizon for either of the sampling dates (Figure 7). In contrast, gross N transformations were significantly higher in the Oie horizon (Figure 8). Mean potential gross N mineralization was a 98.5 (SE: +/- 5.1)  $\mu\text{g gds}^{-1}$  in the Ca-enriched watershed and 71.8

(SE: +/- 3.8)  $\mu\text{g gds}^{-1}$  in the reference watershed, a significant ( $p < 0.001$ ) 37.1% difference. Mean  $\text{NH}_4^+$  immobilization was 70.2 (SE: +/- 3.3)  $\mu\text{g gds}^{-1}$  in the Ca-enriched watershed and 47.0 (SE: +/- 3.0)  $\mu\text{g gds}^{-1}$  in the reference watershed, a significant ( $p < 0.001$ ) 49.6% difference. Gross nitrification was not significantly different in the Oie horizon between watersheds, nor was  $\text{NO}_3^-$  immobilization. The difference in gross N mineralization rates, when multiplied by the greater mass of the Oie horizon in the treated watershed, leads to an estimated 67.8% higher N mineralization rate and 82.8% higher  $\text{NH}_4^+$  immobilization rate in the litter layer of the Ca-enriched watershed, on an areal basis (Figure 9). There were no significant treatment effects on gross N transformations in the Oa or mineral soil horizons.

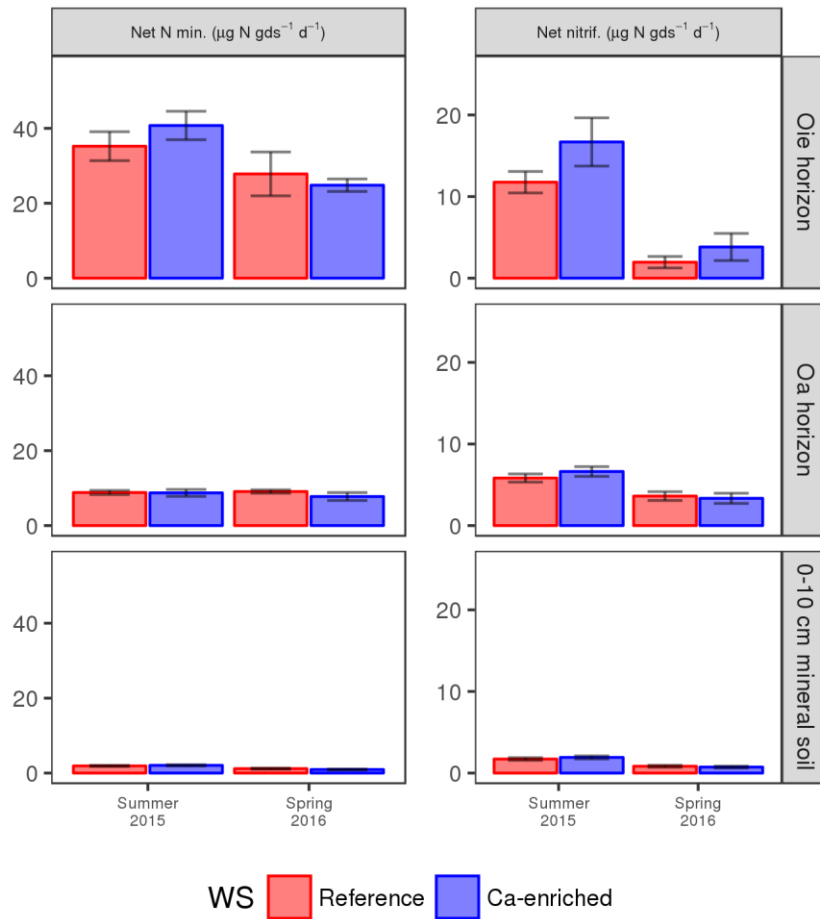


**Figure 7: Net N cycling rates by horizon. Means and standard errors are displayed. There were no significant differences between watersheds for any horizon/time combination.**

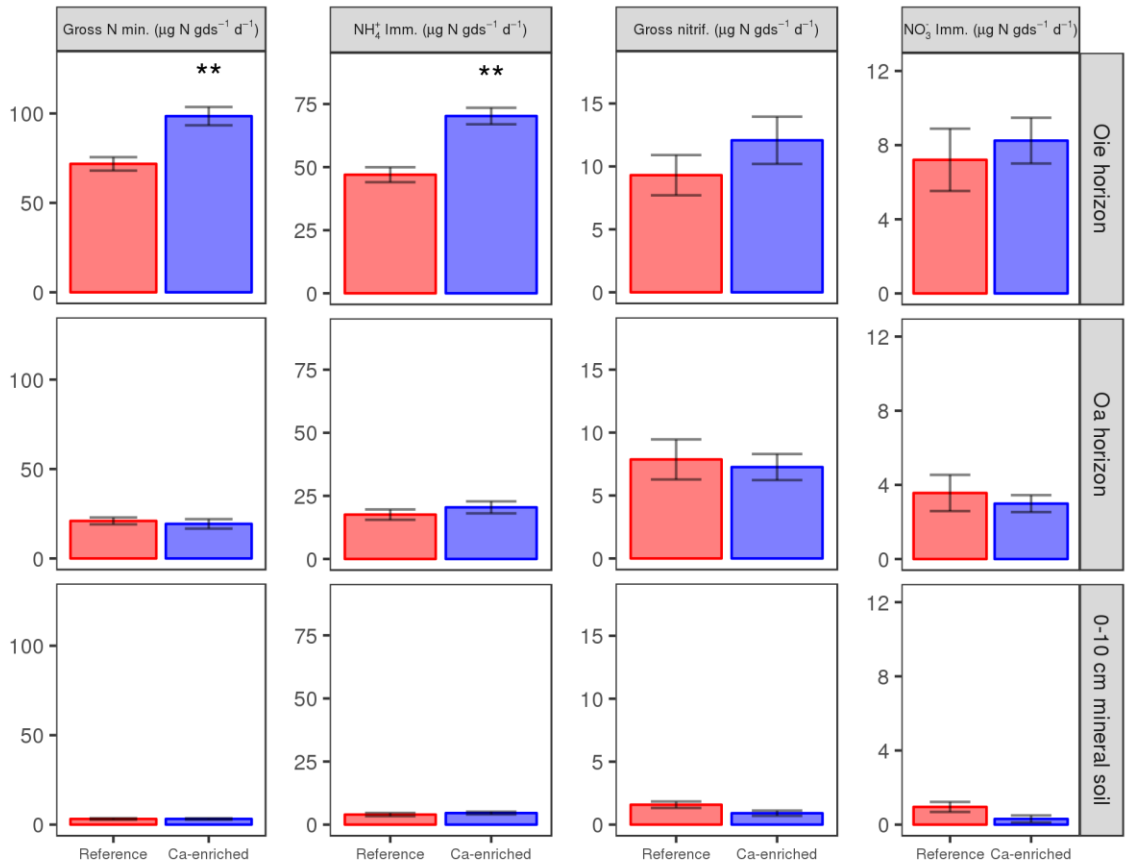
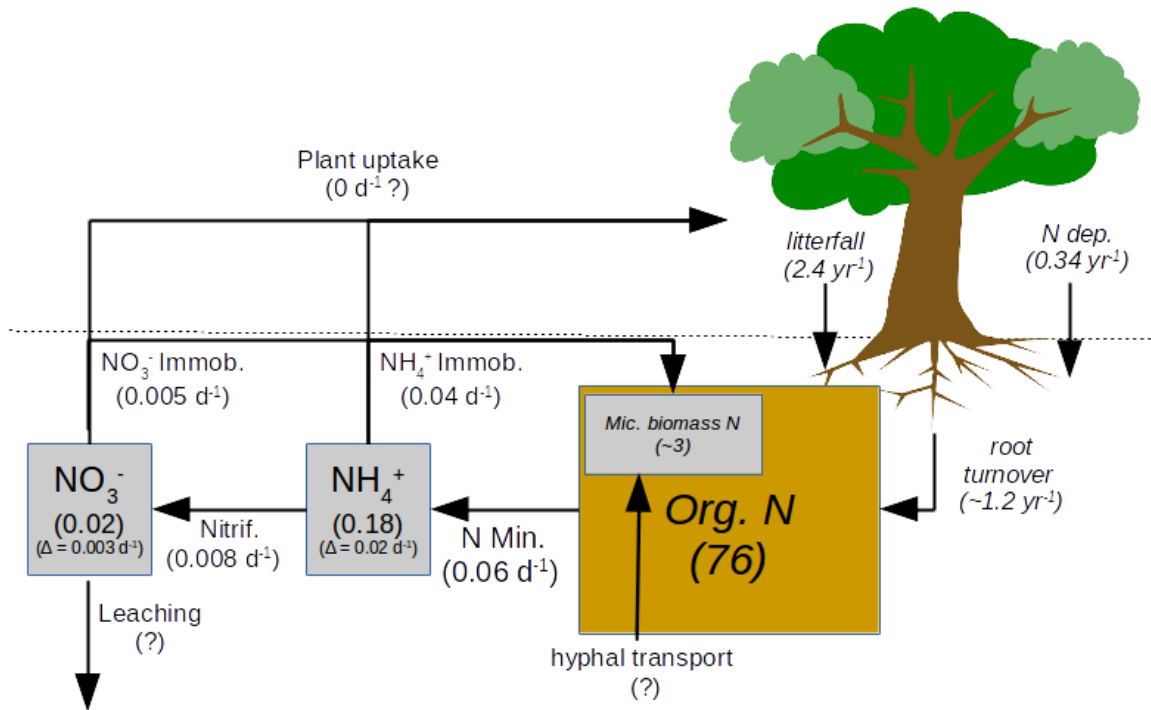


**Figure 8: Gross N cycling rates by horizon for spring 2016 soil samples. Asterisks indicate a significant difference between the Ca enriched watershed and the reference watershed ( $p < 0.05$ ).**

Reference WS, March 29, 2016



Ca-enriched WS, March 29, 2016

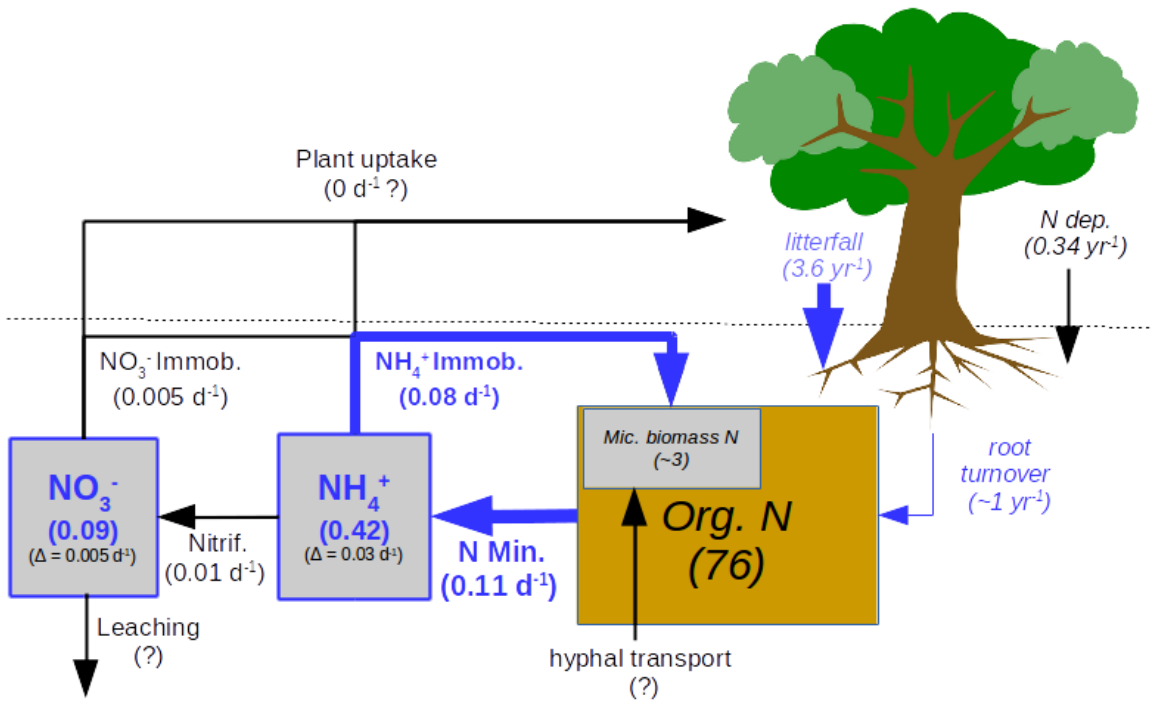


**Figure 9: A N budget “snapshot” for the Oie horizon in spring 2016, reflecting the differences in N pools and gross process rates that were measured. All pools are in units of  $\text{g m}^{-2}$  and fluxes are in units of  $\text{g m}^{-2}$  per unit time indicated. Blue text indicates a pool or flux that is significantly different between the Ca-enriched and reference watersheds. Italics indicate pools or fluxes computed from the literature.**

In some horizons, N cycling rates were positively correlated with soil C mineralization rates but were uncorrelated with any of the any of the soil acid-base properties we measured. Carbon mineralization and gross N mineralization were positively correlated in the Oie horizon ( $r^2 = 0.305$ ,  $p = 0.026$ ), weakly positively correlated in the Oa horizon ( $r^2 = 0.110$ ,  $p = 0.087$ ), and uncorrelated in the mineral horizon (Figure 10a). Carbon mineralization and net N mineralization were strongly positively correlated in the Oa horizon ( $r^2 = 0.490$ ,  $p < 0.001$ ) but uncorrelated in the Oie and mineral horizons (Figure 10b). Carbon mineralization was not significantly different between watersheds for any horizon or sampling date (Table 3). No gross or net N cycling rates were significantly correlated with pH, exchangeable Ca, base saturation, or exchangeable Al in models that included blocking factors for watershed, topographic position, and (where applicable) season. There were no significant differences in gross or net N mineralization or nitrification rates between microtopographic positions, either within or between watersheds, in either spring or summer (Figure 11).

**Table 3: Soil properties related to soil C cycling. Means and standard errors (in parentheses) are reported.**

	Watershed	GWC (%)	SOM (%)	C Mineralization ( $\mu\text{g C gds}^{-1} \text{d}^{-1}$ )	Microbial Biomass ( $\text{mg gds}^{-1}$ )
<i>Summer 2015</i>					
Oie horizon	Reference	67.0 (2.0)	71.3 (3.9)	617 (85)	13.2 (1.0)
	Ca-enriched	69.4 (1.5)	73.8 (1.7)	657 (40)	14.5 (1.4)
Oa horizon	Reference	54.3 (2.1)	34.2 (3.0)	89.4 (6.6)	3.54 (0.27)
	Ca-enriched	51.2 (2.4)	31.6 (3.5)	93.3 (11.0)	3.59 (0.41)
0-10 cm mineral soil	Reference	34.8 (1.6)	10.9 (0.6)	17.4 (0.98)	0.803 (0.076)
	Ca-enriched	34.9 (0.81)	11.7 (0.5)	16.6 (1.20)	0.801 (0.071)
<i>Spring 2016</i>					
Oie horizon	Reference	66.9 (2.3)	73.8 (4.4)	742.0 (82)	13.4 (0.93)
	Ca-enriched	70.8 (1.8)	77.2 (2.1)	880 (58)	15.8 (1.5)
Oa horizon	Reference	57.5 (2.3)	39.7 (4.2)	99.7 (13)	4.04 (0.26)
	Ca-enriched	59.6 (3.0)	44.0 (5.4)	112.0 (20)	4.51 (0.57)
0-10 cm mineral soil	Reference	34.8 (2.1)	10.6 (0.9)	16.3 (1.7)	0.794 (0.088)
	Ca-enriched	35.2 (1.7)	10.6 (0.5)	14.5 (1.1)	0.839 (0.110)

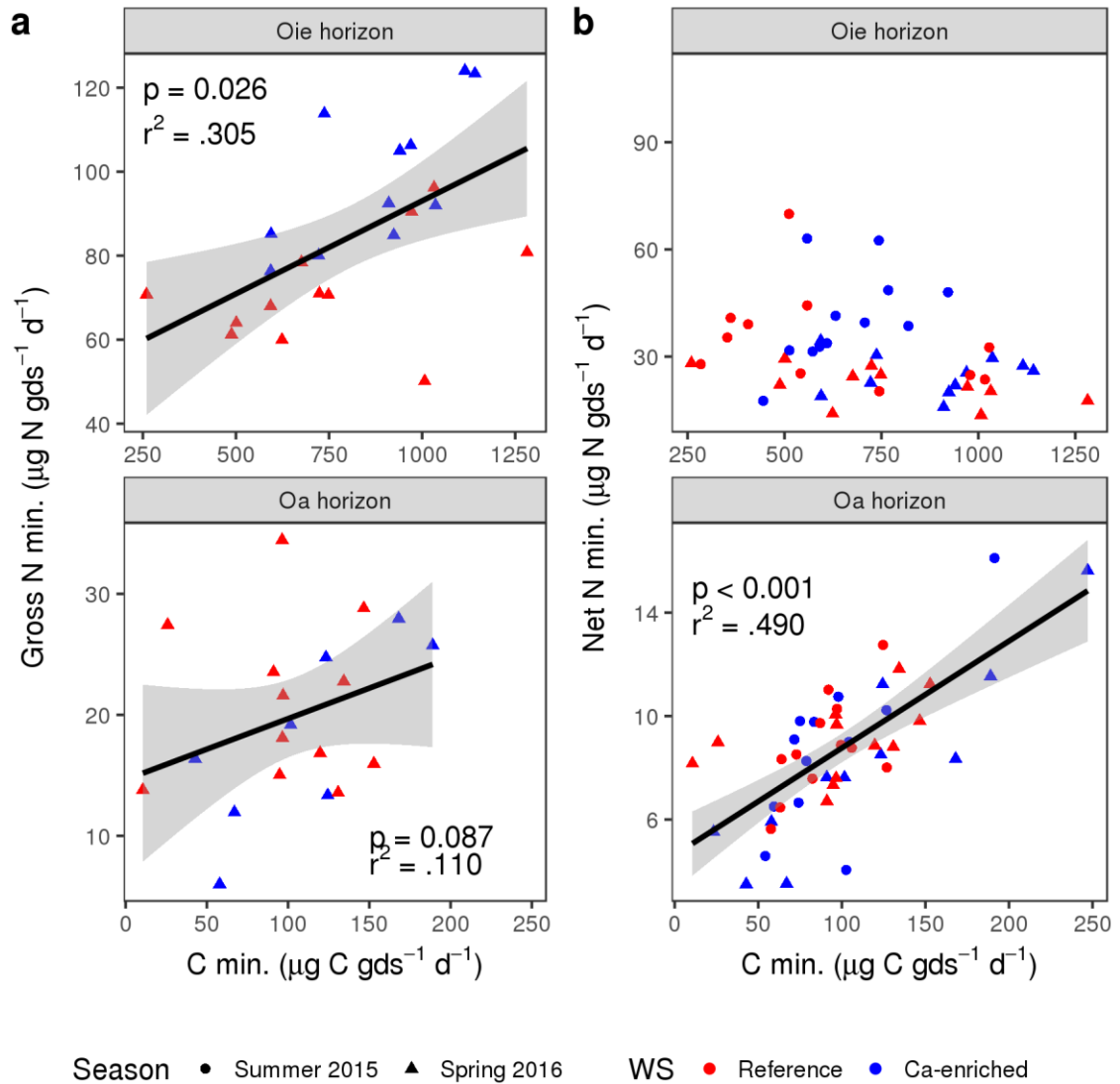


**Figure 10: Correlations between C mineralization and (a) gross and (b) net N mineralization for forest floor soil samples. The significance of the correlation is reported for a full model that included blocking factors for watershed, topographic position, and season, but the correlation coefficient and linear regression displayed here are for the main predictor (C mineralization) only. Only significant linear relationships are shown.**

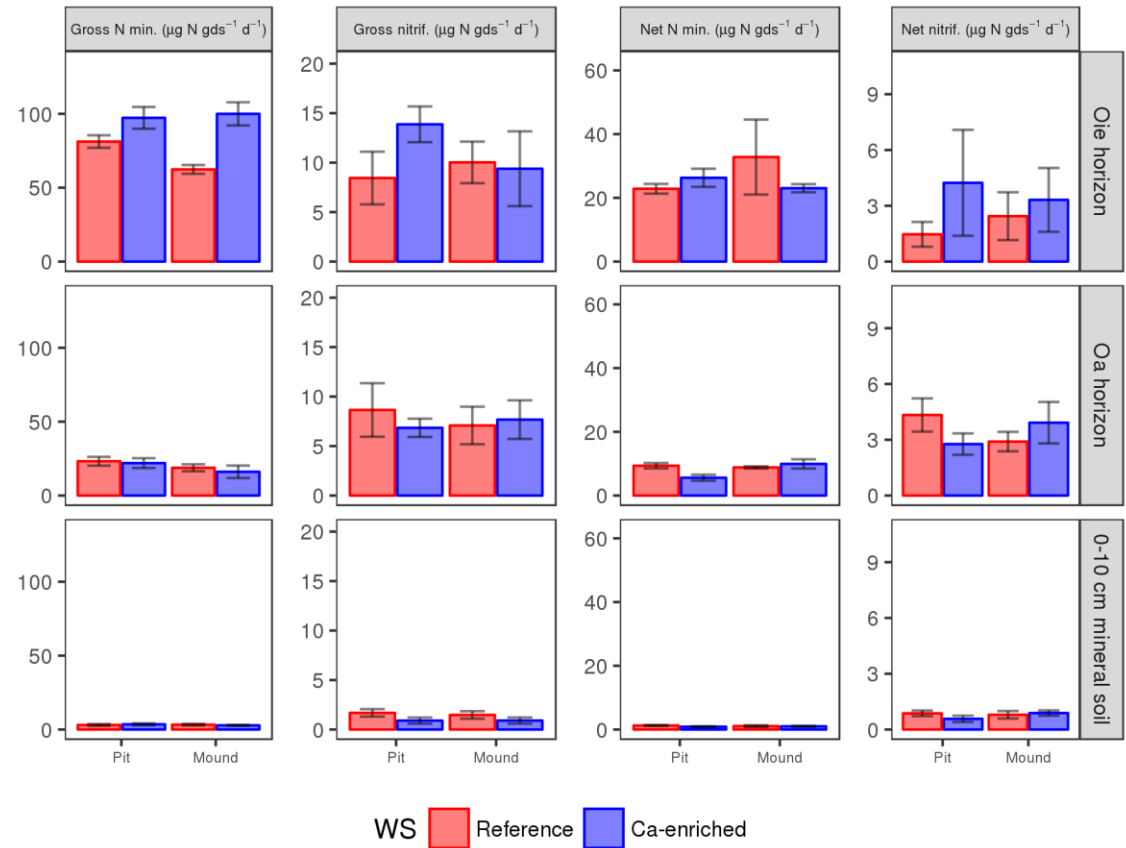


**Figure 11: Gross and net N cycling rates for spring 2016, disaggregated by microtopographic position. No significant differences were found between pit and mound positions.**

### **3.4 Discussion**

We found strong evidence of accelerated N cycling in the Ca-enriched watershed. This accelerated N cycling was only found in the leaf litter layer, though inorganic N pools were enriched throughout the soil profile. Both mineralization and immobilization were accelerated, leading to no measurable change in net mineralization rates. We found little evidence to support our hypothesis that the Ca treatment disproportionately affected N cycling in the non-growing season. Net mineralization

and nitrification rates were similar in both watersheds during both sampling periods, and inorganic N pools were enriched in the treatment watershed in both sampling periods.

The faster N turnover and larger soil inorganic N pools in the treated watershed likely predispose this watershed to hydrologic exports of nitrogen. Higher rates of mineralization and nitrification have previously been linked to increased ecosystem losses of N (Lovett et al. 2002, Phillips et al. 2013). If gross N mineralization is higher, then precipitation percolating through the soil profile will be continually supplied with higher concentrations of inorganic N that can be transported out of zones of high N consumption and into groundwater pools. Such a mechanism may be particularly relevant during times when vertical water movement through the soil is slow but constant, such as during snowmelt. While nitrification is often considered a key step in the mobilization and loss of ecosystem N due to negligible retention on the soil exchange complex (Likens et al. 1969), ammonium can be quite mobile in acid forest soils, particularly in organic horizons (Matschonat and Matzner 1995, Kothawala and Moore 2009). Enhanced nitrification therefore may not be necessary to explain increased ecosystem N loss. If we extrapolate the enhanced N mineralization rates in the Ca-enriched watershed (Figure 10) to an annual time step, we estimate that gross annual leaf litter N mineralization would be increased by  $182.5 \text{ kg ha}^{-1} \text{ y}^{-1}$ . Annual N export in the Ca-enriched has increased by less than  $8 \text{ kg ha}^{-1} \text{ y}^{-1}$ , an increase in watershed N

export that could be explained by less than 5% of this additional mineralized N being lost to streamflow. We conclude that enhanced gross mineralization of N in leaf litter thus represents a plausible mechanism to drive enhanced ecosystem N loss. This proposed mechanism is also entirely consistent with our recent discovery that N export from the Ca-enriched watershed is considerably elevated during storms (see Chapter 4).

Differences in the relationships between C mineralization and both net and gross N mineralization in each soil horizon provides additional, indirect evidence that enhanced N turnover in leaf litter (Oie horizon) may be driving inorganic N losses from this ecosystem. In leaf litter, C mineralization is positively correlated with gross N mineralization but is not correlated with net N mineralization. This discrepancy, together with the high rates of immobilization in this horizon, suggests that microbial demand for N is high in the litter layer. In contrast, in the underlying Oa horizon, C mineralization was strongly positively correlated with net N mineralization. This suggests that more of the N released from decomposition remains in solution and that inorganic N is present in excess of microbial demand in this horizon. Thus, the transition between the Oie and Oa horizons may mark a transition between N-limited and C-limited microbial metabolisms. Considering the whole soil profile then, if faster turnover of N in the Oie horizon results in greater leaching to lower soil horizons, this inorganic N could either accumulate or be transported more conservatively through these presumably C-limited lower horizons. This would account for the fact that we observed

higher inorganic N concentrations throughout the soil profile, despite no difference in gross or net N mineralization in these horizons.

To examine whether soil acid-base properties drove the increased N mineralization in the Ca-enriched watershed, we exploited the natural variability in these properties within each watershed to look for correlations between these properties and rates of N cycling. As an illustration of the natural variability of these properties, in Oie horizon soils of the Ca-enriched watershed, exchangeable Ca ranged from 93 to 267  $\mu\text{mol}_c \text{ gds}^{-1}$ , pH ranged from 4.15 to 4.68, and exchangeable Al ranged from 0 to 2.45  $\mu\text{mol}_c \text{ gds}^{-1}$ . Lovett et al. (2016) proposed that Ca limitation of white rot fungi may inhibit leaf litter decomposition, but we found no correlation between exchangeable Ca and gross or net rates of N cycling in any soil horizon. Others have proposed that low soil pH and associated Al toxicity may suppress soil microbial activity (Illmer et al. 2003, Rousk et al. 2009). We found no relationship between exchangeable Al or soil pH and N cycling rates in any horizon, though, indicating that acid stress was not a strong control on N cycling. These results show that the direct geochemical effects of the treatment are likely not the main cause of enhanced N cycling in the Ca-enriched watershed.

We did find evidence that the mechanism driving enhanced N turnover in the Ca-enriched leaf litter has acted at a substantial lag, and this lag may suggest some possible mechanisms of the enhanced N turnover. Whereas Groffman et al. (2006) found no treatment effect on gross N mineralization one year after the treatment, here we

report a 37% increase in Oie horizon gross N mineralization, fifteen years after the treatment. A mechanism driving this lag may be a gradual shift in forest composition; in the Ca-enriched watershed, sugar maple biomass increased gradually but substantially in the ten years post-treatment, whereas beech biomass decreased (Battles et al. 2014). Sugar maples have been previously shown to support high litter turnover and losses of inorganic N (Lovett et al. 2002, Templer et al. 2005). Further, the simultaneous increase in sugar maple and decrease in beech biomass represents a shift from an ectomycorrhizal-dominated community to an arbuscular mycorrhizal-dominated community, a shift that has been associated with higher C and N turnover and less retentive N cycling (Phillips et al. 2013, Averill and Hawkes 2016). Another possible mechanism to explain the increased leaf litter N cycling may be changes in the leaf litter chemistry of individual species, as leaf N content in sugar maple and yellow birch increased after treatment (Lovett et al. 2016). These changes were more immediate, however, and so would not account for the observed lag. Alternatively, enhanced N cycling could be driven by the gradual recovery of soil fauna adapted to more alkaline conditions. The Ca treatment initially suppressed soil arthropod abundance (Fisk et al. 2006) but soil arthropods have not been measured since. While earthworms are known to be strongly sensitive to pH and to promote ecosystem C and N loss (Groffman et al. 2015), earthworm density in the Ca-enriched watershed is very low (Groffman, personal communication), making this mechanism unlikely. We conclude that the gradual change

in forest composition is therefore the most plausible driver of enhanced N cycling in the Ca-enriched watershed.

### **3.5 Conclusions**

We have shown that watersheds and soils affected by decades of acid rain have likely altered ecosystem N cycles and that natural or experimental remediation of this acidity has the potential to unlock soil N stocks and enhance watershed N losses. This calls for renewed attention to an old problem - acid rain may be a problem that has largely been solved in the developed world, but its legacy will likely continue to alter the carbon and nitrogen cycles of these forests for many decades to come. Concerningly, this may decrease the terrestrial C sink and increase N loading to receiving aquatic ecosystems. In order to anticipate these changes, there is a pressing need for models that predict changes to soil acidity and base cation fertility across different soil parent material geologies and acid deposition gradients. These edaphic factors, alongside climate change and introduced plant pathogens, will likely be dominant anthropogenic controls on temperate forest community structure and biogeochemistry in the coming century.

## **4. A watershed acid rain remediation experiment increases the flashiness of terrestrial nitrogen export but increases in-stream nitrogen retention**

### **4.1 Introduction**

Many forested watersheds across northeastern North America and Europe have shown substantial, unexpected declines in inorganic nitrogen (N) export over the past two decades (Martin et al. 2000, Goodale et al. 2003, Kothawala et al. 2011, Eshleman et al. 2013, Lucas et al. 2016). This reduced stream export coincides with long-term regional declines in soil inorganic N availability (McLauchlan et al. 2017) and N mineralization rates (Duran et al. 2016), suggesting a “tightening” of the N cycle. This tightening of the N cycle runs counter to predictions that anthropogenic N loading would eventually saturate plant N demand and cause increased N export (Aber et al. 1989), but these predictions of increased N export did not account for the accumulation of anthropogenic N in soils (Aber et al. 1998). Soils have been shown to be able to retain anthropogenic inputs of N even when plant demand is saturated (Nave et al. 2009, Van Meter et al. 2016), but the mechanisms that determine this capacity for N retention remain unclear. Some authors have suggested that high N retention in recent decades is due to re-aggradation of soil organic N stocks following catastrophic loss during logging, tillage or other major disturbance (Huntington 2005, Bernal et al. 2012).

An alternative mechanism that has not been extensively examined is that soils have become more retentive of N due to persistent impacts of acid precipitation. Levels

of acid precipitation in the United States and Europe have declined substantially since they peaked in the 1970s, yet forests and the streams that drain them remain severely impaired by the legacy of over a hundred years of acid deposition (Likens et al. 1996). Decades of acid rain have lowered soil pH and reduced the solubility of soil organic matter. (Likens et al. 1996, Driscoll et al. 2001, Erlandsson et al. 2011). This decreased solubility of soil organic matter may reduce the bioavailability of soil organic N to microbes, reducing N mineralization in soils, as well as decreasing dissolved organic N export to streams. Further, low soil pH can suppress turnover of soil organic N by impacting soil microbial communities (Coughlan et al. 2000, Illmer et al. 2003) and soil faunal communities that promote decomposition (Geissen and Brummer 1999).

A watershed acid remediation experiment at Hubbard Brook Experimental Forest (HBEF) (White Mountains National Forest, NH) caused a major increase in watershed N export, suggesting that the legacy of acid precipitation may play a key role in suppressing N export from northern hardwood forests (Rosi-Marshall et al. 2016). In this experiment, researchers replaced increased soil calcium (Ca) fertility and pH by applying wollastonite ( $\text{CaSiO}_3$ ) to a small watershed in 1999 (Johnson et al. 2014). Over the first twelve years of the experiment, upper soil horizons in the  $\text{CaSiO}_3$ -enriched watershed lost  $1333 \text{ kg N ha}^{-1}$ , a 31% loss of soil organic N equivalent to approximately 1.5 times the amount of total N stored in biomass (Johnson et al. 2014). This loss of ecosystem N occurred even as net primary productivity and aboveground biomass

increased (Green et al. 2013, Battles et al. 2014). Ecosystem N export in streams increased substantially but at a lag to the soil and biomass responses to the treatment. From 1970 until 2007, annual N export from the CaSiO<sub>3</sub>-enriched watershed closely tracked export from the biogeochemical reference watershed. Beginning in 2008, N export from the CaSiO<sub>3</sub>-enriched watershed increased gradually such that, by 2013, N export from the CaSiO<sub>3</sub>-enriched watershed was 30-fold higher than from the reference watershed (Rosi-Marshall et al. 2016).

These experimental results raise questions about how soil acidity and alkalinity constrain the mineralization and release of soil organic N. The CaSiO<sub>3</sub>-enrichment created watershed N export patterns consistent with N saturation, despite appreciable declines in N deposition over the past fifteen years and enhanced plant N demand. The nitrogen saturation hypothesis proposes that chronic anthropogenic N deposition to an ecosystem will produce a predictable sequence of changes in ecosystem N retention, reflected in changes to the timing and magnitude of stream N export (Aber et al. 1989, Stoddard 1994, Bernot and Dodds 2005). During the earliest stages of N saturation, stream N concentrations are elevated only during periods of high hydrologic flux, with enhanced primary productivity acting as a sink for elevated levels of N deposition during baseflow conditions. This results in a “flashy” pattern of watershed N export in which a large proportion of the annual N export occurs during transient high flow events, analogous to hydrologic flashiness (Baker et al. 2004). In later stages, the supply

of soil inorganic N completely outstrips autotrophic demand, resulting in elevated baseflow stream N concentrations in addition to still higher storm event concentrations. The progression of N saturation represents a shift from supply limitation of N, when N export from the watershed is limited by the mass of mobile N in soil pools, to transport limitation, where the conveyance of large standing pools of soil N to streams is limited only by the movement of water (Creed et al. 1996).

While the N saturation hypothesis is commonly examined in ecosystems with high external inputs of N, it is also interesting to consider N saturation of an ecosystem as driven by biogeochemical changes that cause extensive release of N from extant ecosystem pools, as is likely the case in the watershed acid remediation experiment at HBEF. In this work, we examine evidence for N saturation in the CaSiO<sub>3</sub>-enriched watershed at HBEF by analyzing stream nitrate (NO<sub>3</sub><sup>-</sup>) dynamics. We focus on NO<sub>3</sub><sup>-</sup> dynamics because the N saturation hypothesis predicts the greatest increases in export of this form of N (Aber et al. 1998), and ammonium and organic nitrogen export remained nearly unchanged in the CaSiO<sub>3</sub>-enriched watershed (Rosi-Marshall et al. 2016). We asked the following questions: 1. Does the CaSiO<sub>3</sub>-enriched watershed at HBEF exhibit symptoms of N saturation? 2. Does an increase in the N export during floods in the early years of the experiment (1999-2007) act as a leading indicator of N saturation, prior to the period of greatly elevated N export (2008-present)? 3. To what

extent does in-stream uptake of inorganic N alter the patterns of increased N export observed in the watershed?

## **4.2 Methods**

### **4.2.1 Study site**

The study was conducted within three small, gauged watersheds at HBEF with areas ranging from 11.8 to 42.6 ha. Vegetation of the watersheds is primarily mixed hardwoods, dominated by American beech (*Fagus grandifolia*), sugar maple (*Acer saccharum*) and yellow birch (*Betula allegheniensis*), with some conifers at higher elevations (Likens 2013). The watersheds are drained by first- and second-order streams, and streamflow is perennial at the base of each watershed except in cases of extreme drought. A full site description can be found in Likens (2013). Hydrologic discharge is continuously measured in each watershed by a V-notch weir. (Buso et al. 2000). Since 1963, the stream chemistry of major inorganic solutes has been measured weekly at the outflows of each of these watersheds. Stream  $\text{NO}_3^-$  concentrations at HBEF show a strongly seasonal, sinusoidal pattern, with highest concentrations observed during the early spring and the lowest concentrations observed in the late summer, a pattern attributed to the degree of biological N demand in each season (Likens 2013).

In October 1999, one of the gauged watersheds was treated with  $1189 \text{ kg Ca ha}^{-1}$  as powdered and pelletized wollastonite ( $\text{CaSiO}_3$ ), applied aerially as an acid remediation treatment. The other two watersheds (the biogeochemical reference and

hydrologic reference watersheds) remained untreated, in a typical paired watershed experimental design. This level of wollastonite application was chosen to replace the amount of Ca estimated to be lost due to anthropogenic acid precipitation, with an additional effect of elevating soil pH (Johnson et al. 2014).

#### **4.2.2 Storm event nitrate dynamics in the long-term record**

We used the long-term HBEF stream chemistry record to examine whether the  $\text{CaSiO}_3$  treatment caused the relationship between streamwater  $\text{NO}_3^-$  concentration and discharge (c-Q relationship) to become more strongly positive, leading to flashier N export at high flow. We analyzed the  $\text{NO}_3^-$  c-Q relationships during high flow events in all three watersheds for three time periods: a pre-treatment period (October 1991 - October 1999), the early post-treatment period (October 1999 - October 2007), and the recent post-treatment period (October 2007 - October 2014). The latter time period corresponds to the period of substantially elevated stream  $\text{NO}_3^-$  flux in the  $\text{CaSiO}_3$ -enriched watershed. The strong seasonality of stream  $\text{NO}_3^-$  concentrations at HBEF complicates an examination of c-Q relationships, so we seasonally detrended the data by looking at c-Q relationships over short timescales, comparing samples taken during high flow events to the immediately antecedent samples taken during baseflow conditions.

To identify stream chemistry samples taken during storm events, we performed a hydrograph separation on the daily HBEF discharge data (Campbell 2015) using the Lynne-Hollick algorithm (Bond 2016). We identified high flow events as days in which

baseflow comprised less than 50% of total discharge. We then paired all stream chemistry samples taken during a high flow event with the antecedent baseflow sample taken one week previously. We did not analyze pairs of samples where the antecedent sample was taken during zero flow (stagnant water) or also during high flow conditions. For each pair of samples, we calculated the slope of the c-Q relationship as follows:

$$m = \frac{[NO_3]_{high\ flow} - [NO_3]_{antecedent}}{\log(Q_{high\ flow}) - \log(Q_{antecedent})} \quad (1)$$

with  $[NO_3]$  in units of  $mg\ L^{-1}$  and discharge (Q) in units of  $mm\ d^{-1}$ . A slope greater than zero indicates flushing behavior of the watershed, where stream  $NO_3^-$  concentrations increase with discharge, and a slope less than zero indicates diluting behavior. We used the Kruskal-Wallis test to test for differences in the median slope of the c-Q relationship among watersheds and across time periods. We adopted this non-parametric approach as the frequency distributions of slopes were substantially non-normal (displaying strong positive skewness). To perform post-hoc comparisons between watersheds and different time periods, we used Dunn's test, correcting for multiple comparisons via Holm's method. To examine the role of N uptake by vegetation in driving event c-Q relationships, we further divided the data into growing season (April - September) and non-growing season events (October - March) and performed the same analyses.

### **4.2.3 High-frequency storm nitrate dynamics**

From August 2015 to December 2016, we employed SUNA optical  $NO_3^-$  analyzers (Sea-Bird Scientific, Halifax, NS) to measure stream  $NO_3^-$  concentrations at

three-hour intervals. These measurements were cross-validated against laboratory analysis of samples. We identified the twelve highest discharge events for which we had data, and we plotted these events in concentration-discharge space.

We analyzed each storm event visually for patterns of hysteresis in the c-Q relationships. To qualitatively infer the source pools of  $\text{NO}_3^-$  export during storm events, we used the analytical framework of Evans and Davies (1998). This framework allows a coarse-scale inference into the concentrations of different ecosystem pools of dissolved solutes based on the direction and curvature of hysteresis in storm event solute concentrations. We classified high flow events based on whether the overall c-Q relationship was positive (flushing) or negative (diluting), as well as if they displayed clockwise, anticlockwise or no hysteresis. In a clockwise hysteresis, for any given discharge, the solute concentration on the rising limb of the hydrograph is higher than on the falling limb. A clockwise hysteresis indicates that proximal sources of water (e.g. channel interception, riparian groundwater) are higher in concentration than distal sources such as soil porewater; in an anticlockwise hysteresis the opposite is indicated (Evans and Davies 1998). When classifying the direction of hysteresis, if the magnitude of the difference between the rising and falling limb  $\text{NO}_3^-$  concentrations never exceeded the published accuracy of the SUNA instrument ( $\pm 28 \mu\text{g-NO}_3\text{-N L}^{-1}$ ), we classified the event as showing no hysteresis.

#### 4.2.4 In-stream nitrate uptake

To measure the impact of in-stream uptake on watershed  $\text{NO}_3^-$  export, we performed a mass balance for the stream channel, calculating net in-stream uptake of  $\text{NO}_3^-$  between the headwaters and the weir of each watershed. Beginning in 1991, streamwater samples were collected approximately monthly at five sites along elevational gradients within the  $\text{CaSiO}_3$ -enriched and biogeochemical reference watersheds. These gradients spanned first flowing water to the weir of the watershed. Unfiltered samples were analyzed for  $\text{NO}_3^-$  by ion chromatography. We calculated  $\text{NO}_3^-$  flux at each sampling location as the product of  $\text{NO}_3^-$  concentration and discharge. Discharge was estimated at ungauged sampling sites by using the mean daily discharge at the weir of each watershed and assuming that discharge at each sampling location was proportional to the upslope accumulated area. This method has been used extensively for computing solute fluxes at HBEF (e.g. Likens et al 1998, Johnson et al. 2000.) We determined upslope accumulated area for each sampling location using a 1m grid DEM produced from a leaf-off LiDAR flight (Photo Science Inc. 2012), coarsened to a 5-m grid and analyzed using ArcGIS 10.2 (ESRI, Redlands, CA).

For each sampling date, we calculated the net proportional decline in  $\text{NO}_3^-$  flux between the headwaters and the watershed weir following the approach of Bernhardt et al. (2003). We calculated a ratio ( $r$ ) as the  $\text{NO}_3^-$  flux at the weir of the watershed divided by the maximum  $\text{NO}_3^-$  flux observed upstream. A ratio below one indicates that  $(1-r)$  of

the  $\text{NO}_3^-$  was removed from the water column by net in-stream  $\text{NO}_3^-$  uptake between the headwaters and the weir of the watershed on that day. A ratio above one indicates that  $\text{NO}_3^-$  exports increased with watershed area on that sampling day (either via new loading or instream production.) This relative method allows comparison of  $\text{NO}_3^-$  uptake across years and widely varying flow conditions. We aggregated net uptake measurements by month and split the data into pre-treatment and post-treatment periods. Each set of aggregated ratios was tested to be significantly less than 1 using a one-way student's t-test ( $\alpha = 0.05$ , corrected for multiple comparisons). This statistical test determined if the mean net retention of  $\text{NO}_3^-$  in a stream was non-zero for a given month. Four outliers out of a total of 373 ratio calculations were excluded from the analysis due to concerns over data quality; exclusion of these data did not impact the statistical significance of any results or our conclusions.

To better understand patterns of growing season net  $\text{NO}_3^-$  uptake over varying flow regimes, we also performed fine-scale longitudinal surveys of stream  $\text{NO}_3^-$  concentrations from June to August 2015. We performed eight surveys in the  $\text{CaSiO}_3$ -enriched watershed and three surveys in the reference watersheds, over flow conditions ranging from 0.2 to 46  $\text{mm d}^{-1}$ . Sampling locations were spaced  $\sim 50$  m apart in stream reaches encompassing first flowing water to the weir of the watershed (550-700m reaches, depending on flow conditions). We measured stream  $\text{NO}_3^-$  concentrations *in situ* using a SUNA optical nitrate analyzer placed in the main channel. Discharge at

ungauged locations was estimated using the upslope area method previously described. We validated this method of discharge estimation by measuring discharge directly using a tracer slug injection method (Kilpatrick and Cobb 1985) during the first four surveys performed. For each survey, we calculated the flux ratio in the same manner as described above for the long-term data.

## **4.3 Results**

### **4.3.1 Storm nitrate c-Q dynamics**

In the pre-treatment and early post-treatment periods, stream  $\text{NO}_3^-$  concentrations increased moderately with discharge (positive c-Q slopes, flushing behavior), and there were no significant differences in median c-Q slopes among the watersheds (Figures 12 and 13). In the recent post-treatment period, event c-Q slopes in the  $\text{CaSiO}_3$ -enriched watershed were significantly higher, resulting in flashier  $\text{NO}_3^-$  export during this period. During the recent post-treatment period, the median slope of the c-Q relationship in the  $\text{CaSiO}_3$ -enriched watershed (0.20, IQR: 0.05 - 0.43) was significantly higher than both the hydrologic reference watershed (0.06, IQR: 0.00 - 0.19;  $p < 0.001$ ) and the biogeochemical reference watershed (0.00, IQR: 0.00 - 0.12;  $p < 0.001$ ). Comparing across time within the  $\text{CaSiO}_3$ -enriched watershed, the median slope in the recent post-treatment period (0.20, IQR: 0.05 - 0.43) was significantly higher than in the pre-treatment period (0.11, IQR: 0.00 - 0.24;  $p = 0.004$ ) and in the early post-treatment period (0.10, IQR: 0.00 - 0.25;  $p = 0.003$ ). In both reference watersheds, there were no

significant differences in median c-Q slopes between time periods. All three watersheds showed a positive excursion in c-Q slope in 1998 and 1999, during which time the forests in each watershed were recovering from a severe ice storm that destroyed up to 30% of the tree canopy (Houlton et al. 2003).

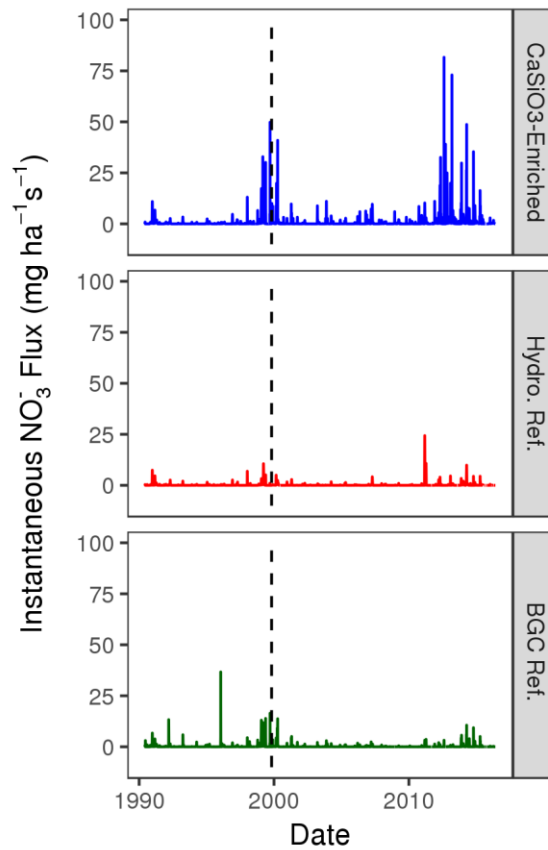


**Figure 12: Instantaneous NO<sub>3</sub><sup>-</sup> flux in three watersheds at HBEF from 1 January 1991 to 30 June 2016. The dashed line indicates the date that the acid mitigation treatment was applied in the CaSiO<sub>3</sub>-enriched watershed. The watershed color scheme used here is maintained throughout the article.**

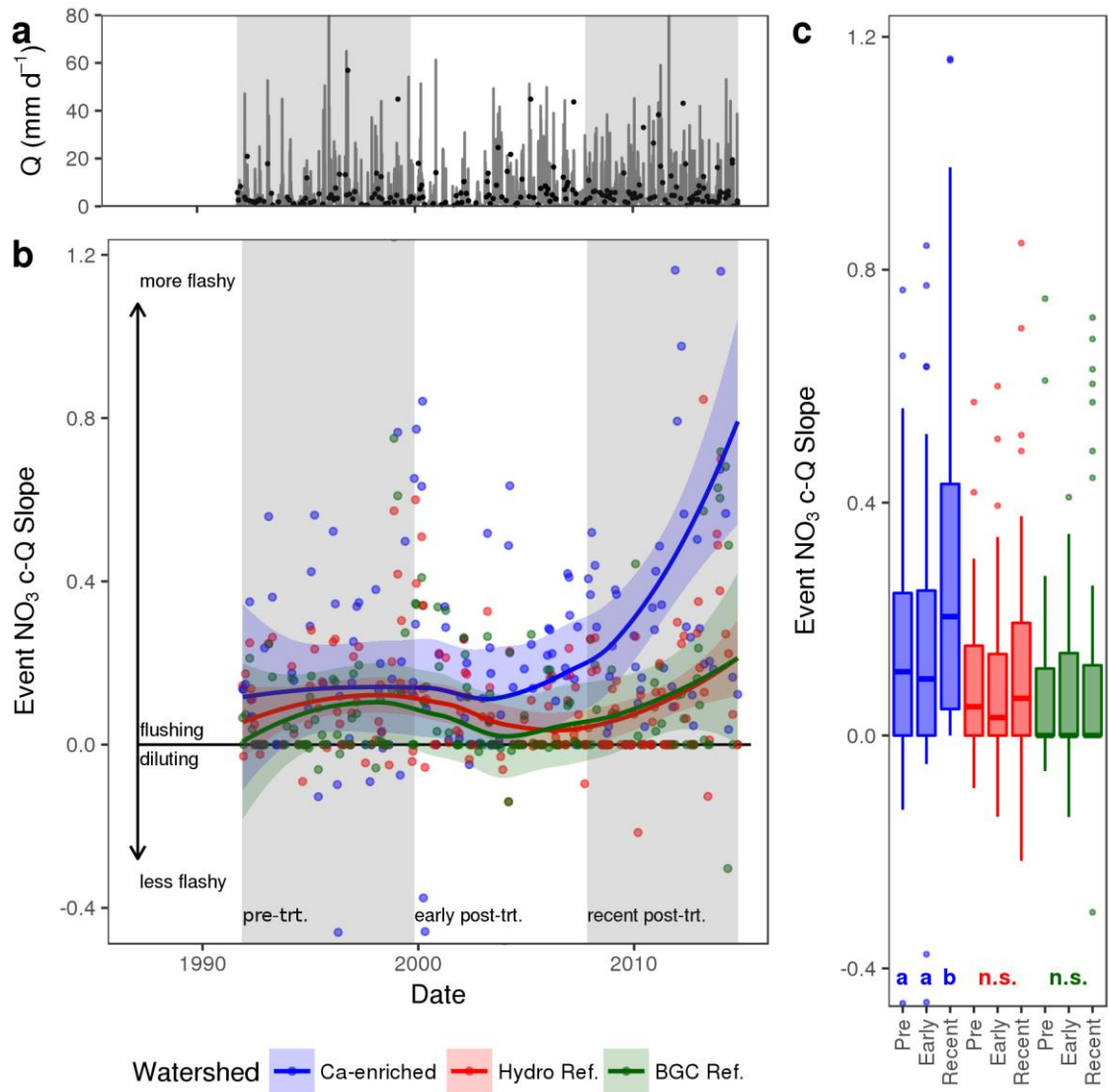
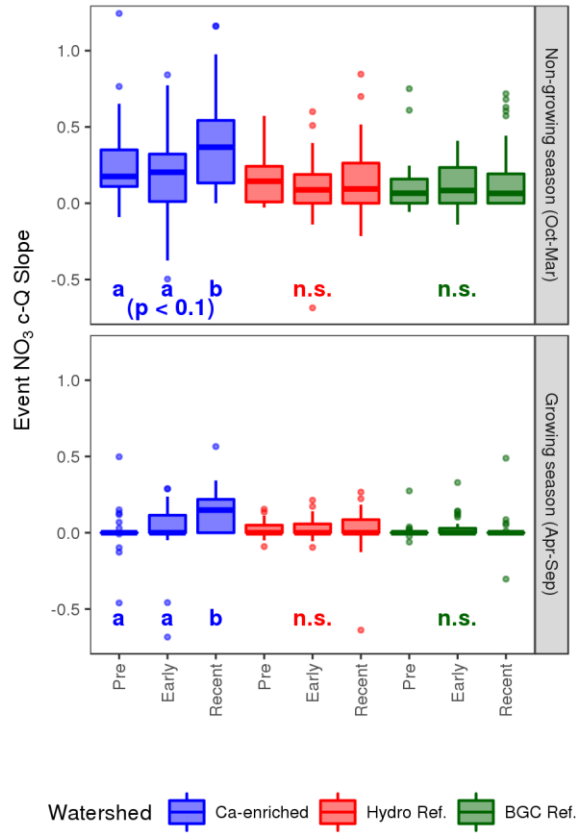


Figure 13: Slopes of the c-Q relationship for high-flow events captured in the weekly HBEF stream chemistry record. Plots show only slopes in the .025 to .975 quantiles to facilitate viewing of detail, but all points are included in statistical analyses. (a) Hydrograph showing sampled events. The grey line shows the daily discharge of the CaSiO<sub>3</sub>-enriched watershed and black points show instantaneous discharge when the event sample was taken. (b) Time series of event c-Q slopes, showing the three time periods analyzed. Curves shown for each watershed are LOESS models (tricubic weights,  $\alpha=0.75$ ) showing means and 95% CIs. (c) Summary statistics by period and watershed of event c-Q slope data. Groups that do not share a letter have significantly different medians.

The higher c-Q slopes of NO<sub>3</sub><sup>-</sup> export in the CaSiO<sub>3</sub>-enriched watershed during the recent post-treatment period were particularly apparent during the growing season (Figure 14). In the recent post-treatment period, the median growing season c-Q slope in the CaSiO<sub>3</sub>-enriched watershed (0.15, IQR: 0.00 - 0.22) was significantly higher than in both the pre-treatment period (0.00, IQR: 0.00-0.00,  $p < 0.001$ ), and the early post-treatment period (0.00, IQR: 0.00 - 0.11;  $p = 0.033$ ), when NO<sub>3</sub><sup>-</sup> concentration was essentially invariant with discharge. In both reference watersheds, median growing season stream NO<sub>3</sub><sup>-</sup> concentrations were at or near the detection limit, both during baseflow and event conditions. In the non-growing season, c-Q slopes were modestly higher in the CaSiO<sub>3</sub>-enriched watershed during the recent post-treatment period, but this difference was only significant at  $\alpha = 0.10$ .



**Figure 14: Summary statistics by period and watershed of event c-Q slope data, disaggregated by season. Groups that do not share a letter have significantly different medians.**

During the twelve storm events analyzed using high-frequency sensor data, c-Q relationships showed markedly different patterns of hysteresis in the CaSiO<sub>3</sub>-enriched watershed compared to the hydrologic reference watershed (Figure 15). In all twelve events for the CaSiO<sub>3</sub>-enriched watershed, stream NO<sub>3</sub><sup>-</sup> concentrations exhibited positive c-Q slopes and strong anticlockwise hysteresis. This indicates the mobilization of distal sources of NO<sub>3</sub><sup>-</sup> containing substantially higher concentrations than near-stream water and channel interception water. By contrast, the hydrologic reference watershed

exhibited no consistent pattern of c-Q slopes or hysteresis. We observed two winter events with anticlockwise c-Q hysteresis (Figure 15b, events 3 and 6) although the magnitude of the hysteresis in the reference watershed was smaller than in the CaSiO<sub>3</sub>-enriched watershed. Four events showed clockwise c-Q hystereses (Figure 15b, events 1, 2, 11 and 12) and in the remaining six events there was no measurable c-Q hysteresis.

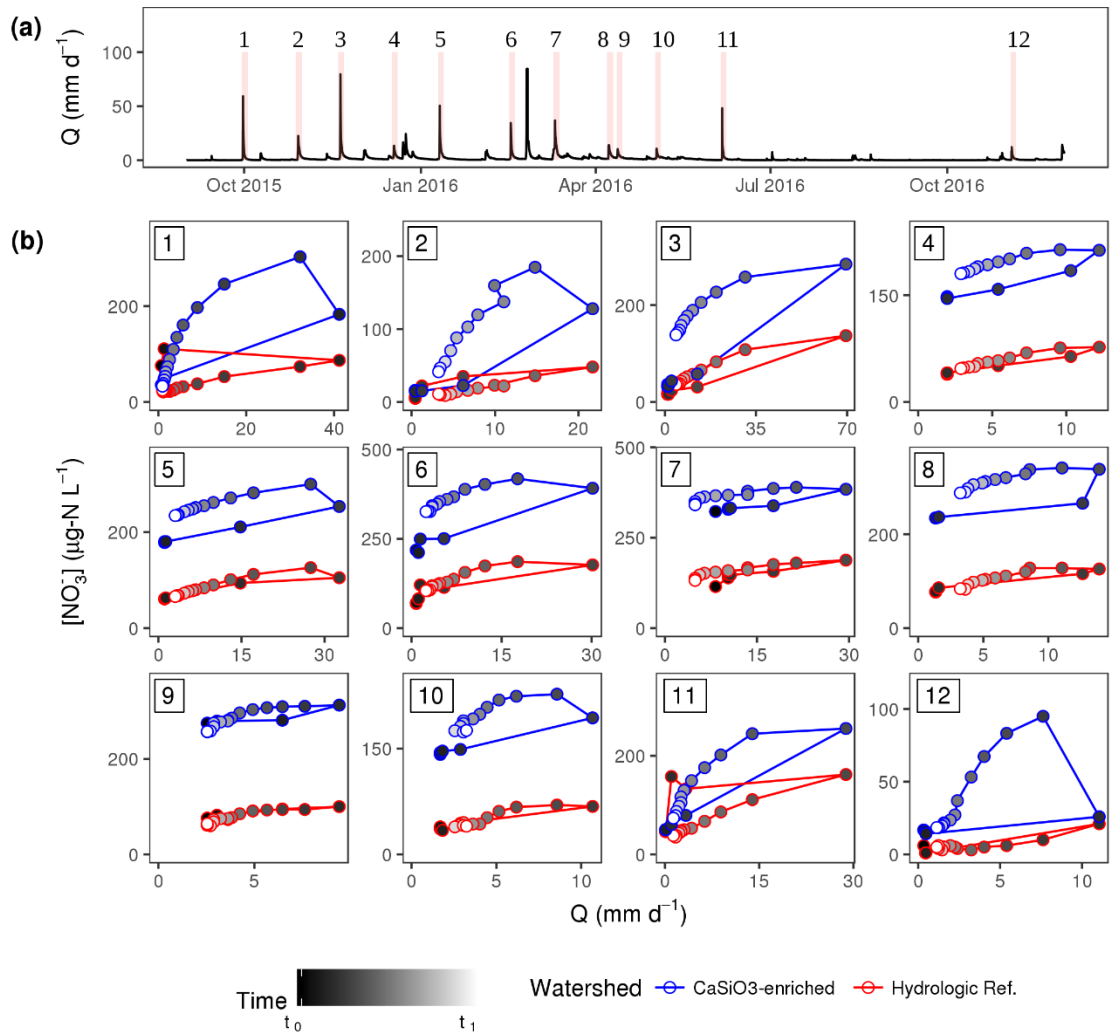


**Figure 15: High-frequency  $NO_3^-$  c-Q relationships for the twelve largest discrete storm events captured using optical  $NO_3^-$  sensors. (a) Discharge of the hydrologic reference watershed, with the sampling periods of the plots in panel (b) indicated. (b) Time series of the  $NO_3^-$  c-Q relationships for the CaSiO<sub>3</sub>-enriched and hydrologic reference watersheds. Direction of the hysteric loops is indicated by greyscale shading. Note that scales of x and y axes are different for each event. Storms 1, 8, 9, 10, and 11 are growing season storms.**

### 4.3.2 In-stream uptake of nitrate

The net rate of in-stream  $\text{NO}_3^-$  uptake was significantly increased in the  $\text{CaSiO}_3$ -enriched watershed during the post-treatment period. In the pre-treatment period (1991-1997), the flux ratio ( $r$ ) was not significantly less than 1 for any month in the record, for either the  $\text{CaSiO}_3$ -enriched or biogeochemical reference watersheds. This indicates that there was no consistent signal of net N retention in either watershed (Figure 16). In the post-treatment period (1999-2012), net in-stream  $\text{NO}_3^-$  uptake significantly reduced the  $\text{NO}_3^-$  flux from the  $\text{CaSiO}_3$ -enriched watershed during three growing-season months: June, July and September. During these months, net in-stream uptake decreased net  $\text{NO}_3^-$  flux from the acid-remediated watershed by a mean of 71.1% in June (SE: +/- 15.9%;  $p = 0.025$ ), 63.0% in July (SE: +/- 10.7%;  $p = 0.023$ ) and 68.0% in September (SE: +/- 9.7%,  $p = 0.005$ ). There was no consistent in-stream uptake of  $\text{NO}_3^-$  in the biogeochemical reference watershed during these months of the post-treatment period, although significant in-stream uptake was detected in the month of November.

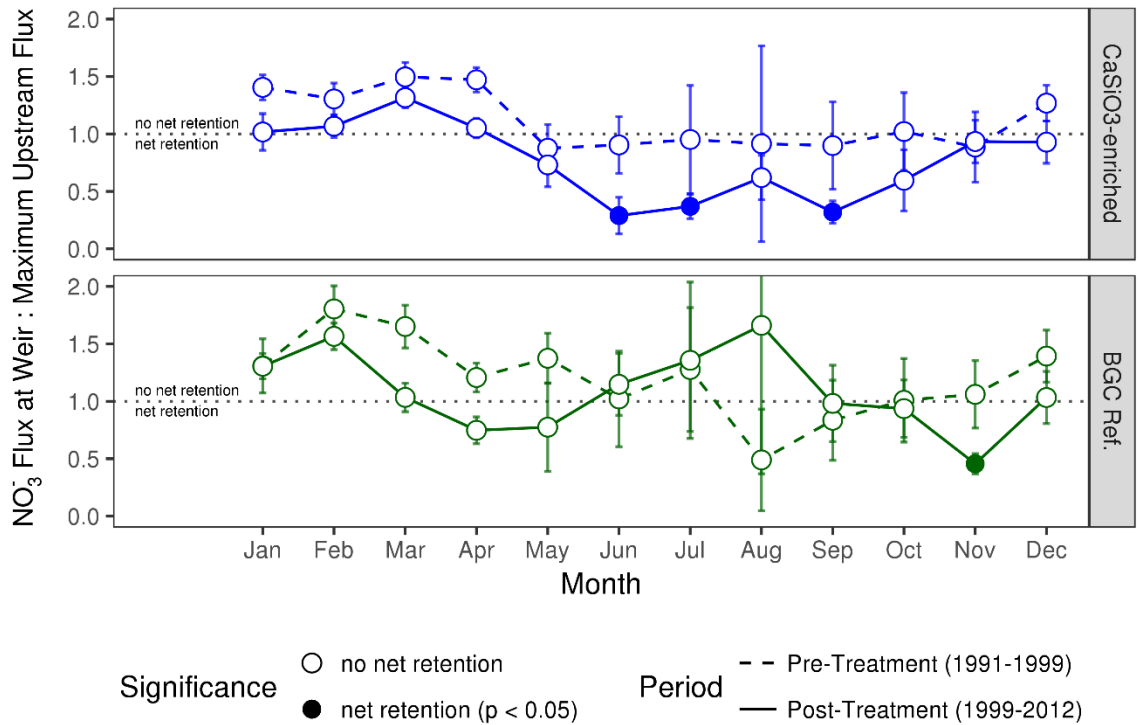


**Figure 16: The mean NO<sub>3</sub><sup>-</sup> flux by month observed at the weir of the CaSiO<sub>3</sub>-enriched and BGC reference watersheds, relative to the maximum flux observed upstream. When this ratio is less than 1, this demonstrates that there is net NO<sub>3</sub><sup>-</sup> retention between the point of maximum NO<sub>3</sub><sup>-</sup> flux and the weir. Filled circles indicate that the mean of the ratio was significantly less than 1, indicating net retention of NO<sub>3</sub><sup>-</sup> in that month. Error bars are +/- 1 SE.**

The fine-scale longitudinal surveys conducted from June to August 2015 showed that in-stream uptake continued to result in reduced NO<sub>3</sub><sup>-</sup> fluxes from the CaSiO<sub>3</sub>-enriched watershed during the growing season. Net in-stream uptake reduced net NO<sub>3</sub><sup>-</sup> flux from the watershed by 0 - 77.1% (median: 28.9%) across the eight surveys. The flux ratio was strongly positively correlated with the logarithm of discharge ( $p < 0.001$ ) (Figure 17). The greatest proportional in-stream uptake was therefore observed at low-flow conditions, whereas at high flow conditions, there was no detectable in-stream

uptake of  $\text{NO}_3^-$ . In the surveys performed in the reference watersheds, there was no observed net in-stream uptake, regardless of discharge.

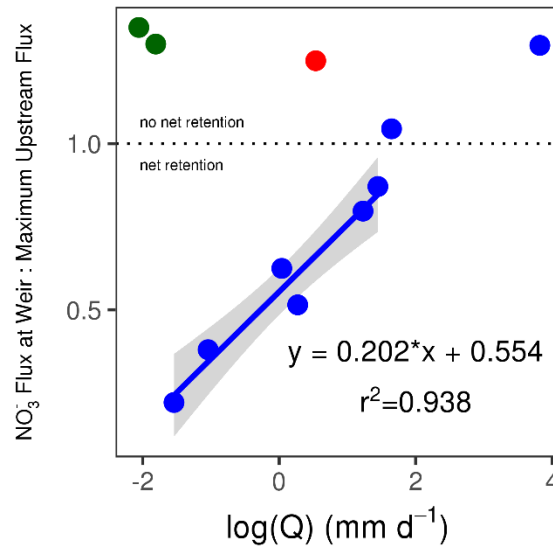


**Figure 17: The relationship between the  $\text{NO}_3^-$  flux ratio and discharge. Data calculated from synoptic surveys performed in the  $\text{CaSiO}_3$ -enriched watershed (blue points) from June to August 2015. Surveys performed in the biogeochemical reference (green points) and hydrologic reference (red point) watersheds are shown for comparison. For points above the dashed line, there was no net in-stream  $\text{NO}_3^-$  uptake.**

#### **4.4 Discussion**

We found several lines of evidence that show that the  $\text{CaSiO}_3$ -enriched watershed shows a shift from supply limitation to transport limitation of  $\text{NO}_3^-$  in streams, consistent with symptoms of N saturation. Foremost, we found that streams demonstrated a pronounced increase in the positive relationship between discharge and streamwater  $\text{NO}_3^-$  concentrations, resulting in significantly increased  $\text{NO}_3^-$  export during high flow events. Previous work at HBEF has shown a positive relationship between discharge and stream  $\text{NO}_3^-$  concentrations during the non-growing season (Johnson et al.

1969, Buso et al. 2000), but as Likens (2013) notes, in recent decades this relationship has nearly disappeared as N deposition and stream N efflux have decreased markedly. While we did find evidence limited evidence that the c-Q relationship became more positive during the non-growing season in the CaSiO<sub>3</sub>-enriched watershed, the most striking changes happened during the growing season. This suggests that in the CaSiO<sub>3</sub>-enriched watershed, NO<sub>3</sub><sup>-</sup> is produced in excess of biological demand and is retained in hydrologically-isolated pools which then become mobilized during storm events. Even during the 1960s, when annual watershed export of N at HBEF was an order of magnitude higher than today, growing-season stream NO<sub>3</sub><sup>-</sup> concentrations were uniformly low and did not vary with discharge (Johnson et al. 1969), likely due to strong biotic demand for N (Likens et al. 1970). This shift in the CaSiO<sub>3</sub>-enriched watershed toward flashy growing-season NO<sub>3</sub><sup>-</sup> export thus represents a profound shift in ecosystem N balance.

Consistent with Stoddard's (1994) model of N saturation, we had initially hypothesized that an increase in the flashiness of NO<sub>3</sub><sup>-</sup> export in the CaSiO<sub>3</sub>-enriched watershed would appear in the early post-treatment period as a leading indicator of the greater annual NO<sub>3</sub><sup>-</sup> flux observed in the recent post-treatment period. We did not find support for this hypothesis, however, as the median c-Q slope in the early post-treatment period was no different than in the pre-treatment period. Instead, the observed increased flashiness of NO<sub>3</sub><sup>-</sup> export was coincident with the increase in total

annual  $\text{NO}_3^-$  flux, with the watershed rapidly transitioning from very low annual N stream flux in the early period to symptoms of intermediate N saturation. The reasons behind this delayed but pronounced change in N export remain unclear, but we speculate that it may relate to a time lag between the surface application of the  $\text{CaSiO}_3$  treatment and the migration of the treatment into deep, hydrologically active soil horizons, which Johnson et al. (2014) document.

The patterns of  $\text{NO}_3^-$  c-Q hysteresis observed during storm events offers some suggestion as to the character and location of the concentrated  $\text{NO}_3^-$  pools that are mobilized during high flow events. The anti-clockwise hystereses that we document show that high- $\text{NO}_3^-$  waters are arriving late to the stream from distal sources. Perhaps the most likely mechanism driving this pattern is that the  $\text{NO}_3^-$  is being mobilized late in the storm event from large standing pools in surficial soils throughout the watershed. This mechanism has been shown to be possible through modeling and empirical work if the hydrologic routing of a watershed has a large preferential flow component (Band et al. 2001). In this framework, water on the rising limb and at peak flow is efficiently routed to the stream through preferential flowpaths, with minimal contact time and exchange with soil porewater. The water that arrives on the falling limb of the hydrograph then represents matric flow with much longer travel times and exchange with surficial soil porewater. The late-arriving water is thus in a sense vertically distal from the stream, arriving from top soil layers. Extensive preferential flow has been

documented at HBEF (Detty and McGuire 2010), and  $\text{NO}_3^-$  concentrations in organic horizon lysimeter samples have recently increased substantially (Driscoll 2016), making this mechanism plausible.

Patterns of hysteresis in the  $\text{CaSiO}_3$ -enriched watershed remained constant regardless of season, suggesting that these high  $\text{NO}_3^-$  source areas remain active even in periods of high plant demand.

The reference watershed showed greater seasonal variability in patterns of hysteresis, similar to patterns observed in other headwater catchments throughout the region. During the non-growing season there was a slightly positive c-Q relationship and some examples of counterclockwise hysteresis, but during the growing season c-Q relationship became near-zero and displayed clockwise or no hysteresis. Koenig et al. (2017) found that this seasonal pattern was common across forested watersheds in the region. Inamdar et al. (2004) also showed flushing but clockwise  $\text{NO}_3^-$  storm hysteresis during the growing season in Adirondack headwater catchments, and still other regional examples (Vaughn et al. 2017) show strongly negative c-Q relationships during the growing season. We do not have pre-treatment data to conclusively show that the atypical patterns of hysteresis in the  $\text{CaSiO}_3$ -enriched watershed are due to the treatment rather than intrinsic differences in the watersheds, though we have demonstrated that the overall c-Q relationship changed positively compared to pre-treatment conditions. Overall, the  $\text{CaSiO}_3$ -enriched watershed now demonstrates  $\text{NO}_3^-$

export characteristics that are atypical for headwaters in the region, both in the magnitude of the c-Q relationship, hysteresis, and the aseasonality of these relationships. These differences suggest a substantial alteration of watershed N cycling.

In addition to flushing of  $\text{NO}_3^-$ -rich waters during storms, net in-stream  $\text{NO}_3^-$  uptake during baseflow conditions may contribute as well to the enhanced flashiness of the  $\text{NO}_3^-$  c-Q relationship in the  $\text{CaSiO}_3$ -enriched watershed; a more strongly positive c-Q relationship can result both from elevated event concentrations as well as suppressed baseflow concentrations. During the growing season, we documented a strong signal of net in-stream uptake of  $\text{NO}_3^-$  and found that the proportional rate of  $\text{NO}_3^-$  uptake was strongly inversely correlated with discharge (Figure 5). This inverse relationship would be a prerequisite for in-stream uptake impacting the flashiness of stream N export. In-stream uptake of N is known to be tightly coupled to contact time between stream water and benthic sediments (Peterson 2001). Contact time is lower at high discharge due to higher stream velocity and a greater cross-sectional area to wetted perimeter ratio. We therefore conclude that the observed relationship between discharge and N uptake is consistent with increased uptake by benthic microbiota. This uptake resulted in lower baseflow stream  $\text{NO}_3^-$  concentrations that likely contributed to more positive, flashier  $\text{NO}_3^-$  c-Q relationships during the growing season, although this contribution is difficult to directly quantify.

The high rates of net in-stream N uptake observed in the CaSiO<sub>3</sub>-enriched watershed are a sharp contrast to the view of some authors that solute fluxes in the streams of small watersheds are almost always at steady state, with no net retention or release of solutes (Brookshire et al. 2009). Among other studies that do show net in-stream uptake, our result is remarkable both for the amount of net uptake (up to 77% in the lowest flow conditions) and the lack of an obvious sink for this NO<sub>3</sub><sup>-</sup>. Other work has shown moderate net in-stream uptake in conjunction with very high rates of algal primary productivity (Grimm et al. 1981) or in conjunction with pulses of organic matter inputs, either during autumn (Roberts and Mulholland 2007, Bernal et al. 2012b) or after a disturbance event. In previous work at HBEF, high rates of net in-stream uptake were measured in the aftermath of the 1998 ice storm that resulted in ~ 30% canopy destruction at HBEF (Bernhardt et al. 2003). In this earlier instance, researchers speculated that high in-stream N retention was driven by the large inputs of terrestrial litter from downed trees and higher in-stream productivity resulting from an opening of the forest canopy. We measured similar rates of net NO<sub>3</sub><sup>-</sup> uptake in the post-treatment period, despite no apparent increase in detrital inputs to the stream, and no observed algal productivity during the growing season.

Given the apparent lack of algal productivity or enhanced carbon inputs to the CaSiO<sub>3</sub>-enriched stream, we hypothesize that higher instream NO<sub>3</sub> uptake results from an increase in denitrification. Denitrification can substantially attenuate N fluxes in

streams (Mulholland et al. 2004) and is favored under the conditions of higher stream pH and high  $\text{NO}_3^-$  availability observed in the  $\text{CaSiO}_3$ -enriched watershed (Groffman et al. 2009). Limited data (Appendix B) show elevated denitrification potential in the sediments of the  $\text{CaSiO}_3$ -enriched stream, but further work would be required to quantify a potentially enhanced denitrification sink in the watershed. If the observed increase in N uptake is driven by denitrification, this would represent a permanent, dissimilatory sink of N, in contrast to assimilatory uptake, in which assimilated N could be re-released as organisms die. This permanent sink of N could potentially alter the watershed N budget, particularly if in-stream processes are reliable proxies for metabolisms also occurring in saturated soils.

We found that stream  $\text{NO}_3^-$  concentrations in the  $\text{CaSiO}_3$ -enriched watershed became substantially flashier post-treatment, consistent with saturation of ecosystem N demand. It is possible that this experiment may foreshadow changes in N cycling that will occur in acid-impacted forests over the coming decades as they recover from acid deposition. Many forests are showing incipient signs of recovery in soil acid-base properties (Lawrence et al. 2015), and this recovery has been linked to enhanced decomposition of soil organic matter stocks, which are the largest pool of soil N in forested ecosystems (Oulehle et al. 2011, Lawrence et al. 2012). This raises the intriguing possibility that acid precipitation, of which a large portion is deposited as nitric acid, may have paradoxically reduced watershed N export through stabilization of soil

organic N at low soil pH (see Clarholm and Skjellberg (2013) for a review of possible mechanisms). With declines in acid forcing on soils, this stabilized legacy N may be released causing ecosystem N saturation, in a mechanism analogous to the internal eutrophication of lakes by remobilization of sediment phosphorus (Smolders et al. 2006). As ecosystems continue to recover from acid precipitation, this hypothesis should be examined across continental-scale gradients of acid deposition severity.

## 5. Conclusions

Natural recovery of soils from acid deposition has recently been shown to have substantial effects on ecosystem C and N cycling, driving changes in forest biomass and composition (Lawrence et al. 2017), soil C and N stocks (Oulelhe et al. 2011, Lawrence et al. 2012), organic C and N mobility in soils (Evans et al. 2010, Oulehle et al. 2013), and delivery of DOM to aquatic ecosystems (Monteith et al. 2007, de Wit et al. 2007, Evans et al. 2008). Nonetheless, substantial uncertainty remains around the speed and extent to which ecosystems will continue to recover, given the ongoing legacies of past and present acid deposition. The watershed acid remain remediation study at HBEF offers a useful end-member of full ecosystem recovery, allowing researchers to rapidly and unmistakably observe changes in ecosystem structure and function that are occurring far more gradually in unmanipulated ecosystems. Because the changes in ecosystem C and N cycling in response to this acid rain mitigation experiment have been so profound, this whole watershed experiment is a good laboratory for exploring the mechanisms via which soil alkalinity and ecosystem C and N cycling are linked. In my dissertation, I examined the impacts of this acid mitigation experiment on plant and soil cycling of C and N, and the consequences of this for watershed N export.

A consistent theme that emerged throughout this work is the importance of the interplay among soil geochemistry, watershed hydrology, and vegetation dynamics in controlling C and N cycling as ecosystems recover from acid precipitation. In Chapter 2,

I showed that changes in soil pH drove increases in both the respiration and mobility of soil C, but that these changes were driven by plant-soil interactions and not direct geochemical effects. In Chapter 3, I demonstrated enhanced N cycling in leaf litter in the experimental watershed that was temporally correlated to changes in forest species composition. Further, I showed enhanced soil inorganic N availability throughout the soil profile, suggesting the hydrologic propagation of N cycling effects occurring only in the uppermost soil horizons. Finally, in Chapter 4, I demonstrated that, in the experimental watershed, storms played an increasingly important role in controlling watershed export of N. This work showed that changes in terrestrial N cycling are driving accumulation of inorganic N pools that are only mobilized during high flow. While this work has contributed to understanding how ecosystem recovery from acid deposition impacts C and N cycling, it also highlights some old questions and suggests new ones, both at HBEF and in the larger context of temperate forest ecology.

This work was motivated by the desire to understand the drivers behind two observations in the experimental watershed that I thought were almost certainly related: a) the loss of over a third of the soil C and N in the humic (Oa/A) soil horizon, and b) the later thirtyfold increase in watershed N export. My dissertation research suggests that there is not a causal link. I found that enhanced N cycling in the litter layer (Oie horizon) could easily account for the observed increase in watershed N export (Chapter 3). This enhanced N cycling in the litter layer occurred contemporaneously with the increased N

export, whereas N loss from the Oa horizon had ceased by the time watershed N export increased. If litter turnover is the cause of the high ecosystem N losses, then it makes it even more difficult to determine the fate of the C and N stocks lost from surficial soils (Figure 18). An estimated 11.3 Mg ha<sup>-1</sup> of soil C and 420 kg ha<sup>-1</sup> N have been lost from this watershed's surficial soils over the last decade. Our inability to explain either the mechanisms for this loss or the fate of these liberated elements in one of the world's best-studied forests is forcing ecosystem scientists to ask new questions about how shifting soil acidity may alter the magnitude, form and timing of C and N transfers within and from natural ecosystems.

The most plausible fate of this of this missing C and N is retention in the deep soil. Soil respiration has not increased post-treatment (Groffman 2013) and respiratory loss for the missing C would pose a significant N mass balance problem. If this entire mass of N had been mineralized, it would have almost certainly been subject to flushing in storms. In Chapter 5, I showed no evidence for increased flushing during the time period that the Oa horizon mass decreased. Measurement error of surficial soil pools is also unlikely, as Johnson et al.'s (2014) sampling scheme was extensive, robust to outliers, and showed a consistent multi-year trend. In Chapter 2, I showed that, while changes in soil pH drove both enhanced microbial respiration and SOM solubility, the changes in solubility were of a greater magnitude than changes

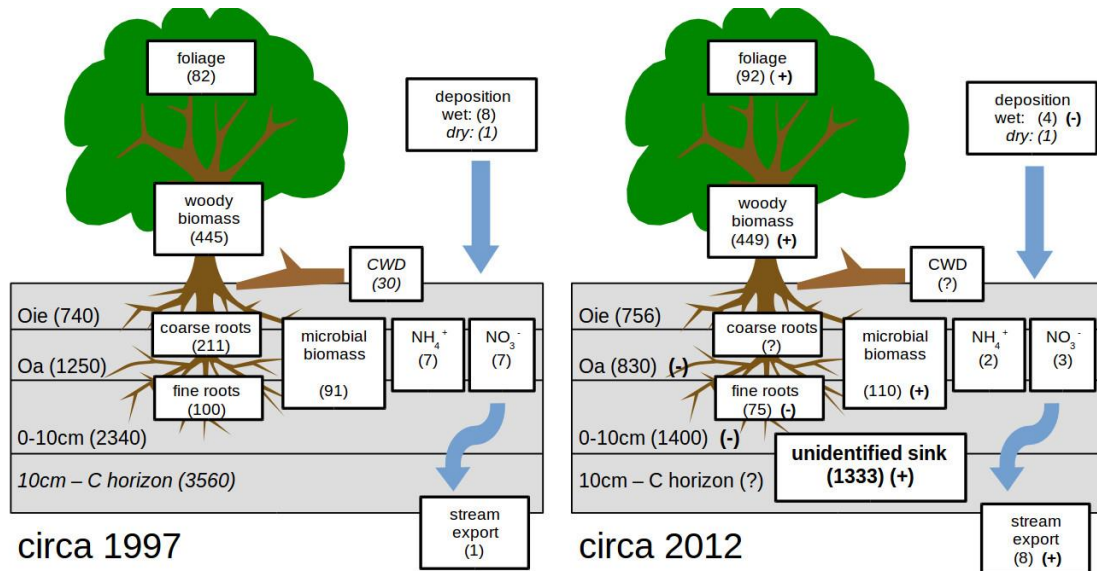


**Figure 18: A nitrogen budget for the Ca-enriched watershed, highlighting the large discrepancy in ecosystem N balance that continues to be a mystery. Pools are expressed in units of kg ha<sup>-1</sup> and fluxes as kg ha<sup>-1</sup> y<sup>-1</sup>. Changes between 1997 and 2012 are indicated by the sign next to the pools or fluxes. Italics indicate estimates that are not well-constrained. Total N by soil horizon excludes root biomass N but includes inorganic and microbial N. Soil inorganic N pools show high annual and interannual variation and are included only to illustrate their order of magnitude relative to other pools. Microbial biomass N and inorganic N pools were calculated from Johnson et al. (2014) and Groffman (2013). Coarse and fine root N data were calculated from Fahey et al. (1988), Battles et al. (2014), and Fahey (2016). Aboveground biomass N was calculated from Battles et al. (2014), Juice et al. (2005), and Yanai et al. (2013). Total soil pool data is from Johnson et al. (2014). CWD data are from Yanai et al. (2013). Wet deposition and stream export are from Rosi Marshall et al. (2016), and dry deposition is estimated from Yanai et al. (2013).**

in soil respiration. Loss to deep soil therefore remains the most plausible explanation.

This is despite soil solution DOC flux calculations, based on zero tension lysimeter

samples, that show that eluviation of DOC could account for less than 10% of the

observed loss in the Oa horizon (data from Driscoll, personal communication). As others

have eloquently put it, “Once you eliminate the impossible, whatever remains, no matter how improbable, must be the truth.” (Doyle 1890, Nimoy et al. 1991)

If retention in the deep soil is the sink of this SOM, this raises important questions about what determines the capacity of mineral soils to retain and protect SOM from decomposition. DOM export regionally has increased significantly with much smaller changes in alkalinity, yet it would seem that the Ca-enriched watershed has nearly quantitatively retained the SOM lost from organic soil horizons. Differences in the capacity of watersheds to re-sequester mobilized DOM may result from differences in soil texture, clay mineralogy, and watershed hydrology. No studies, to my knowledge, currently link edaphic properties of deep soils to the relative retention or export of DOM from recovering watersheds experiencing organic horizon SOM loss. These factors may be a primary control on the great variability in the extent to which headwater streams are browning. Cross-site comparisons of deep soil properties with stream DOC export would be a fruitful line of future research.

This also raises the question of whether losses of surficial pools of SOC, as forests recover from acid precipitation, are indicative of decreases in total ecosystem C stocks, or if paradoxically this might drive an increase in ecosystem retention of C in deep soil pools. If soil C in organic horizons is more mobile due to decreases in soil acidity, this may drive a redistribution of soil C from organic horizons into deep horizons where organo-mineral associations can protect SOC from degradation. In this manner,

ecosystem recovery from acid precipitation could *increase* the terrestrial C sink, rather than decrease it, as others have proposed (Oulelhe et al. 2011, Lawrence et al. 2012). Acid rain may have driven accumulation of SOM in surficial soils, but this retention of soils in upper horizons may have caused depletion of SOM in deep soils, meaning that deep mineral soils are under-saturated with SOM, relative to their capacity to adsorb it. If greater ecosystem C is being sequestered in deep soil, an important question then becomes how readily exhaustible this storage capacity is. Testing this hypothesis would require long-term soil monitoring across acid-impacted regions that a) puts focus on whole-profile SOM stocks, rather than just surficial soils, and b) embraces a three-dimensional model of soil development and C redistribution, rather than traditional one-dimensional models of soil C movement (*sensu* Bailey et al. 2014). Further, evidence for this hypothesis would need to be weighed against alternative drivers of C accumulation in deep soil, such as long-term recovery from disturbance (Huntington 2005, Lovett et al. *in review*).

Finally, this work refocuses attention on the role that shifts in plant community composition may have in determining ecosystem C and N cycling. In Chapter 2 I showed that the presence of sugar maple saplings enhanced DOC solubility and soil respiration in soils when soil pH was altered. In chapter 3, I showed that accelerated leaf litter N cycling was coincident with recovery in sugar maple biomass. Further work is called for to concretely link changes in maple abundances with differences in N cycling.

While sugar maples in the past have been linked to enhanced N cycling (Lovett et al. 2002), and maples have recently been shown to have a positive growth response to ecosystem recovery from acid rain (Lawrence et al. 2017), it remains an open question how much this natural recovery of maples may affect ecosystem N retention. Again, the Hubbard Brook experiment may be a useful end member of recovery of maple populations, but given that stream inorganic N concentrations across the region are at historic lows (Bernal et al. 2012), it is unclear if the patterns of high watershed N export observed at HBEF represent a likely future scenario in unmodified ecosystems.

Even if the Ca-enriched watershed is a harbinger of changes to come in N cycling and forest demography across temperate forests in the Northeast, it is also important to bear in mind other possible drivers for these changes. For example, others have proposed that less retentive N cycling can result in communities dominated by arbuscular mycorrhizal associated trees generally (Phillips et al. 2013), and declines in ectomycorrhizal species (e.g. via beech bark disease) may shift forests toward more arbuscular mycorrhizal domination. It is therefore important to consider whether any observed changes in ecosystem N retention are due to recovery of a Ca-sensitive species such as sugar maple, or if these effects are due to demographic factors unrelated to acid precipitation. This emphasizes the need to consider all acid rain recovery research in the context of multiple other anthropogenic stressors, such as introduced pests and diseases, climate change, and N deposition.

## **Appendix A: Soil carbon losses due to higher pH offset vegetation gains due to calcium enrichment in an acid mitigation experiment: Supplement**

### ***A.1 Preliminary Experiment: Laboratory Soil Manipulations***

#### **A.1.1 Supplemental methods**

In addition to examining the long-term soil response to the chemical amendments in the mesocosm experiment, we also performed laboratory chemical manipulations of soils from the same pedon to measure the immediate impact of the chemical amendments on soil respiration potential. In August 2016, we excavated a soil immediately adjacent to the mesocosm excavation site, applied the same chemical amendments as in the mesocosm experiment (n = 5), and measured short-term soil respiration potential immediately following excavation and treatment. The same protocols were followed as in the mesocosm experiments.

#### **A.1.2 Supplemental results**

In the laboratory soil experiment, Ca amendment had a negative effect on respiration for soils from all horizons (Figure 19). The Ca treatment decreased respiration by 39.3%, 17.4%, and 9.5% in the leaf litter, humic horizon, and mineral horizon, respectively ( $p < 0.05$ ). In all horizons, a similar decrease in respiration was noted in the KCl amendment, supporting the conclusion that this decrease in respiration potential was a result of salt stress, rather than inhibition by Ca per se. In contrast, the alkalinity-only treatment resulted in significant increases in respiration of 10.5%, 16.5%,

and 7.0% above controls in the leaf litter, humic horizon, and mineral horizon, respectively ( $p < 0.05$ .) Post-hoc comparisons (Tukey's method) showed that the Ca x alkalinity treatment was not significantly different from the Ca treatment for any horizon, suggesting that salt stress more than offset any of the positive effects of alkalinity on microbial respiration.

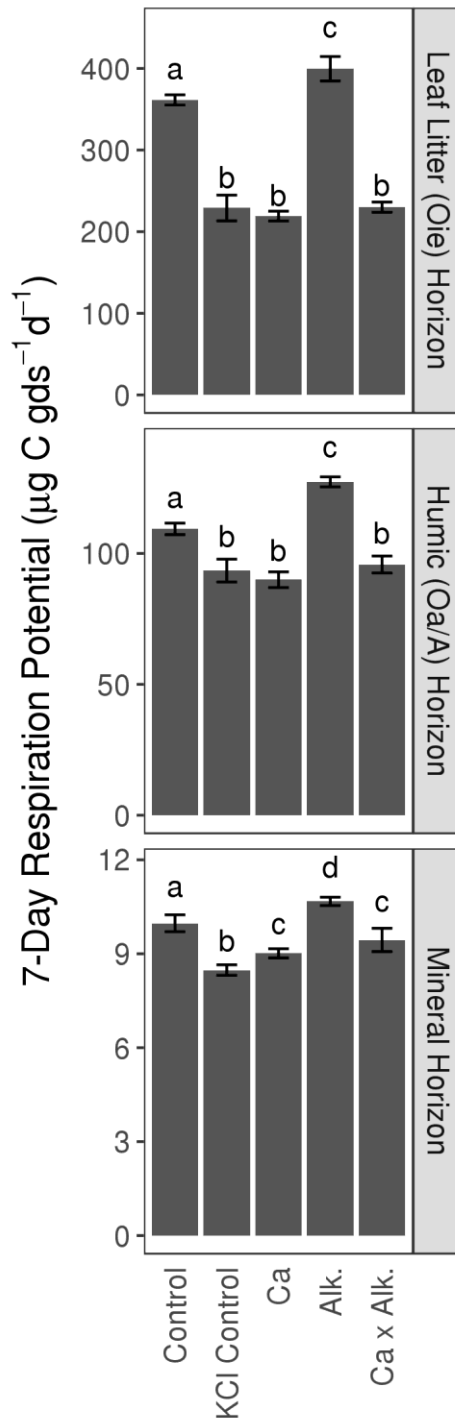


Figure 19: Short term soil microbial respiration potential of soils in laboratory soil manipulations. Error bars are 95% confidence intervals. Letters indicate significant differences between treatments within soil horizon. (Tukey's test,  $p < 0.05$ ).

## ***A.2 Plant morphological trait analysis***

### **A.2.1 Supplemental methods**

Plants were kept moist and plant traits were measured within 4 hours of harvest. We separated each plant into leaves, aboveground woody biomass, coarse roots (> 2mm) and fine roots (<2mm). Coarse roots and fine roots were treated separately because the great majority of fine root biomass was produced during the duration of the experiment, whereas the coarse root fraction was substantially established before planting. We scanned leaves and roots and measured leaf and root traits with WinFolia (Regent Instruments 2009a) and WinRhizo (Regent Instruments 2009b). We measured leaf area and root length in 0.5 mm size class increments from 0 to 4.5mm, as well as root tip counts.

In some samples, the software identified > 2mm roots that we had mistakenly identified as < 2 mm roots. We corrected the fine root mass to reflect this, multiplying the root mass by the proportion of root volume composed of < 2 mm roots. This correction did not change the conclusions of our analysis.

Root to shoot ratio was calculated as the total aboveground biomass divided by the total belowground biomass. Specific root length (SRL) was calculated as the total root length of all size classes divided by the total belowground biomass. Since the root mass was dominated by the large taproot that was already established pre-planting, we also calculated the fine root SRL as the length of roots < 2mm divided by the mass of

roots < 2 mm. We felt that this would better capture root properties of roots that were grown during the experiment. We calculated specific leaf area as the total leaf area divided by the mass of leaves. Root tips per unit biomass were calculated using the entire plant biomass.

## A.2.2 Supplemental results

We found no significant effects of any treatment (2-way ANOVA,  $\alpha=0.05$ ) for any of the plant morphological traits that we measured. Means and standard errors of ten replicates are reported in Table 4.

**Table 4: Plant biomass and morphological traits. Means and standard errors of ten replicates are reported.**

	Treatment			
	<u>Control</u>	<u>Ca</u>	<u>Alk.</u>	<u>Ca x Alk.</u>
Initial plant biomass (g)	7.72 (0.61)	5.61 (0.68)	5.22 (0.5)	6.34 (0.54)
Plant biomass (g)	14.3 (1.3)	13.1 (1.8)	11.2 (1.3)	14 (1.3)
Aboveground biomass (g)	6.84 (0.68)	5.9 (0.84)	5.09 (0.66)	6.78 (0.69)
Belowground Biomass (g)	7.50 (0.72)	7.18 (0.95)	6.13 (0.71)	7.20 (0.65)
Leaf biomass (g)	3.10 (0.31)	3.23 (0.46)	2.82 (0.37)	3.38 (0.4)
Fine root (< 2 mm) biomass (g)	0.465 (0.098)	0.437 (0.058)	0.402 (0.052)	0.367 (0.061)
Root:shoot ratio	0.937 (0.079)	0.823 (0.035)	0.839 (0.042)	0.933 (0.035)
Specific root length (m g <sup>-1</sup> )	0.218 (0.02)	0.296 (0.04)	0.35 (0.04)	0.251 (0.028)
Fine root (< 2 mm) SRL (m g <sup>-1</sup> )	4.10 (0.75)	4.17 (0.34)	4.82 (0.49)	5.00 (0.63)
Specific leaf area (m <sup>2</sup> kg <sup>-1</sup> )	16.9 (0.54)	16.3 (0.36)	16.3 (0.70)	16.1 (0.59)
Root Tips (#)	3360 (390)	3920 (460)	3930 (470)	3620 (450)
Root tips per unit biomass (# g <sup>-1</sup> )	242 (24)	332 (40)	394 (53)	279 (42)

## **A.3 Soil analyses**

### **A.3.1 Supplemental methods**

#### **A.3.1.1 Soil physical and chemical analyses**

We measured soil gravimetric water content (GWC) by drying soils at 105 °C for 24h, and soil organic matter content by loss on ignition at 550 °C, a reliable metric of organic matter content in these soils (Johnson et al. 2014). We determined soil pH potentiometrically in a 2:1 water : soil slurry using a DL-25 pH probe (Mettler-Toledo, Columbus, OH). We extracted exchangeable Ca with 1 M ammonium acetate and exchangeable Al using 2 M potassium chloride, following Robertson et al. (1999a). We filtered all extracts through Acrodisc 0.2 µm polysulfone membrane filters (Pall Corporation, Port Washington, NY) and analyzed them by flame AA spectrometry on a PE 3100 spectrometer (Perkin-Elmer, Waltham, MA). As an index of ionic strength, we measured the electroconductivity of 5:1 water : soil extracts and converted this to mass of total dissolved solids (Richards et al. 1954).

#### **A.3.1.2 Microbial respiration potential assays**

We performed long-term soil respiration potential assays following a modified version of the protocol presented in Robertson et al. (1999b). The incubations were performed in 60 ml i-Chem vials (Thermo Fisher, Waltham, MA) with PTFE-silicone septa. We measured cumulative respiration over 24 h on days 1, 2, 4, 8, 16, 35, and 75 post-harvest. On the day preceding the measurement day, vials were thoroughly vented

to the atmosphere by repeatedly blowing laboratory air into the headspaces of the vials. Vials were then immediately capped, recording the incubation start time, and allowed to incubate in a dark cabinet at 21 °C for approximately 24h. Following incubation, headspace carbon dioxide concentrations were sampled using a gas syringe and measured using a LI-820 infrared gas analyzer (Li-Cor Biosciences, Lincoln, NE) in a flow injection configuration. We calculated total carbon dioxide production per day based on the final headspace gas concentration and the total time elapsed between capping and measurement; initial headspace gas concentrations of each vial were assumed to be equal to the mean concentration of the blank samples. Vials were stored loosely capped in a dark cabinet between measurements. Soil water content was held relatively stable throughout the incubations. Mean initial soil water content was 52.7% (SD = 4.5%) for organic soils and 38.3% (SD = 3.1%) for mineral horizon soils. Soil respiration on day 1 was measured at the unadjusted water content of each sample. After the day 1 assay, we adjusted the water content of dry soils to within 5% of the initial mean water content. Six out of two hundred samples required such adjustment. Beginning with the day 16 assay, we adjusted soil moisture content of all soils to the mean initial moisture content of each horizon, at least five days before performing each assay.

### **A.3.2 Supplemental results**

Here we report the individual results of extracellular enzyme assays for five carbon-degrading enzymes as well as phosphatase. There were no significant treatment effects within groups (2-way ANOVA,  $\alpha=0.0125$ ). The phosphatase enzyme assay was excluded from the C-degrading enzyme sum that we report in Tables 1 and 2. Means and standard errors of ten replicates are presented in Table 5.

**Table 5: Soil exoenzyme potential assays. All measurements are in units of nmol gds<sup>-1</sup> h<sup>-1</sup>. Means and standard errors (in parentheses) of ten replicates are reported.**

	Unplanted			
	Control	Ca	Alk.	Ca x Alk.
<b><u>Organic Horizon</u></b>				
α-glucosidase (AG)	11.7 (0.55)	15.9 (0.41)	14.5 (0.45)	15.7 (0.78)
β-glucosidase (BG)	150 (4.2)	168 (3.7)	182 (3.6)	189 (6.4)
Cellobiohydrolase (CB)	31.3 (1.3)	37.3 (1.2)	35 (0.99)	39.2 (2)
β-xylosidase (XYL)	73.1 (2.7)	76.7 (1.7)	86.7 (2.1)	85.3 (3.1)
N-acetylglucosaminadase (NAG)	189 (7.4)	193 (5.4)	184 (5.3)	184 (6.3)
Acid phosphatase (PHOS)	373 (12)	454 (11)	548 (16)	709 (65)
<b><u>Mineral Horizon</u></b>				
α-glucosidase (AG)	3.28 (0.24)	2.78 (0.14)	3.57 (0.25)	3.48 (0.18)
β-glucosidase (BG)	81.6 (3.1)	73.6 (1.5)	79.8 (2.5)	82.5 (2.3)
Cellobiohydrolase (CB)	23.2 (1.0)	20.6 (0.51)	22.8 (0.82)	23.3 (0.83)
β-xylosidase (XYL)	53.4 (1.8)	48 (0.89)	55.7 (1.6)	55.7 (1.5)
N-acetylglucosaminadase (NAG)	45.2 (2.0)	45.8 (1.6)	51.9 (1.9)	49.2 (1.7)
Acid phosphatase (PHOS)	242 (6.2)	253 (5.7)	269 (7.3)	307 (11)
	Planted			
	Control	Ca	Alk.	Ca x Alk.
<b><u>Organic Horizon</u></b>				
α-glucosidase (AG)	18.1 (0.9)	17.1 (0.47)	16.8 (0.56)	14.8 (0.59)
β-glucosidase (BG)	206 (7.3)	203 (4.5)	202 (5.9)	186 (6.4)
Cellobiohydrolase (CB)	49.4 (2.6)	44.6 (1.1)	41.7 (1.9)	40.2 (1.9)
β-xylosidase (XYL)	103 (3.5)	103 (2.2)	104 (3.2)	90.2 (3.5)
N-acetylglucosaminadase (NAG)	297 (11)	319 (7.5)	297 (5.9)	250 (11)
Acid phosphatase (PHOS)	472 (16)	514 (12)	520 (11)	437 (15)
<b><u>Mineral Horizon</u></b>				
α-glucosidase (AG)	3.09 (0.28)	2.74 (0.14)	2.9 (0.15)	3.57 (0.19)
β-glucosidase (BG)	77.2 (3.4)	71.5 (1.8)	72.9 (2.1)	81.2 (2.7)
Cellobiohydrolase (CB)	23.2 (1.2)	20.2 (0.55)	19.2 (0.47)	23.1 (0.89)
β-xylosidase (XYL)	51.5 (1.9)	45.5 (1.1)	49.3 (1.2)	55.4 (1.8)
N-acetylglucosaminadase (NAG)	47.6 (2.7)	44.5 (1.6)	47.4 (1.5)	43 (1.7)
Acid phosphatase (PHOS)	234 (8.7)	239 (6.9)	236 (5.4)	242 (6.8)

We found that WEOC and microbial respiration were not strongly correlated, either within treatment groups or across treatment groups, as shown in Figure 20.

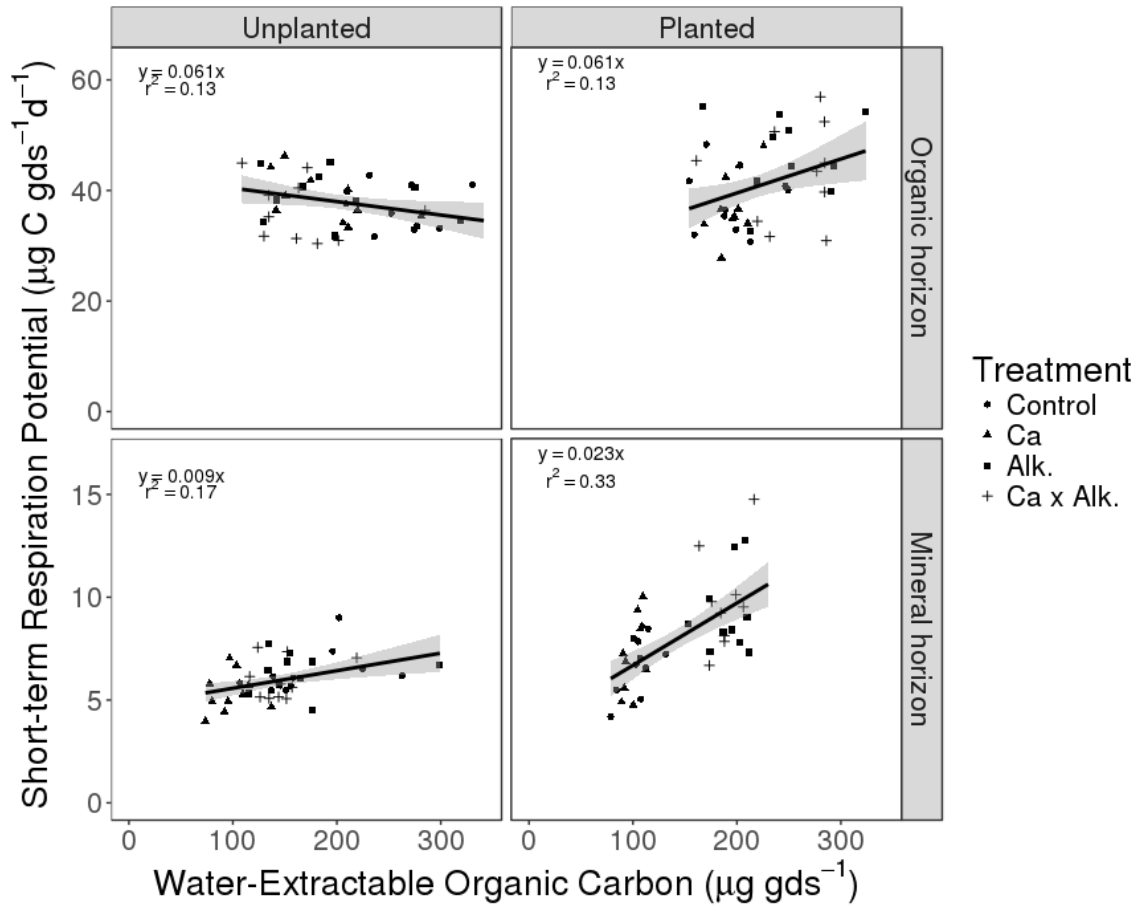


**Figure 20: Relationships between WEOC and short-term soil microbial respiration across treatment groups. Only significant linear regressions are displayed. These single-predictor regressions do not include terms for treatment and are for data visualization purposes only.**

## **Appendix B: A watershed acid rain remediation experiment increases the flashiness of terrestrial nitrogen export but increases in-stream nitrogen retention: Supplement**

### ***B.1 Supplemental methods***

In early September 2015, we sampled five debris dams in both the stream draining the CaSiO<sub>3</sub>-enriched watershed and Bear Brook, immediately downstream of the biogeochemical reference watershed. We used a slide hammer corer to sample sediments to 10 cm or refusal, taking 5 cores in each debris dam. We bulked the sediments by watershed and homogenized them by hand.

We performed potential denitrification enzyme activity assays on these sediments in the laboratory. For each sample, we performed four replicate denitrification enzyme activity assays following the protocol of Groffman et al. (1999), amending each sample with 10 ml of 2.5 mg N L<sup>-1</sup> KNO<sub>3</sub> solution, but no glucose addition. We analyzed N<sub>2</sub>O concentrations on a Shimadzu GC17A gas chromatograph. We used a student's t-test to test for differences in mean denitrification rates.

### ***B.2 Supplemental results and discussion***

Denitrification potential rates were significantly higher in the Ca-enriched watershed compared to the reference watershed ( $p = 0.036$ ) (Figure 21). The mean rate in the reference watershed was 1.48 (SE: +/-0.77)  $\mu\text{g N gds}^{-1} \text{d}^{-1}$ , and in the 4.18 (SE: +/- 0.18)  $\mu\text{g N gds}^{-1} \text{d}^{-1}$  in the Ca-enriched watershed, a 2.8-fold difference. We emphasize that the

scope of this sampling and replication scheme is very limited, and that these data only suggest a potentially enhanced denitrification sink.

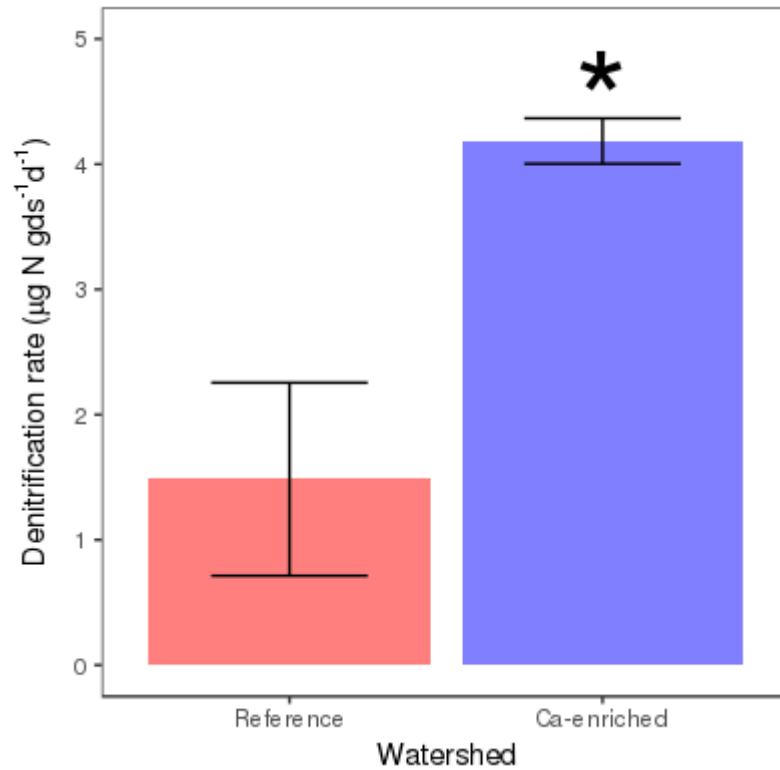


**Figure 21: Potential denitrification rates of four replicate debris dam sediment samples. The asterisk indicates a significant difference ( $p < 0.05$ ) between reference and Ca-enriched sediments. Means and standard errors are shown.**

## Works Cited

- Aber, J., G. Berntson, W. Currie, I. Fernandez, M. Kamakea, A. Magill, W. McDowell, S. McNulty, K. Nadelhoffer, and L. Rustad. 1998. Nitrogen saturation in temperate forest ecosystems: hypotheses revisited. *BioScience* 48:921.
- Aber, J. D., K. J. Nadelhoffer, P. Steudler, and J. M. Melillo. 1989. Nitrogen Saturation in Northern Forest Ecosystems. *Bioscience* 39:378.
- Aber, S. V. Ollinger, C. T. Driscoll, G. E. Likens, R. T. Holmes, R. J. Freuder, and C. L. Goodale. 2002. Inorganic nitrogen losses from a forested ecosystem in response to physical, chemical, biotic and climatic perturbations. *Ecosystems* 5:648–658.
- Abreu, C., C. Hamilton, T. Muraoka, and A. F. Lavorante. 2003. Exchangeable aluminum evaluation in acid soils. *Scientia Agricola* 60:543–548.
- Avagyan, A., B. R. K. Runkle, and L. Kutzbach. 2014. Application of high-resolution spectral absorbance measurements to determine dissolved organic carbon concentration in remote areas. *Journal of Hydrology* 517:435–446.
- Averill, C., and C. V. Hawkes. 2016. Ectomycorrhizal fungi slow soil carbon cycling. *Ecology Letters* 19:937–947.
- B J Peterson, W. M. W. 2001. Control of Nitrogen Export From Watersheds By Headwater Streams. *Science (New York, N.Y.)* 292:86–90.
- Bailey, S. W. 2000. Geologic and Edaphic Factors Influencing Susceptibility of Forest Soils to Environmental Change. Pages 27–49 *Responses of Northern U.S. Forests to Environmental Change*. Springer, New York, NY.
- Bailey, S. W., P. A. Brousseau, K. J. McGuire, and D. S. Ross. 2014. Influence of landscape position and transient water table on soil development and carbon distribution in a steep, headwater catchment.
- Baker, D. B., R. P. Richards, T. T. Loftus, and J. W. Kramer. 2004. A New Flashiness Index: Characteristics and Applications to Midwestern Rivers and Streams. *JAWRA Journal of the American Water Resources Association* 40:503–522.

- Balaria, A., C. E. Johnson, P. M. Groffman, and M. C. Fisk. 2015. Effects of calcium silicate treatment on the composition of forest floor organic matter in a northern hardwood forest stand. *Biogeochemistry* 122:313–326.
- Band, L. E., C. L. Tague, P. Groffman, and K. Belt. 2001. Forest ecosystem processes at the watershed scale: hydrological and ecological controls of nitrogen export. *Hydrological Processes* 15:2013–2028.
- Battles, J. J., T. J. Fahey, C. T. Driscoll, J. D. Blum, and C. E. Johnson. 2014. Restoring Soil Calcium Reverses Forest Decline. *Environmental Science & Technology Letters* 1:15–19.
- Bell, C. W., B. E. Fricks, J. D. Rocca, J. M. Steinweg, S. K. McMahon, and M. D. Wallenstein. 2013. High-throughput Fluorometric Measurement of Potential Soil Extracellular Enzyme Activities. *Journal of Visualized Experiments*.
- Bernal, S., L. O. Hedin, G. E. Likens, S. Gerber, and D. C. Buso. 2012a. Complex response of the forest nitrogen cycle to climate change. *Proceedings of the National Academy of Sciences*:201121448.
- Bernal, S., D. Schiller, E. Martí, and F. Sabater. 2012b. In-stream net uptake regulates inorganic nitrogen export from catchments under base flow conditions. *Journal of Geophysical Research: Biogeosciences* 117.
- Bernhardt, E. S., G. E. Likens, D. C. Buso, and C. T. Driscoll. 2003. In-stream uptake dampens effects of major forest disturbance on watershed nitrogen export. *Proceedings of the National Academy of Sciences* 100:10304–10308.
- Bernhardt, E. S., G. E. Likens, R. O. Hall, D. C. Buso, S. G. Fisher, T. M. Burton, J. L. Meyer, W. H. McDowell, M. S. Mayer, W. B. Bowden, S. E. G. Findlay, K. H. Macneale, R. S. Stelzer, and W. H. Lowe. 2005. Can't See the Forest for the Stream? In-stream Processing and Terrestrial Nitrogen Exports. *BioScience* 55:219–230.
- Bernot, M. J., and W. K. Dodds. 2005. Nitrogen Retention, Removal, and Saturation in Lotic Ecosystems. *Ecosystems* 8:442–453.
- Bond, N. 2016. hydrostats: Hydrologic Indices for Daily Time Series Data. CRAN.

- Bormann, F. H., and G. E. Likens. 1979. Pattern and process in a forested ecosystem: disturbance, development, and the steady state based on the Hubbard Brook ecosystem study. Springer-Verlag.
- Boyer, J. N., and P. M. Groffman. 1996. Bioavailability of water extractable organic carbon fractions in forest and agricultural soil profiles. *Soil Biology and Biochemistry* 28:783–790.
- Brookshire, E. N. J., H. M. Valett, and S. Gerber. 2009. Maintenance of terrestrial nutrient loss signatures during in-stream transport. *Ecology* 90:293–299.
- Burns, D. A., M. R. McHale, C. T. Driscoll, and K. M. Roy. 2006. Response of surface water chemistry to reduced levels of acid precipitation: comparison of trends in two regions of New York, USA. *Hydrological Processes* 20:1611–1627.
- Buso, D. C., G. E. Likens, and J. S. Eaton. 2000. Chemistry of precipitation, streamwater, and lakewater from the Hubbard Brook Ecosystem Study: a record of sampling protocols and analytical procedures. Gen. Tech. Rep. NE-275. Newtown Square, PA: U.S. Department of Agriculture, Forest Service, Northeastern Research Station. 52 p. 275.
- Campbell, J. 2015. Hubbard Brook Experimental Forest (US Forest Service): Daily Streamflow by Watershed, 1956 - present. Environmental Data Initiative.
- Chapin, F. S., L. R. Walker, C. L. Fastie, and L. C. Sharman. 1994. Mechanisms of Primary Succession Following Deglaciation at Glacier Bay, Alaska. *Ecological Monographs* 64:149–175.
- Chin, Y.-P., G. Aiken, and E. O'Loughlin. 1994. Molecular Weight, Polydispersity, and Spectroscopic Properties of Aquatic Humic Substances. *Environmental Science & Technology* 28:1853–1858.
- Cho, Y., C. T. Driscoll, C. E. Johnson, J. D. Blum, and T. J. Fahey. 2012. Watershed-Level Responses to Calcium Silicate Treatment in a Northern Hardwood Forest. *Ecosystems* 15:416–434.
- Cho, Y., C. T. Driscoll, C. E. Johnson, and T. G. Siccama. 2009. Chemical changes in soil and soil solution after calcium silicate addition to a northern hardwood forest. *Biogeochemistry* 100:3–20.

- Clarholm, M., and U. Skyllberg. 2013. Translocation of metals by trees and fungi regulates pH, soil organic matter turnover and nitrogen availability in acidic forest soils. *Soil Biology and Biochemistry* 63:142–153.
- Coughlan, A. P., Y. Dalpé, L. Lapointe, and Y. Piché. 2000. Soil pH-induced changes in root colonization, diversity, and reproduction of symbiotic arbuscular mycorrhizal fungi from healthy and declining maple forests. *Canadian Journal of Forest Research* 30:1543–1554.
- Covington, W. W. 1981. Changes in Forest Floor Organic Matter and Nutrient Content Following Clear Cutting in Northern Hardwoods. *Ecology* 62:41–48.
- Creed, I. F., L. E. Band, N. W. Foster, I. K. Morrison, J. A. Nicolson, R. S. Semkin, and D. S. Jeffries. 1996. Regulation of Nitrate-N Release from Temperate Forests: A Test of the N Flushing Hypothesis. *Water Resources Research* 32:3337–3354.
- Curtin, D., M. E. Peterson, and C. R. Anderson. 2016. pH-dependence of organic matter solubility: Base type effects on dissolved organic C, N, P, and S in soils with contrasting mineralogy. *Geoderma* 271:161–172.
- Detty, J. M., and K. J. McGuire. 2010. Threshold changes in storm runoff generation at a till-mantled headwater catchment. *Water Resources Research* 46:W07525.
- Donnelly, J. 1973. Duration of cold storage alters time required for seedling bud-break. University of Vermont, Montpelier, VT.
- Doyle, A. C. 1890. *The Sign of Four*. Penguin, London ; New York.
- Driscoll, C. 2016a. Chemistry of freely-draining soil solutions at the Hubbard Brook Experimental Forest, Watershed 1, 1996 - present. Environmental Data Initiative.
- Driscoll, C. T. 2016b. Longitudinal Stream Chemistry at the Hubbard Brook Experimental Forest, Watershed 6, 1982 - present. Environmental Data Initiative.
- Driscoll, C. T. 2016c. Longitudinal Stream Chemistry at the Hubbard Brook Experimental Forest, Watershed 1, 1991 - present. Environmental Data Initiative.
- Driscoll, C. T., C. P. Cirimo, T. J. Fahey, V. L. Blette, P. A. Bukaveckas, D. A. Burns, C. P. Gubala, D. J. Leopold, R. M. Newton, D. J. Raynal, C. L. Schofield, J. B. Yavitt,

- and D. B. Porcella. 1996. The experimental watershed liming study: Comparison of lake and watershed neutralization strategies. *Biogeochemistry* 32:143–174.
- Driscoll, C. T., K. M. Driscoll, H. Fakhraei, and K. Civerolo. 2016. Long-term temporal trends and spatial patterns in the acid-base chemistry of lakes in the Adirondack region of New York in response to decreases in acidic deposition. *Atmospheric Environment*.
- Driscoll, C. T., G. B. Lawrence, A. J. Bulger, T. J. Butler, C. S. Cronan, C. Eagar, K. F. Lambert, G. E. Likens, J. L. Stoddard, and K. C. Weathers. 2001. Acidic Deposition in the Northeastern United States: Sources and Inputs, Ecosystem Effects, and Management Strategies. *BioScience* 51:180–198.
- DS Jenkinson, D. P. 1976. The Effects of Biocidal Treatments on Metabolism in Soil – V. A Method for Measuring Soil Biomass. *Soil Biology & Biochemistry* 8:209–213.
- Durán, J., J. L. Morse, P. M. Groffman, J. L. Campbell, L. M. Christenson, C. T. Driscoll, T. J. Fahey, M. C. Fisk, G. E. Likens, J. M. Melillo, M. J. Mitchell, P. H. Templer, and M. A. Vadeboncoeur. 2016. Climate change decreases nitrogen pools and mineralization rates in northern hardwood forests. *Ecosphere* 7:n/a-n/a.
- Ekström, S. M., E. S. Kritzberg, D. B. Kleja, N. Larsson, P. A. Nilsson, W. Graneli, and B. Bergkvist. 2011. Effect of Acid Deposition on Quantity and Quality of Dissolved Organic Matter in Soil–Water. *Environmental Science & Technology* 45:4733–4739.
- Erlandsson, M., N. Cory, J. Fölster, S. Köhler, H. Laudon, G. A. Weyhenmeyer, and K. Bishop. 2011. Increasing Dissolved Organic Carbon Redefines the Extent of Surface Water Acidification and Helps Resolve a Classic Controversy. *BioScience* 61:614–618.
- Eshleman, K. N., R. D. Sabo, and K. M. Kline. 2013. Surface Water Quality Is Improving due to Declining Atmospheric N Deposition. *Environmental Science & Technology* 47:12193–12200.
- Evans, C. D., C. L. Goodale, S. J. M. Caporn, N. B. Dise, B. A. Emmett, I. J. Fernandez, C. D. Field, S. E. G. Findlay, G. M. Lovett, H. Meesenburg, F. Moldan, and L. J. Sheppard. 2008. Does elevated nitrogen deposition or ecosystem recovery from acidification drive increased dissolved organic carbon loss from upland soil? A

- review of evidence from field nitrogen addition experiments. *Biogeochemistry* 91:13–35.
- Evans, C. D., T. G. Jones, A. Burden, N. Ostle, P. Zieliński, M. D. A. Cooper, M. Peacock, J. M. Clark, F. Oulehle, D. Cooper, and C. Freeman. 2012. Acidity controls on dissolved organic carbon mobility in organic soils. *Global Change Biology* 18:3317–3331.
- Evans, C., and T. D. Davies. 1998. Causes of concentration/discharge hysteresis and its potential as a tool for analysis of episode hydrochemistry. *Water Resources Research* 34:129–137.
- Fahey, T. J. 2016. Coarse Litterfall Data at the Hubbard Brook Experimental Forest, 1996 - present. Environmental Data Initiative.
- Fahey, T. J., A. K. Heinz, J. J. Battles, M. C. Fisk, C. T. Driscoll, J. D. Blum, and C. E. Johnson. 2016. Fine root biomass declined in response to restoration of soil calcium in a northern hardwood forest. *Canadian Journal of Forest Research* 46:738–744.
- Fahey, T. J., and J. W. Hughes. 1994. Fine Root Dynamics in a Northern Hardwood Forest Ecosystem, Hubbard Brook Experimental Forest, NH. *Journal of Ecology* 82:533–548.
- Fahey, T. J., T. G. Siccama, C. T. Driscoll, G. E. Likens, J. Campbell, C. E. Johnson, J. J. Battles, J. D. Aber, J. J. Cole, M. C. Fisk, P. M. Groffman, S. P. Hamburg, R. T. Holmes, P. A. Schwarz, and R. D. Yanai. 2005. The Biogeochemistry of Carbon at Hubbard Brook. *Biogeochemistry* 75:109–176.
- Fierer, N., J. P. Schimel, and P. A. Holden. 2003. Variations in microbial community composition through two soil depth profiles. *Soil Biology and Biochemistry* 35:167–176.
- Finzi, A. C., R. Z. Abramoff, K. S. Spiller, E. R. Brzostek, B. A. Darby, M. A. Kramer, and R. P. Phillips. 2015. Rhizosphere processes are quantitatively important components of terrestrial carbon and nutrient cycles. *Global Change Biology* 21:2082–2094.

- Fisher, S. G., and G. E. Likens. 1973. Energy Flow in Bear Brook, New Hampshire: An Integrative Approach to Stream Ecosystem Metabolism. *Ecological Monographs* 43:421–439.
- Fisk, M. C., W. R. Kessler, A. Goodale, T. J. Fahey, P. M. Groffman, and C. T. Driscoll. 2006. Landscape variation in microarthropod response to calcium addition in a northern hardwood forest ecosystem. *Pedobiologia* 50:69–78.
- Fontaine, S., S. Barot, P. Barré, N. Bdioui, B. Mary, and C. Rumpel. 2007. Stability of organic carbon in deep soil layers controlled by fresh carbon supply. *Nature* 450:277–280.
- Gächter, R., and B. Müller. 2003. Why the phosphorus retention of lakes does not necessarily depend on the oxygen supply to their sediment surface. *Limnology and Oceanography* 48:929–933.
- Gbondo-Tugbawa, S. S., C. T. Driscoll, J. D. Aber, and G. E. Likens. 2001. Evaluation of an integrated biogeochemical model (PnET-BGC) at a northern hardwood forest ecosystem. *Water Resources Research* 37:1057–1070.
- Geissen, V., and G. W. Brümmer. 1999. Decomposition rates and feeding activities of soil fauna in deciduous forest soils in relation to soil chemical parameters following liming and fertilization. *Biology and Fertility of Soils* 29:335–342.
- Goodale, C. L., J. D. Aber, and P. M. Vitousek. 2003. An Unexpected Nitrate Decline in New Hampshire Streams. *Ecosystems* 6:0075–0086.
- Green, M. B., A. S. Bailey, S. W. Bailey, J. J. Battles, J. L. Campbell, C. T. Driscoll, T. J. Fahey, L. C. Lepine, G. E. Likens, S. V. Ollinger, and P. G. Schaberg. 2013. Decreased water flowing from a forest amended with calcium silicate. *Proceedings of the National Academy of Sciences* 110:5999–6003.
- Grimm, N. B., S. G. Fisher, and W. L. Minckley. 1981. Nitrogen and phosphorus dynamics in hot desert streams of Southwestern U.S.A. *Hydrobiologia* 83:303–312.
- Groffman, P. 2013a. Long-term measurements of microbial biomass and activity at the Hubbard Brook Experimental Forest, 1994 - present. Environmental Data Initiative.

- Groffman, P. M. 2013b. Microbial biomass and activity.  
<http://hubbardbrook.org/data/dataset.php?id=67>.
- Groffman, P. M., K. Butterbach-Bahl, R. W. Fulweiler, A. J. Gold, J. L. Morse, E. K. Stander, C. Tague, C. Tonitto, and P. Vidon. 2009. Challenges to incorporating spatially and temporally explicit phenomena (hotspots and hot moments) in denitrification models. *Biogeochemistry* 93:49–77.
- Groffman, P. M., T. J. Fahey, M. C. Fisk, J. B. Yavitt, R. E. Sherman, P. J. Bohlen, and J. C. Maerz. 2015. Earthworms increase soil microbial biomass carrying capacity and nitrogen retention in northern hardwood forests. *Soil Biology and Biochemistry* 87:51–58.
- Groffman, P. M., M. C. Fisk, C. T. Driscoll, G. E. Likens, T. J. Fahey, C. Eagar, and L. H. Pardo. 2006. Calcium Additions and Microbial Nitrogen Cycle Processes in a Northern Hardwood Forest. *Ecosystems* 9:1289–1305.
- Grogan, P., T. D. Burns, and F. S. Chapin Iii. 2000. Fire effects on ecosystem nitrogen cycling in a Californian bishop pine forest. *Oecologia* 122:537–544.
- Gu, W., C. T. Driscoll, S. Shao, and C. E. Johnson. 2017. Aluminum is more tightly bound in soil after wollastonite treatment to a forest watershed. *Forest Ecology and Management* 397:57–66.
- Halman, J. M., P. G. Schaberg, G. J. Hawley, C. F. Hansen, and T. J. Fahey. 2014. Differential impacts of calcium and aluminum treatments on sugar maple and American beech growth dynamics. *Canadian Journal of Forest Research* 45:52–59.
- Halman, J. M., P. G. Schaberg, G. J. Hawley, L. H. Pardo, and T. J. Fahey. 2013. Calcium and aluminum impacts on sugar maple physiology in a northern hardwood forest. *Tree Physiology* 33:1242–1251.
- Hart, S. C., G. E. Nason, D. D. Myrold, and D. A. Perry. 1994. Dynamics of Gross Nitrogen Transformations in an Old-Growth Forest: The Carbon Connection. *Ecology* 75:880–891.
- Hobbie, S. E., M. Ogdahl, J. Chorover, O. A. Chadwick, J. Oleksyn, R. Zytowskiak, and P. B. Reich. 2007. Tree species effects on soil organic matter dynamics: The role of soil cation composition. *Ecosystems* 10:999–1018.

- Houlton, B. Z., C. T. Driscoll, T. J. Fahey, G. E. Likens, P. M. Groffman, E. S. Bernhardt, and D. C. Buso. 2003. Nitrogen Dynamics in Ice Storm-Damaged Forest Ecosystems: Implications for Nitrogen Limitation Theory. *Ecosystems* 6:431–443.
- Hruska, J., F. Moldan, and P. Krám. 2002. Recovery from acidification in central Europe--observed and predicted changes of soil and streamwater chemistry in the Lysina catchment, Czech Republic. *Environmental Pollution (Barking, Essex: 1987)* 120:261–274.
- Hunt, R. 1982. *Plant Growth Curves: The Functional Approach to Plant Growth Analysis*. Cambridge University Press.
- Huntington, T. G. 2005. Can Nitrogen Sequestration Explain the Unexpected Nitrate Decline in New Hampshire Streams? *Ecosystems; New York* 8:331–333.
- Illmer, P., K. Marschall, and F. Schinner. 1995. Influence of available aluminium on soil micro-organisms. *Letters in Applied Microbiology* 21:393–397.
- Illmer, P., U. Obertegger, and F. Schinner. 2003. Microbiological Properties in Acidic Forest Soils with Special Consideration of KCl Extractable Al. *Water, Air, and Soil Pollution* 148:3–14.
- Inamdar, S. P., S. F. Christopher, and M. J. Mitchell. 2004. Export mechanisms for dissolved organic carbon and nitrate during summer storm events in a glaciated forested catchment in New York, USA. *Hydrological Processes* 18:2651–2661.
- Johnson, C. E., C. T. Driscoll, J. D. Blum, T. J. Fahey, and J. J. Battles. 2014. Soil Chemical Dynamics after Calcium Silicate Addition to a Northern Hardwood Forest. *Soil Science Society of America Journal* 78:1458.
- Johnson, C. E., C. T. Driscoll, T. G. Siccama, and G. E. Likens. 2000. Element Fluxes and Landscape Position in a Northern Hardwood Forest Watershed Ecosystem. *Ecosystems* 3:159–184.
- Johnson, C., and S. P. Hamburg. 2015. Mass and Chemistry of Organic Horizons and Surface Mineral Soils on Watershed 6 at the Hubbard Brook Experimental Forest, 1976 - present. Environmental Data Initiative.
- Johnson, N. M., G. E. Likens, F. H. Bormann, D. W. Fisher, and R. S. Pierce. 1969. A Working Model for the Variation in Stream Water Chemistry at the Hubbard

- Brook Experimental Forest, New Hampshire. *Water Resources Research* 5:1353–1363.
- Joslin, J., J. Kelly, and H. V. Miegroet. 1992. Soil Chemistry and Nutrition of North American Red Spruce-Fir Stands: Evidence for Recent Change. *Journal of Environmental Quality* 21:12–29.
- Judd, K. E., G. E. Likens, and P. M. Groffman. 2007. High Nitrate Retention during Winter in Soils of the Hubbard Brook Experimental Forest. *Ecosystems* 10:217–225.
- Juice, S. M., T. J. Fahey, T. G. Siccama, C. T. Driscoll, E. G. Denny, C. Eagar, N. L. Cleavitt, R. Minocha, and A. D. Richardson. 2006. Response of sugar maple to calcium addition to northern hardwood forest. *Ecology* 87:1267–1280.
- Kalbitz, K., S. Solinger, J.-H. Park, B. Michalzik, and E. Matzner. 2000. Controls on the dynamics of dissolved organic matter in soils: A review. *Soil Science* 165:277–304.
- Kätterer, T., M. Reichstein, O. Andrén, and A. Lomander. 1998. Temperature dependence of organic matter decomposition: a critical review using literature data analyzed with different models. *Biology and Fertility of Soils* 27:258–262.
- Kilpatrick, F. A., and E. D. Cobb. 1985. Measurement of Discharge Using Tracers. Pages 1–49 *Applications of Hydraulics*.
- Kirk, G. J. d., P. H. Bellamy, and R. M. Lark. 2010. Changes in soil pH across England and Wales in response to decreased acid deposition. *Global Change Biology* 16:3111–3119.
- Koenig, L. E., M. D. Shattuck, L. E. Snyder, J. D. Potter, and W. H. McDowell. 2017. Deconstructing the Effects of Flow on DOC, Nitrate, and Major Ion Interactions Using a High-Frequency Aquatic Sensor Network. *Water Resources Research* 53:10655–10673.
- Kooch, Y., S. M. Darabi, and S. M. Hosseini. 2015. Effects of Pits and Mounds Following Windthrow Events on Soil Features and Greenhouse Gas Fluxes in a Temperate Forest. *Pedosphere* 25:853–867.
- Kothawala, D. N., and T. R. Moore. 2009. Adsorption of dissolved nitrogen by forest mineral soils. *Canadian Journal of Forest Research* 39:2381–2390.

- Kothawala, D. N., S. A. Watmough, M. N. Futter, L. Zhang, and P. J. Dillon. 2011. Stream Nitrate Responds Rapidly to Decreasing Nitrate Deposition. *Ecosystems* 14:274–286.
- Kreutzweiser, D. P., P. W. Hazlett, and J. M. Gunn. 2008. Logging impacts on the biogeochemistry of boreal forest soils and nutrient export to aquatic systems: A review. *Environmental Reviews* 16:157–179.
- Lawrence, G. B., P. W. Hazlett, I. J. Fernandez, R. Ouimet, S. W. Bailey, W. C. Shortle, K. T. Smith, and M. R. Antidormi. 2015. Declining Acidic Deposition Begins Reversal of Forest-Soil Acidification in the Northeastern U.S. and Eastern Canada. *Environmental Science & Technology* 49:13103–13111.
- Lawrence, G. B., T. C. McDonnell, T. J. Sullivan, M. Dovciak, S. W. Bailey, M. R. Antidormi, and M. R. Zarfos. 2017. Soil Base Saturation Combines with Beech Bark Disease to Influence Composition and Structure of Sugar Maple-Beech Forests in an Acid Rain-Impacted Region. *Ecosystems*:1–16.
- Lawrence, G. B., W. C. Shortle, M. B. David, K. T. Smith, R. A. F. Warby, and A. G. Lapenis. 2012. Early indications of soil recovery from acidic deposition in U.S. red spruce forests. *Soil Science Society of America Journal* 76:14071417.
- Li, Y., S. J. Chapman, G. W. Nicol, and H. Yao. 2018. Nitrification and nitrifiers in acidic soils. *Soil Biology and Biochemistry* 116:290–301.
- Likens, G. E. 2013. *Biogeochemistry of a Forested Ecosystem*. Springer Science & Business.
- Likens, G. E., F. H. Bormann, and N. M. Johnson. 1969. Nitrification: Importance to Nutrient Losses from a Cutover Forested Ecosystem. *Science* 163:1205–1206.
- Likens, G. E., F. H. Bormann, N. M. Johnson, D. W. Fisher, and R. S. Pierce. 1970. Effects of Forest Cutting and Herbicide Treatment on Nutrient Budgets in the Hubbard Brook Watershed-Ecosystem. *Ecological Monographs* 40:23–47.
- Likens, G. E., and D. C. Buso. 2012. Dilution and the Elusive Baseline. *Environmental Science & Technology* 46:4382–4387.
- Likens, G. E., C. T. Driscoll, and D. C. Buso. 1996. Long-Term Effects of Acid Rain: Response and Recovery of a Forest Ecosystem. *Science* 272:244–246.

- Likens, G. E., C. T. Driscoll, D. C. Buso, T. G. Siccama, C. E. Johnson, G. M. Lovett, T. J. Fahey, W. A. Reiners, D. F. Ryan, C. W. Martin, and S. W. Bailey. 1998. The biogeochemistry of calcium at Hubbard Brook. *Biogeochemistry* 41:89–173.
- Lindeman, R. L. 1942. The Trophic-Dynamic Aspect of Ecology. *Ecology* 23:399–417.
- Liu, B., P. T. Mørkved, Å. Frostegård, and L. R. Bakken. 2010. Denitrification gene pools, transcription and kinetics of NO, N<sub>2</sub>O and N<sub>2</sub> production as affected by soil pH. *FEMS Microbiology Ecology* 72:407–417.
- Lovett, G. M., M. A. Arthur, and K. F. Crowley. 2016. Effects of Calcium on the Rate and Extent of Litter Decomposition in a Northern Hardwood Forest. *Ecosystems* 19:87–97.
- Lovett, G. M., and C. L. Goodale. 2011. A New Conceptual Model of Nitrogen Saturation Based on Experimental Nitrogen Addition to an Oak Forest. *Ecosystems* 14:615–631.
- Lovett, G. M., K. C. Weathers, and M. A. Arthur. 2002. Control of Nitrogen Loss from Forested Watersheds by Soil Carbon:Nitrogen Ratio and Tree Species Composition. *Ecosystems* 5:712–718.
- Lu, X., Q. Mao, F. S. Gilliam, Y. Luo, and J. Mo. 2014. Nitrogen deposition contributes to soil acidification in tropical ecosystems. *Global Change Biology* 20:3790–3801.
- Lucas, R. W., R. A. Sponseller, M. J. Gundale, J. Stendahl, J. Fridman, P. Högberg, and H. Laudon. 2016. Long-term declines in stream and river inorganic nitrogen (N) export correspond to forest change. *Ecological Applications* 26:545–556.
- Martin, C. W., C. T. Driscoll, and T. J. Fahey. 2000. Changes in streamwater chemistry after 20 years from forested watersheds in New Hampshire, U.S.A. *Canadian Journal of Forest Research* 30:1206–1213.
- Matschonat, G., and E. Matzner. 1995. Quantification of ammonium sorption in acid forest soils by sorption isotherms. *Plant and Soil* 168–169:95–101.
- McHale, M. R., J. J. McDonnell, M. J. Mitchell, and C. P. Cirimo. 2002. A field-based study of soil water and groundwater nitrate release in an Adirondack forested watershed. *Water Resources Research* 38:2–1.

- McLauchlan, K. K., L. M. Gerhart, J. J. Battles, J. M. Craine, A. J. Elmore, P. E. Higuera, M. C. Mack, B. E. McNeil, D. M. Nelson, N. Pederson, and S. S. Perakis. 2017. Centennial-scale reductions in nitrogen availability in temperate forests of the United States. *Scientific Reports* 7:7856.
- Melvin, A. M., J. W. Lichstein, and C. L. Goodale. 2013. Forest liming increases forest floor carbon and nitrogen stocks in a mixed hardwood forest. *Ecological Applications: A Publication of the Ecological Society of America* 23:1962–1975.
- Minick, K. J., M. C. Fisk, and P. M. Groffman. 2017. Soil Ca alters processes contributing to C and N retention in the Oa/A horizon of a northern hardwood forest. *Biogeochemistry* 132:343–357.
- Monteith, D. T., J. L. Stoddard, C. D. Evans, H. A. de Wit, M. Forsius, T. Høgåsen, A. Wilander, B. L. Skjelkvåle, D. S. Jeffries, J. Vuorenmaa, B. Keller, J. Kopáček, and J. Vesely. 2007. Dissolved organic carbon trends resulting from changes in atmospheric deposition chemistry. *Nature* 450:537–540.
- Mouvenchery, Y. K., J. Kučerík, D. Diehl, and G. E. Schaumann. 2012. Cation-mediated cross-linking in natural organic matter: a review. *Reviews in Environmental Science and Bio/Technology* 11:41–54.
- Mueller, K. E., D. M. Eissenstat, S. E. Hobbie, J. Oleksyn, A. M. Jagodzinski, P. B. Reich, O. A. Chadwick, and J. Chorover. 2012. Tree species effects on coupled cycles of carbon, nitrogen, and acidity in mineral soils at a common garden experiment. *Biogeochemistry* 111:601–614.
- Mulholland, P. J., H. M. Valett, J. R. Webster, S. A. Thomas, L. W. Cooper, S. K. Hamilton, and B. J. Peterson. 2004. Stream denitrification and total nitrate uptake rates measured using a field  $^{15}\text{N}$  tracer addition approach. *Limnology and Oceanography* 49:809–820.
- Nave, L. E., E. D. Vance, C. W. Swanston, and P. S. Curtis. 2009. Impacts of elevated N inputs on north temperate forest soil C storage, C/N, and net N-mineralization. *Geoderma* 153:231–240.
- Newcomb, C. J., N. P. Qafoku, J. W. Grate, V. L. Bailey, and J. J. D. Yoreo. 2017. Developing a molecular picture of soil organic matter–mineral interactions by quantifying organo–mineral binding. *Nature Communications* 8:396.

- Nezat, C. A., J. D. Blum, A. Klaue, C. E. Johnson, and T. G. Siccama. 2004. Influence of landscape position and vegetation on long-term weathering rates at the Hubbard Brook Experimental Forest, New Hampshire, USA. *Geochimica et Cosmochimica Acta* 68:3065–3078. Associate editor: K. L. Nagy.
- Niemi, R. M., and M. Vepsäläinen. 2005. Stability of the fluorogenic enzyme substrates and pH optima of enzyme activities in different Finnish soils. *Journal of Microbiological Methods* 60:195–205.
- Nilsson, I., S. Andersson, I. Valeur, T. Persson, J. Bergholm, and A. Wirén. 2001. Influence of dolomite lime on leaching and storage of C, N and S in a Spodosol under Norway spruce (*Picea abies* (L.) Karst.). *Forest Ecology and Management* 146:55–73.
- Nilsson, L. O., E. Bååth, U. Falkengren-Grerup, and H. Wallander. 2007. Growth of ectomycorrhizal mycelia and composition of soil microbial communities in oak forest soils along a nitrogen deposition gradient. *Oecologia* 153:375–384.
- Nimoy, L., G. Roddenberry, N. Meyer, and D. Flinn. 1991. *Star Trek VI: The Undiscovered Country*. Paramount Pictures.
- Odum, E. P. *The Strategy of Ecosystem Development*. 1969. *Science* 3877: 262-270.
- Oleson, K., M. Lawrence, B. Bonan, B. Drewniak, M. Huang, D. Koven, S. Levis, F. Li, J. Riley, M. Subin, S. Swenson, E. Thornton, A. Bozbiyik, R. Fisher, L. Heald, E. Kluzek, J.-F. Lamarque, J. Lawrence, R. Leung, W. Lipscomb, P. Muszala, M. Ricciuto, J. Sacks, Y. Sun, J. Tang, and Z.-L. Yang. 2013. Technical description of version 4.5 of the Community Land Model (CLM).
- Olsson, P. A., and N. C. Johnson. 2005. Tracking carbon from the atmosphere to the rhizosphere. *Ecology Letters* 8:1264–1270.
- Oulehle, F., C. D. Evans, J. Hofmeister, R. Krejci, K. Tahovska, T. Persson, P. Cudlin, and J. Hruska. 2011. Major changes in forest carbon and nitrogen cycling caused by declining sulphur deposition. *Global Change Biology* 17:3115–3129.
- Oulehle, F., T. G. Jones, A. Burden, M. D. A. Cooper, I. Lebron, P. Zieliński, and C. D. Evans. 2013. Soil–solution partitioning of DOC in acid organic soils: results from a UK field acidification and alkalization experiment. *European Journal of Soil Science* 64:787–796.

- Pan, Y., R. A. Birdsey, J. Fang, R. Houghton, P. E. Kauppi, W. A. Kurz, O. L. Phillips, A. Shvidenko, S. L. Lewis, J. G. Canadell, P. Ciais, R. B. Jackson, S. W. Pacala, A. D. McGuire, S. Piao, A. Rautiainen, S. Sitch, and D. Hayes. 2011. A Large and Persistent Carbon Sink in the World's Forests. *Science* 333:988–993.
- Pardo, L. H., C. Kendall, J. Pett-Ridge, and C. C. Y. Chang. 2004. Evaluating the source of streamwater nitrate using  $\delta^{15}\text{N}$  and  $\delta^{18}\text{O}$  in nitrate in two watersheds in New Hampshire, USA. *Hydrological Processes* 18:2699–2712.
- Parton, W. J., M. Hartman, D. Ojima, and D. Schimel. 1998. DAYCENT and its land surface submodel: description and testing. *Global and Planetary Change* 19:35–48.
- Peterjohn, W. T., M. B. Adams, and F. S. Gilliam. 1996. Symptoms of nitrogen saturation in two central Appalachian hardwood forest ecosystems. *Biogeochemistry* 35:507–522.
- Phillips, J. D., P. Šamonil, L. Pawlik, J. Trochta, and P. Daněk. 2017. Domination of hillslope denudation by tree uprooting in an old-growth forest. *Geomorphology* 276:27–36.
- Phillips, R. P., E. Brzostek, and M. G. Midgley. 2013. The mycorrhizal-associated nutrient economy: a new framework for predicting carbon–nutrient couplings in temperate forests. *New Phytologist* 199:41–51.
- Phillips, R. P., and T. J. Fahey. 2005. Patterns of rhizosphere carbon flux in sugar maple (*Acer saccharum*) and yellow birch (*Betula allegheniensis*) saplings. *Global Change Biology* 11:983–995.
- Photo Science Inc. 2012. White Mountain National Forest Lidar (USGS Contract: G10PC00026 Task Order Numbers: G12PD00775). <http://lidar.unh.edu/map/>.
- Post, W. M., and K. C. Kwon. 2000. Soil carbon sequestration and land-use change: processes and potential. *Global Change Biology* 6:317–327.
- R Core Team. 2013. R: A Language and Environment for Statistical Computing. R Foundation for Statistical Computing, Vienna, Austria.
- Reich, P. B., J. Oleksyn, J. Modrzyński, P. Mrozinski, S. E. Hobbie, D. M. Eissenstat, J. Chorover, O. A. Chadwick, C. M. Hale, and M. G. Tjoelker. 2005. Linking litter

- calcium, earthworms and soil properties: a common garden test with 14 tree species. *Ecology Letters* 8:811–818.
- Richards, L. A., editor. 1954. *Diagnosis and improvement of saline and alkali soils*. United States Department of Agriculture.
- Richter, D. D., D. Markewitz, S. E. Trumbore, and C. G. Wells. 1999. Rapid accumulation and turnover of soil carbon in a re-establishing forest. *Nature* 400:56–58.
- Roberts, B. J., and P. J. Mulholland. 2007. In-stream biotic control on nutrient biogeochemistry in a forested stream, West Fork of Walker Branch. *Journal of Geophysical Research: Biogeosciences* 112:G04002.
- Robertson, G. P., P. Sollins, B. G. Ellis, and K. Lajtha. 1999a. Exchangable Ions, pH, and Cation Exchange Capacity. Page *in* G. P. Robertson, D. C. Coleman, C. S. Bledsoe, and P. Sollins, editors. *Standard Soil Methods for Long-Term Ecological Research*. Oxford University Press, New York.
- Robertson, G. P., D. Wedin, P. M. Groffmann, J. M. Blair, E. A. Holland, K. J. Nadelhoffer, and D. Harris. 1999b. Soil carbon and nitrogen availability: Nitrogen mineralization, nitrification, and soil respiration potentials. Pages 258–271 *in* P. Robertson, D. C. Coleman, C. Bledsoe, and P. Sollins, editors. Oxford University Press, New York.
- Rosi-Marshall, E. J., E. S. Bernhardt, D. C. Buso, C. T. Driscoll, and G. E. Likens. 2016. Acid rain mitigation experiment shifts a forested watershed from a net sink to a net source of nitrogen. *Proceedings of the National Academy of Sciences* 113:7580–7583.
- Rousk, J., P. C. Brookes, and E. Bååth. 2009. Contrasting Soil pH Effects on Fungal and Bacterial Growth Suggest Functional Redundancy in Carbon Mineralization. *Applied and Environmental Microbiology* 75:1589–1596.
- Schaetzl, R. J., S. F. Burns, D. L. Johnson, and T. W. Small. 1988. Tree uprooting: review of impacts on forest ecology. *Vegetatio* 79:165–176.
- Scharlemann, J. P., E. V. Tanner, R. Hiederer, and V. Kapos. 2014. Global soil carbon: understanding and managing the largest terrestrial carbon pool. *Carbon Management* 5:81–91.

- Schmidt, M. W. I., M. S. Torn, S. Abiven, T. Dittmar, G. Guggenberger, I. A. Janssens, M. Kleber, I. Kögel-Knabner, J. Lehmann, D. A. C. Manning, P. Nannipieri, D. P. Rasse, S. Weiner, and S. E. Trumbore. 2011. Persistence of soil organic matter as an ecosystem property. *Nature* 478:49–56.
- Simek, M., and J. E. Cooper. 2002. The influence of soil pH on denitrification: progress towards the understanding of this interaction over the last 50 years. *European Journal of Soil Science* 53:345–354.
- Slessarev, E. W., Y. Lin, N. L. Bingham, J. E. Johnson, Y. Dai, J. P. Schimel, and O. A. Chadwick. 2016. Water balance creates a threshold in soil pH at the global scale. *Nature* 540:567–569.
- Smolders, A. J. P., L. P. M. Lamers, E. C. H. E. T. Lucassen, G. V. D. Velde, and J. G. M. Roelofs. 2006. Internal eutrophication: How it works and what to do about it—a review. *Chemistry and Ecology* 22:93–111.
- Søndergaard, M., J. P. Jensen, and E. Jeppesen. 2003. Role of sediment and internal loading of phosphorus in shallow lakes. *Hydrobiologia* 506–509:135–145.
- Sørensen, P., and E. S. Jensen. 1991. Sequential diffusion of ammonium and nitrate from soil extracts to a polytetrafluoroethylene trap for <sup>15</sup>N determination. *Analytica Chimica Acta* 252:201–203.
- Stempfhuber, B., M. Engel, D. Fischer, G. Neskovic-Prit, T. Wubet, I. Schöning, C. Gubry-Rangin, S. Kublik, B. Schloter-Hai, T. Rattei, G. Welzl, G. W. Nicol, M. Schrupf, F. Buscot, J. I. Prosser, and M. Schloter. 2015. pH as a Driver for Ammonia-Oxidizing Archaea in Forest Soils. *Microbial Ecology* 69:879–883.
- Stempfhuber, B., T. Richter-Heitmann, L. Bienek, I. Schöning, M. Schrupf, M. Friedrich, S. Schulz, and M. Schloter. 2017. Soil pH and plant diversity drive co-occurrence patterns of ammonia and nitrite oxidizer in soils from forest ecosystems. *Biology and Fertility of Soils* 53:691–700.
- Stoddard, J. L. 1994. Long-term changes in watershed retention of nitrogen: Its causes and aquatic consequences. *Adv. Chem.* 237:223–284.
- Stoddard, J. L., D. S. Jeffries, A. Lükewille, T. A. Clair, P. J. Dillon, C. T. Driscoll, M. Forsius, M. Johannessen, J. S. Kahl, J. H. Kellogg, A. Kemp, J. Mannio, D. T. Monteith, P. S. Murdoch, S. Patrick, A. Rebsdorf, B. L. Skjelkvåle, M. P. Stainton,

- T. Traaen, H. van Dam, K. E. Webster, J. Wieting, and A. Wilander. 1999. Regional trends in aquatic recovery from acidification in North America and Europe. *Nature* 401:575–578.
- Stream Solute Workshop. 1990. Concepts and Methods for Assessing Solute Dynamics in Stream Ecosystems. *Journal of the North American Benthological Society* 9:95–119.
- Sullivan, T. J., G. B. Lawrence, S. W. Bailey, T. C. McDonnell, C. M. Beier, K. C. Weathers, G. T. McPherson, and D. A. Bishop. 2013. Effects of Acidic Deposition and Soil Acidification on Sugar Maple Trees in the Adirondack Mountains, New York. *Environmental Science & Technology* 47:12687–12694.
- Sutton, R., and G. Sposito. 2005. Molecular Structure in Soil Humic Substances: The New View. *Environmental Science & Technology* 39:9009–9015.
- Templer, P. H., G. M. Lovett, K. C. Weathers, S. E. Findlay, and T. E. Dawson. 2005. Influence of Tree Species on Forest Nitrogen Retention in the Catskill Mountains, New York, USA. *Ecosystems* 8:1–16.
- Thornton, P. E. 2005. Biome-BGC: Modeling Effects of Disturbance and Climate. Oak Ridge, TN.
- Tierney, G., and T. Fahey. 2002. Fine root turnover in a northern hardwood forest: a direct comparison of the radiocarbon and minirhizotron methods. *Can. J. For. Res.* 32:1692–1697.
- Ulrich, B., R. Mayer, and P. K. Khanna. 1980. Chemical changes due to acid precipitation in a loess-derived soil in Central Europe. *Soil Science* 130:193.
- Valtera, M., and R. J. Schaetzl. 2017. Pit-mound microrelief in forest soils: Review of implications for water retention and hydrologic modelling. *Forest Ecology and Management* 393:40–51.
- Van Meter, K. J., N. B. Basu, J. J. Veenstra, and C. Burras. 2016. The nitrogen legacy: emerging evidence of nitrogen accumulation in anthropogenic landscapes. *Environmental Research Letters*:035014.
- Vaughan, M. C. H., W. B. Bowden, J. B. Shanley, A. Vermilyea, R. Sleeper, A. J. Gold, S. M. Pradhanang, S. P. Inamdar, D. F. Levia, A. S. Andres, F. Birgand, and A. W.

- Schroth. 2017. High-frequency dissolved organic carbon and nitrate measurements reveal differences in storm hysteresis and loading in relation to land cover and seasonality. *Water Resources Research* 53:5345–5363.
- Veneman, P. L. M., P. V. Jacke, and S. M. Bodine. 1984. Soil formation as affected by pit and mound microrelief in Massachusetts, USA. *Geoderma* 33:89–99.
- Venterea, R. T., P. M. Groffman, L. V. Verchot, A. H. Magill, and J. D. Aber. 2004. Gross nitrogen process rates in temperate forest soils exhibiting symptoms of nitrogen saturation. *Forest Ecology and Management* 196:129–142.
- Vitousek, P. M., and W. A. Reiners. 1975. Ecosystem Succession and Nutrient Retention: A Hypothesis. *BioScience* 25:376–381.
- de Wit, H. A., J. Mulder, A. Hindar, and L. Hole. 2007. Long-Term Increase in Dissolved Organic Carbon in Streamwaters in Norway Is Response to Reduced Acid Deposition. *Environmental Science & Technology* 41:7706–7713.
- Wolters, V., and M. Schaefer. 1994. Effects of acid deposition on soil organisms and decomposition processes. Pages 83–127.
- Yanai, R. D., M. A. Vadeboncoeur, S. P. Hamburg, M. A. Arthur, C. B. Fuss, P. M. Groffman, T. G. Siccama, and C. T. Driscoll. 2013. From Missing Source to Missing Sink: Long-Term Changes in the Nitrogen Budget of a Northern Hardwood Forest. *Environmental Science & Technology* 47:11440–11448.
- Zhou, G., S. Liu, Z. Li, D. Zhang, X. Tang, C. Zhou, J. Yan, and J. Mo. 2006. Old-Growth Forests Can Accumulate Carbon in Soils. *Science* 314:1417–1417.
- Zhu, Q., W. De Vries, X. Liu, M. Zeng, T. Hao, E. Du, F. Zhang, and J. Shen. 2016. The contribution of atmospheric deposition and forest harvesting to forest soil acidification in China since 1980. *Atmospheric Environment* 146:215–222.

## Biography

Richard Marinos was born September 8, 1985 outside Chicago. He grew up in Wenonah, NJ, where he spent his formative years getting dirty in the forests surrounding the town, and Tuscaloosa, AL. He graduated from Kenyon College, in Gambier, OH, in 2007 with an A.B. degree in philosophy. Through his work at the Brown Family Environmental Center and the mentorship of Siobhan Fennessy, Richard found his love of ecology late in his undergraduate career. He spent two and a half years in the Peace Corps, living outside Bangangte, Cameroon and working as an agroforestry extension agent. It was through this work in the Peace Corps that Richard became fascinated with soils and nutrient cycling. He came to the Nicholas School of the Environment as a Ph.D. student in 2012, first as a student of Rob Jackson and then Emily Bernhardt. At Duke, he has worked on anthropogenic disturbances to carbon and nitrogen cycling in terrestrial and aquatic ecosystems. He has been awarded an NSF Graduate Research Fellowship, an NSF Doctoral Dissertation Improvement Grant, and awards from Duke's Data+ big data initiative, the William and Janet Hunt Graduate Fellowship Fund, and the Aleane Webb Dissertation Research Fellowship. He is married to his college sweetheart Cari Ficken and they have a newborn daughter Lillian.